APPENDIX B

FULL-SCALE FIELD TESTS

CONTENTS

Two full-scale field tests were conducted at the University of Massachusetts at Amherst (UMass) to investigate the structural behavior of large-span culverts under shallow fills. The tests investigated the culvert response to forces resulting from erection, placement, and compaction of backfill as well as from live loads. Field measurements of culvert behavior, soil behavior, and culvert-soil interaction during backfilling and live loading are presented in this Appendix. Long-term monitoring of the culverts for about 9 months after completion of the live-load testing is also discussed. Complete details are presented by Webb (1998) and Webb et al. (1998).

TEST PLAN

The field tests were conducted at a dormant gravel pit 4 km (2.5 mi) north of the UMass campus. The test plan called for installing a 9.1-m (30-ft) span × 3.5-m (11-ft 4-in.) rise (inside dimensions) × 12.8-m (42-ft)-long reinforced concrete arch culvert and a 9.50-m (31-ft 2-in.) span at the footings × 3.7-m (12-ft 1-in.) rise × 12.2-m (40-ft)-long structural plate metal arch culvert end to end in a pre-excavated wide trench as illustrated in Figures B-1 and B-2. Ordinarily, there would be concern that interaction between two dissimilar culverts placed next to each other would affect the test results; however, because the focus of the tests was to evaluate performance under live-load conditions, where the structural response is primarily under the vehicle, the risk of such interaction was minimal. Placing the culverts end to end allowed a shorter length of test structure and allowed backfill placement for both structures to be undertaken in a single operation.

The culverts were installed with the top of the culvert approximately 0.6 m (2 ft) above the existing ground surface (Figure B-1). Each culvert was placed on continuous reinforced concrete footings. The footing had one joint where the metal and concrete culverts came together. The trench was then backfilled with existing site material, a well-graded sand with gravel. Live-load testing was conducted with a tandem-axle truck, loaded with 310 kN (70,000 lb) on the tandem axles. Tests were carried out at depths of fill of 0.9 m (3 ft), 0.6 m (2 ft), and 0.3 m (1 ft). The backfill placement and live-load procedures were carried out twice: once with backfill compacted to 92 percent of maximum density (AASHTO T99) and once with backfill compacted to 87 percent of maximum density.

After completion of Test 2, embankment material was added over the top of the two culverts to bring the height of cover to about 1.4 m (4.5 ft). This cover height remained in place for about 9 months, at which time the culverts were excavated and dismantled.

MEASUREMENT PLAN

The measured parameters are listed in Table B-1. Webb et al. (1999) provide more information about the instrumentation.

SOIL PROPERTIES

The in situ and backfill soil were the same material, a well-graded sand with gravel with 1 percent fines, classified SW per ASTM D2487, and A-1-b per AASHTO. Details of laboratory testing of the material are presented by Webb (1998) and Sussmann et al. (1998). Tests included sieve analyses, relative density tests, reference compaction tests (standard and variable

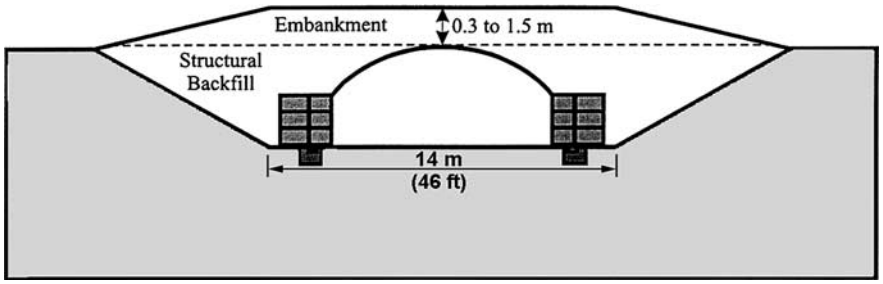

Figure B-1. Cross-sectional view of culvert installation.

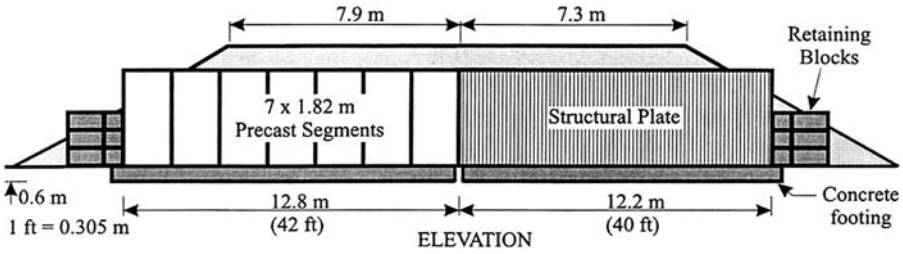

Figure B-2. End-to-end installation of culverts.

effort Proctor tests), California bearing ratio tests, and static triaxial compression tests.

TEST CULVERTS

Test Arrangement

The concrete and metal arch culverts were installed end to end (Figure B-2) extending over a length of 25 m (82 ft). Reinforced concrete blocks stacked 1.8 m (6 ft) high were used at the ends of the combined culverts to confine the backfill. The joint between the two culverts was wrapped with plastic sheeting but was otherwise unrestrained.

The concrete culvert arch segments were shipped to the site in trucks and placed on the footings with a crane. The structural plates for the metal culvert were shipped to the site and erected by a local contractor and UMass personnel.

TABLE B-1 Field test measurements

Element	Measurement
Metal Culvert	Deformation Strain Interface Pressure Wall Temperature
Concrete Culvert	Deformation Interface Pressure Crack Length and Width Relative Segment Movement Wall Temperature
Foundation	Settlement Transverse Spread Rotation
Soil	Stress Strain Moisture Unit Weight Stiffness Surface Elevations
Other	Photographs Live Load Magnitude Temperature and Rainfall

Reinforced Concrete Culvert

The concrete culvert was a 9.1-m (30-ft) span × 3.5-m (11-ft 4-in.) rise (inside dimensions), BEBO arch culvert that was manufactured by a local licensee, Rotondo Precast of Avon, Connecticut. The arch was BEBO Type E30/3. The concrete arch had a constant wall thickness of 254 mm (10 in.). The arch was made up of precast segments with a width of 1.82 m (5 ft 11½ in.). Culvert dimensions and properties are summarized in Table B-2.

Corrugated Metal Culvert

The metal culvert selected for field testing was a Contech Construction Products Type 108A30 nongalvanized corrugated steel arch culvert with a 9.50-m (31-ft 2-in.) span at the footings and a 3.7-m (12-ft 1-in.) total rise. The culvert was manufactured from structural plates with 152 × 51 mm (6 × 2 in.) corrugations. The plate thickness was 5.5 mm (0.218 in.), designated as 5 gauge. The metal culvert was tested without longitudinal thrust beams, which would be the typical installation recommended by Contech. Section properties of the

TABLE B-2 Reinforced concrete culvert properties

Culvert Properties	Metric Units		U.S. Customary Units	
	Inside	Outside	Inside	Outside
	m	m	ft-in.	ft-in.
Span	9.15	9.65	30-0	31-8
Rise	3.46	3.71	11-4	12-2
Wall Thickness	0.254		0-10	
Compressive Strength, f'c	29	MPa	4,200	psi
Poisson's Ratio	0.17			
Reinforcement Details (Circumferential)	**Metric Units**		**U.S. Customary Units**	
Area of Inside Steel, A_{si}	1.15	sq mm/mm	0.0451	sq in./in.
Area of Outside Steel, A_{so}	1.15	sq mm/mm	0.0451	sq in./in.
Yield strength, F_y (rebar & welded wire fabric)	482	MPa	70	ksi
Cover – Inside Surface	38	mm	1.5	in.
Cover – Outside Surface	51	mm	2	in.

structural plate and culvert dimensions are summarized in Table B-3.

Footings

Each culvert was supported on 1.5-m wide × 0.6-m deep (4.9 × 2 ft) continuous, reinforced concrete spread footings with a joint at the transition between types of culvert. A keyway was formed in the footing for the concrete culvert to seat the arch elements with the aid of grout and hardened plastic shims. The metal arch culvert was bolted to base channel connections cast into the footing.

PLACEMENT AND COMPACTION OF FILL

The extent of the structural backfill zone is similar for both culverts, as depicted in Figure B-1. The structural backfill material for Test 1 was placed and compacted with a vibratory plate compactor (close to the culvert) or a vibratory roller to a target value of 95 percent of AASHTO T99 maximum dry density. For Test 2, the soil was placed and spread with a backhoe with a grading bucket. No compaction effort was applied to backfill soil during Test 2 except for the layers above the top of the culverts. These layers were placed and compacted with a vibratory roller to a target 95 percent of AASHTO T99 to support the live-load test vehicle. A water truck and spray system were used to maintain the moisture content close to the optimum of 5.5 percent during construction.

The structural backfill was placed in lifts approximately 300 mm (12 in.) thick, measured before compaction, for both types of culverts. The maximum difference in backfill surface elevation between the two sides of the culverts did not exceed 0.6 m (2 ft) during construction operations. Heavy construction equipment was operated far enough from the culverts to avoid causing excessive deformations or distress of the culverts.

TABLE B-3 Properties of structural steel plates and culvert dimensions

Culvert Properties	Metric Units		U.S. Customary Units	
Bottom Span	9.50	m	31-2	ft-in.
Maximum Span	9.63	m	31-7	ft-in.
Total Rise	3.68	m	12-1	ft-in.
Top Radius, R_t	6.275	m	20-7	ft-in.
Side Radius, R_s	2.210	m	7-3	ft-in.
Angle below Horizontal	14° 3'			
R_t/R_s	2.84			
Sectional Plate Properties	**Metric Units**		**U.S. Customary Units**	
Corrugation Pitch and Depth	152.4 x 50.8	mm	6 x 2	in.
Uncoated Plate Thickness	5.45	mm	0.215	in.
Nominal Uncoated Section Depth	56.2	mm	2.215	in.
Cross-Sectional Area per Unit Length, A	6.77	sq mm/mm	0.267	$in.^2/in.$
Moment of Inertia per Unit Length, I	2,080	sq mm/mm	0.127	$in.^4/in.$
Section Modulus, S	74.0	sq mm/mm	0.115	$in.^3/in.$
Young's Modulus, E	200	GPa	29×10^6	psi
Poisson's Ratio	0.3			
Yield Strength, F_y (from test results)	282	MPa	40.9	ksi
Ultimate Strength, F_u (from test results)	379	MPa	55.0	ksi

During backfilling, the crown of the metal culvert moved upward (peaked) more than recommended by the manufacturer. This motion was controlled by placing a line of concrete blocks on the crown of the culvert. The blocks were placed when the backfill was approximately 2.5 m above the footings.

LIVE-LOAD TESTING

The live-load test vehicle had tandem axles with dual tires. Center-to-center axle spacing was 1.4 m (4 ft 7 in.). Center-to-center spacing between the wheels of the tandem axles was 1.96 m (6 ft 5 in.). The width of one set of dual wheels was about 0.58 m (23 in.). The test vehicle was loaded with concrete blocks to achieve the test load. The target load was the LRFD tandem truck, 222 kN (50,000 lb) distributed to two axles, plus 40 percent impact, for a total load of 310 kN (70,000 lb). This load was applied to both culverts. Some testing was also conducted with the metal culvert using 50 percent of the target load. The wheel loads were verified with portable scales maintained by the Massachusetts State Police.

Measurements of culvert response were taken for five load positions across the culvert, starting with the tandem axles centered approximately over the south springline, 4.6 m (15 ft) from the crown, and advancing in 2.3-m (7.5-ft) increments toward the north springline (NS). The live-load positions are therefore designated SS (south springline), SH (south shoulder), CR (crown), NH (north shoulder), and NS (north springline).

The live-load tests were conducted with the 100-percent load level at 0.9 m of soil cover. Then the fill was removed in increments of 300 mm (12 in.), and the live-load tests were repeated at 0.6 and 0.3 m of soil cover. For the metal culvert at 0.9 and 0.3 m of soil cover, the 50-percent load level was used first, and then the 100-percent load level was used. However, the 50-percent load level was not used for the metal culvert of Test 2 at 0.9 m (3 ft) of soil cover. For each cover depth, two passes of the live-load vehicle were made. For the first pass, the wheels of the live-load vehicle were positioned over the primary instrument stations (Stations P1 and P2); for the second pass, the vehicle was offset 0.9 m toward the outside of the culvert (toward east over the metal culvert and toward west over the concrete culvert). However, for the concrete culvert at 0.9 m of soil cover (Test 1), the live-load vehicle was offset 0.9 m toward the east for Test 1. Plan views of live-load positions relative to earth pressure cells for the concrete and metal culverts are shown in Figures B-3 and B-4, respectively. Wheel contact areas are shown in these figures. Field measurements showed the contact area to be about 300 mm long × 200 mm wide (12 in. long × 8 in. wide). In these figures, a, b, c, and d refer to Pass 1 with the tandem-axle wheels positioned over both springlines, the south shoulder, the crown, and the north shoulder, respectively; e, f, g, and h refer to similar live-load positions for Pass 2. In these figures, the front wheels are always positioned to the right of the tandem axles. The front wheels are not shown when they were beyond the springlines.

RESULTS

Deformation

Deformation measurements were made with the laser, digital level, structural extensometers and the manual tape extensometer. The measurement locations are summarized in Figures B-5 and B-6 for the metal and concrete culverts, respectively. A total of 26 locations around the circumference of the metal culvert and 23 locations for the concrete culvert were selected for the detailed laser measurements at each of the three monitoring stations. A conventional level survey with a digital level was used to obtain level measurements of crown and points of radius change at two stations along the top of each culvert. Structural extensometers were used to measure relative horizontal movement between points of radius change at two stations along the length of each culvert.

Deformations During Backfilling

Vertical deformations of the metal culvert during backfilling operations, measured with the laser device and with the digital level at the crown and curvature locations and averaged for the respective stations, are shown in Figure B-7 for Tests 1 and 2. For Test 1, a systematic difference exists between the laser device and level surveys. Digital-level measurements of Test 1 are shown before and after compaction. These measurements indicate that most of the structural displacements occurred because of placement and spreading of the backfill with small compaction-induced deformations. In both tests, the crown continued to rise until earth was placed over the top of the structure, at which point the movement was reversed. In Test 1, with backfill compacted to 95 percent of maximum density, crown peaking deformation exceeded the subsequent downward movement during overfilling. For Test 2, with no compactive effort applied, the downward movement of the crown was about the same as the upward movement during sidefilling. Maximum peakings during backfilling were about 80 mm (3.1 in.) and 72 mm (2.8 in.) for Tests 1 and 2, respectively. Both tests show fairly similar trends for movements of the curvature points. Also, for both tests, the south curvature points showed more downward movement than the north points. This trend was also noted visually as more flattening of the side plates on the south side than on the north side. The effect of top loading the metal structure as well as the significance of having less stiff soil support for Test 2 is shown in Figure B-7.

Horizontal changes in top chord measurements of both culverts during backfilling operations are shown in Figure B-8. The measurements in this figure represent average values

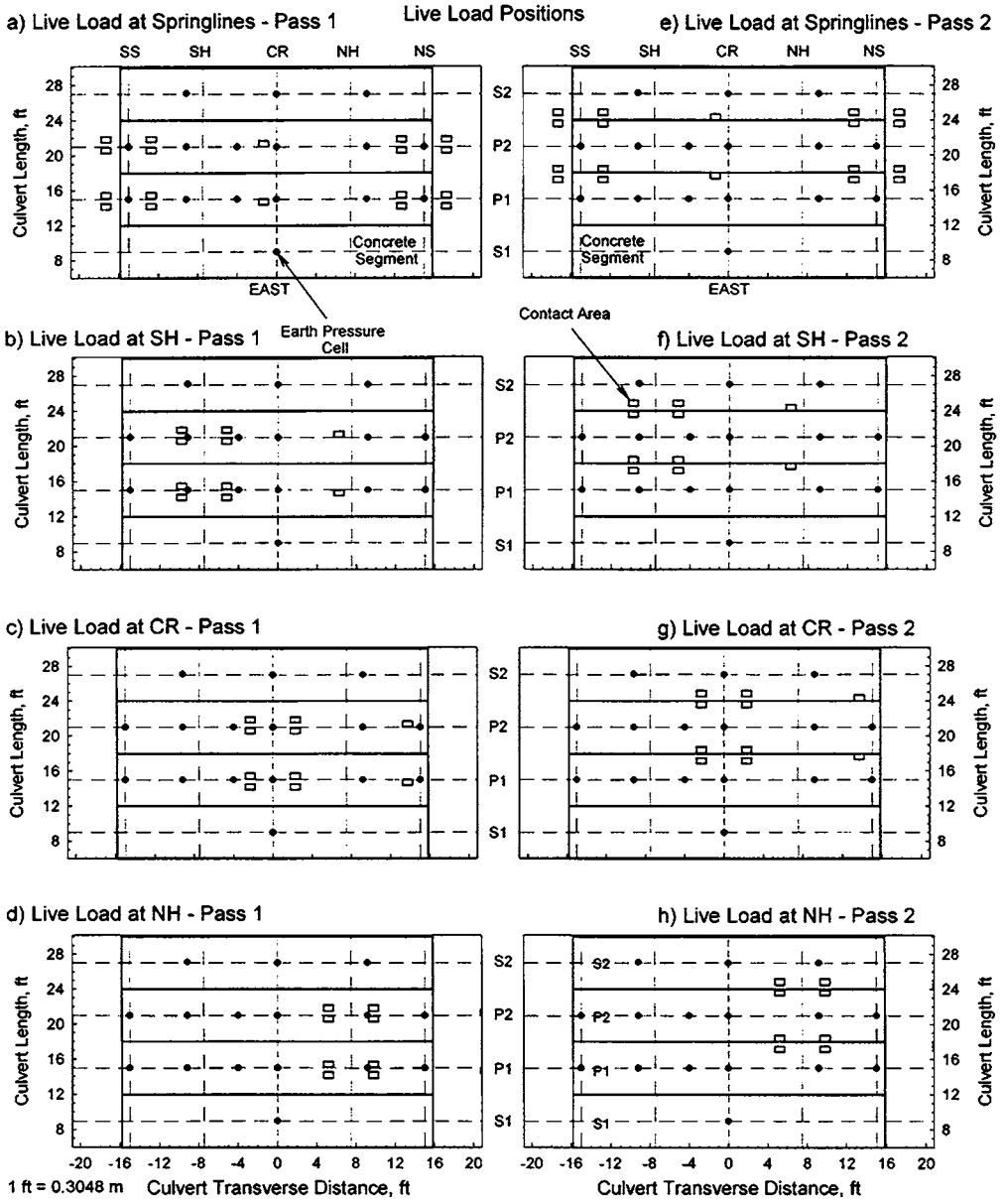

Figure B-3. Plan view of live-load positions for concrete culvert.

at the two monitoring stations along the length of each culvert. The concrete culvert showed very little movement between the curvature points for both tests. For the concrete culvert, compacted Test 1 produced slightly more inward movement (contraction) of the curvature points compared with Test 2. The metal culvert produced similar changes in top chord measurements during sidefilling and before top loading for both tests (inward movement of the curvature points and thus contraction). However, during placement of the last two layers of soil cover, significant extension of the top chord occurred in Test 2 compared with Test 1, which showed small extension. Furthermore, the effect of top loading the metal structure and having less stiff soil support in Test 2 can also be seen.

Deformed metal culvert shapes due to backfilling operations are shown in Figure B-9 for both tests as measured with the laser device. This figure shows the maximum peaking of the structure at 0.3 m (1 ft) of soil cover and the final shape after backfilling. Culvert displacements have been magnified 7.5 times. Test 1 shows slightly more peaking than Test 2. More flattening of the south plates occurred in Test 2 than in Test 1.

The concrete culvert did not significantly deform for either of the tests during backfilling or during live-load testing. Measurements indicate a maximum downward movement of the crown of less than 2 mm at the end of backfilling. Also, maximum outward movement (spreading) of the arch legs was less than about 2 mm for both tests.

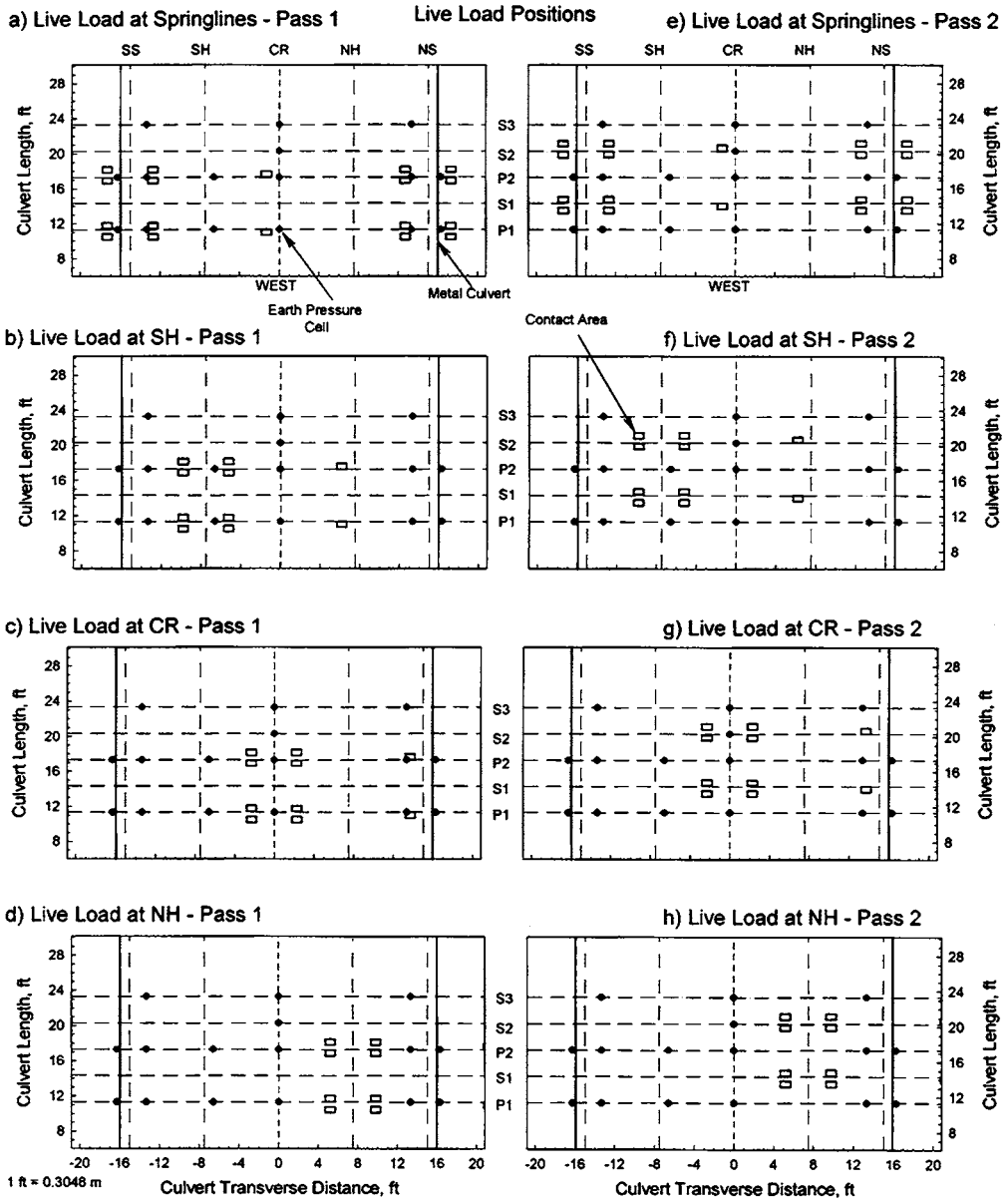

Figure B-4. Plan view of live-load positions for metal culvert.

A comparison of all the deformation measurements is given in Table B-4a and b for the metal culvert and in Table B-5 for the concrete culvert. The shoulder locations on the metal culvert showed upward movement during Test 1, which is consistent with the observed peaking behavior of the crown and subsequent decrease of the top chord distance (about 0.6 percent compared with the design dimension). However, for Test 2, the south shoulder on the metal culvert was pushed downward at the end of backfilling, which is consistent with the observed flattening of the south plates. For this test, the top chord contracted by about 0.4 percent compared with the design dimension.

As noted previously, movements in the concrete culvert were small at all times.

Average movements of the metal culvert springlines during backfilling are presented in Figure B-10 for both tests, as measured with the laser device. In general, the springlines showed similar trends. For Test 2, the springlines moved inward about the same amount during placement of the sidefill material, even though no compaction effort was applied. This was also seen in the vertical displacement of the culvert shown in Figure B-7, in which most of the peaking displacements are similar in both tests. Test 1 shows almost no outward movement of the walls during placement of the embankment material over the crown, whereas Test 2 shows movement approximately equal to the total inward movement during sidefilling. This is undoubtedly due to the stiffer backfill material in Test 1.

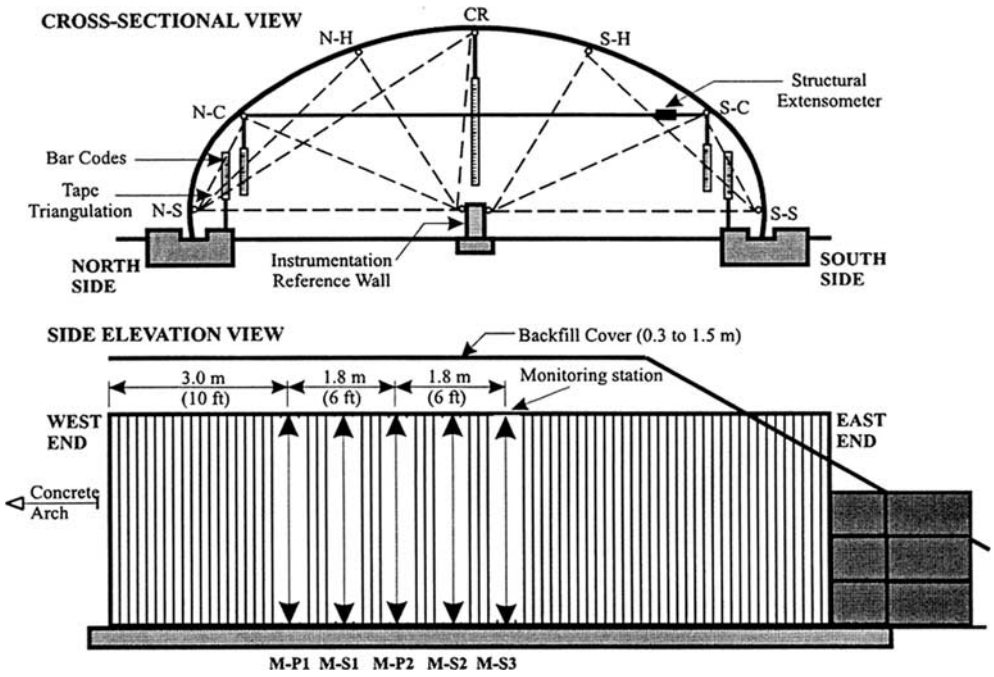

Figure B-5. Instrumentation for monitoring deformation in metal culvert.

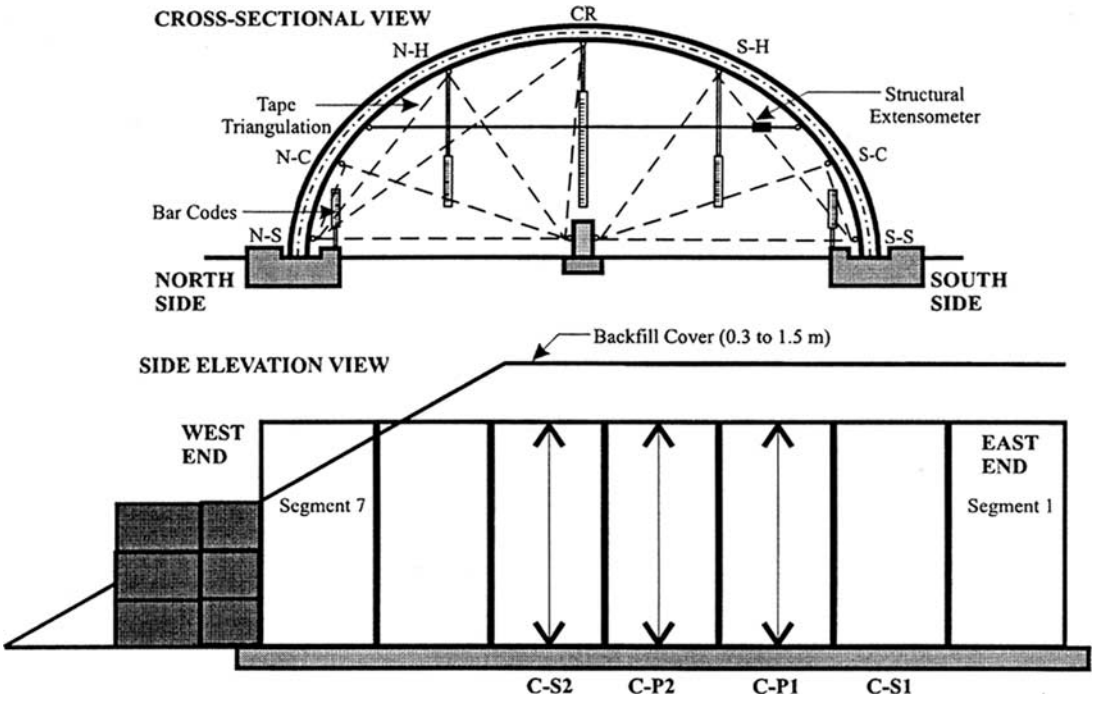

Figure B-6. Instrumentation for monitoring deformation in concrete culvert.

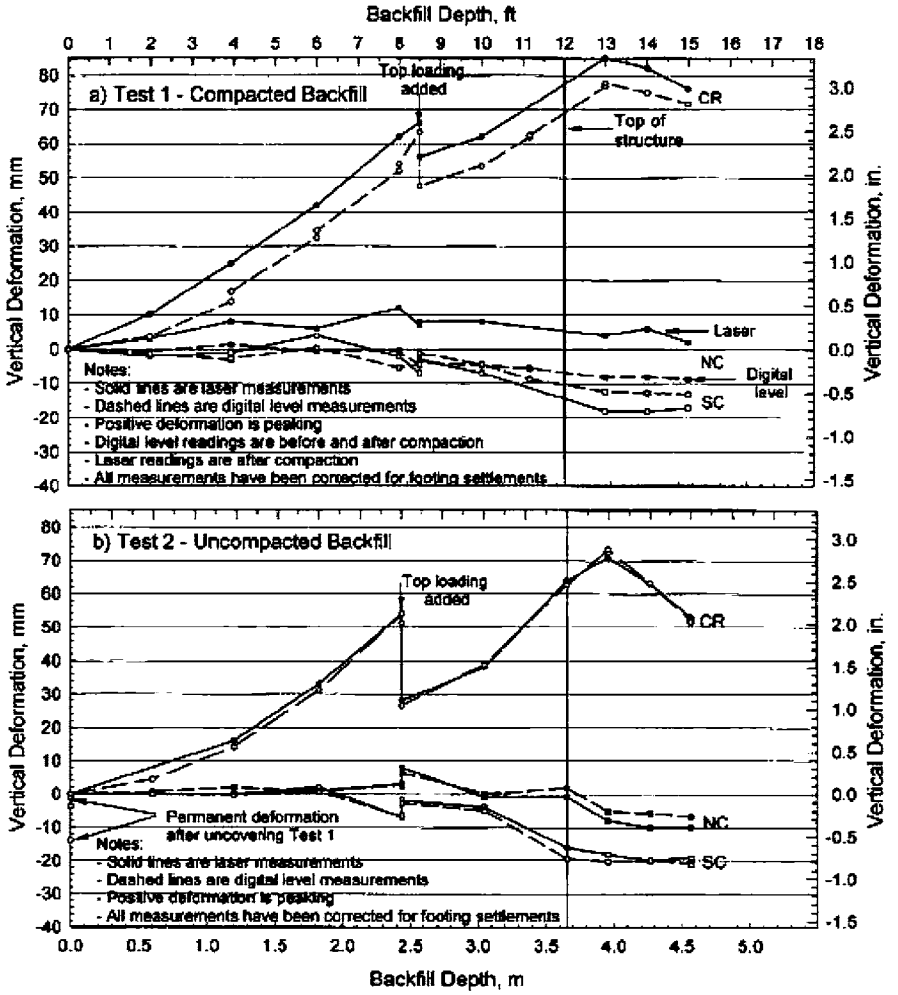

Figure B-7. Structural deformations of metal culvert during backfilling.

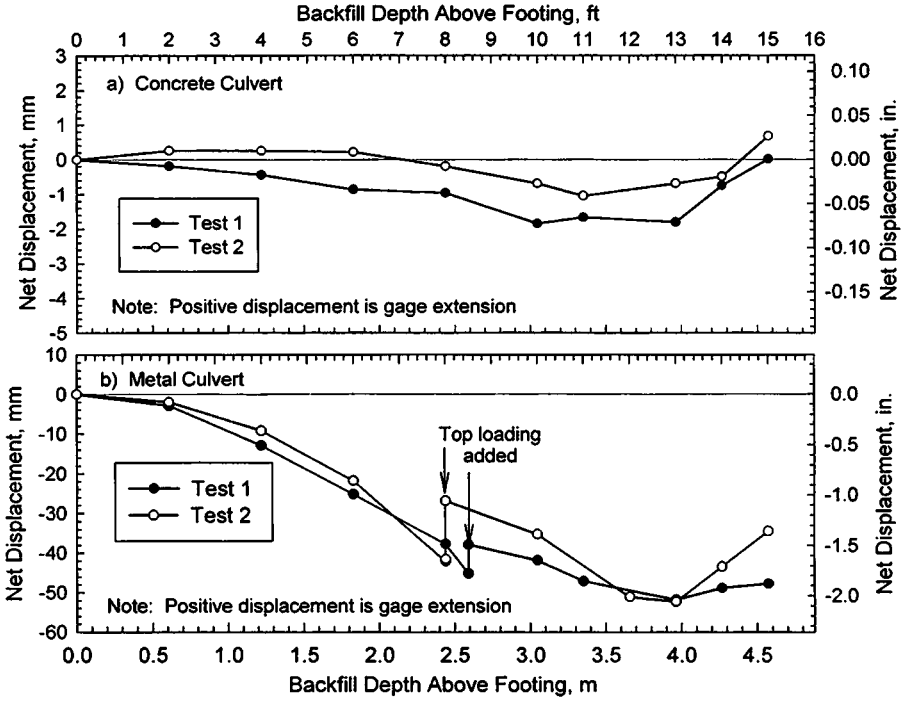

Figure B-8. Horizontal change in top chord measurements during backfilling.

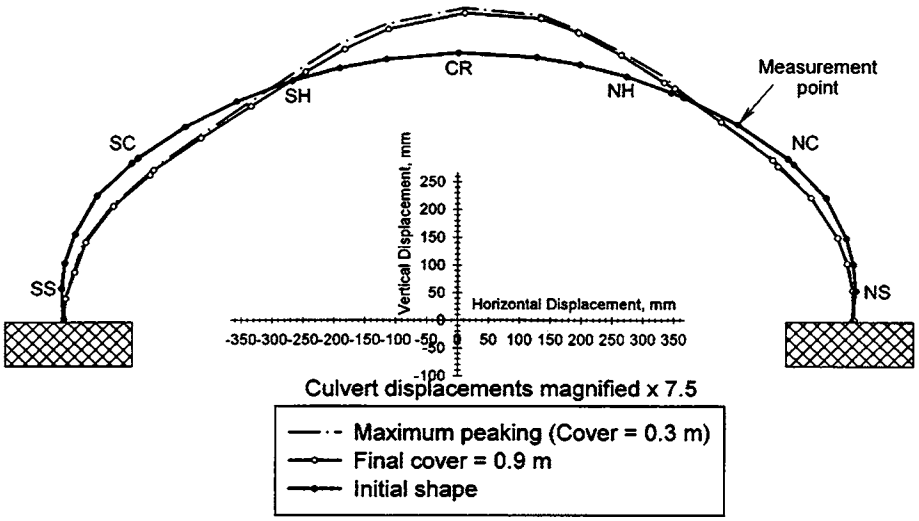

a) Average Displacements for Test 1

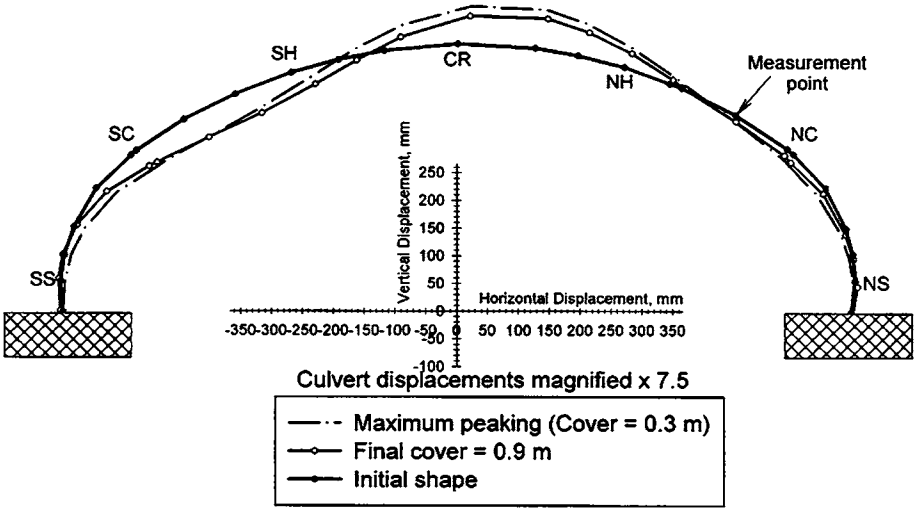

b) Average Displacements for Test 2

Figure B-9. Deformed culvert shapes after backfilling.

Deformations During Live-Load Testing

Sample plots of metal culvert displacements during live-load testing at 0.3 m (1 ft) of soil cover are shown in Figures B-11 and B-12 for Tests 1 and 2, respectively. These figures show the three monitoring stations where laser measurements were obtained (P1, P2, and S3) with the tandem axles of the live-load vehicle positioned over the south shoulder, crown, and north shoulder for Pass 1. A magnification factor of 15 has been used. For the tandem axles of the live-load vehicle positioned over the springlines, the live-load deformations were small based on the digital-level measurements. At 0.3 m (1 ft) of soil cover, most deformation occurred at the station directly under the tandem axles of the live-load vehicle (Stations P1 and P2) with less deformation further away (Station S3). Also, very similar deformed shapes were obtained at Stations P1 and P2. When the tandem axles of the live-load vehicle were positioned over the south shoulder, upward movement of the crown occurred (Figures B-11 and B-12). Test 2 displacements were slightly larger than those for Test 1. After the live-load vehicle was removed, most of the live-load-induced deformations were recovered.

Longitudinal deflection profiles measured along the metal culvert crown with the tandem axles of the live-load vehicle over the crown are shown in Figures B-13 and B-14 for Tests 1 and 2, respectively. Arrows denote the longitudinal positions of the live-load vehicle. The most significant difference between Test 1 and Test 2 deflection profiles was the more gradual deflection basin for Test 2. Also, the pattern did not shift as much as expected from Pass 1 to Pass 2 for either test. The data showed very small movements at the curvature loca-

TABLE B-4 Metal culvert backfilling deformations (readings with laser)

a. Test 1

Reading Location	3.05 m (10 ft) of Backfill		End of Backfill	
	Vertical (mm)	Horizontal (mm)	Vertical (mm)	Horizontal (mm)
SS		-8		-6
NS		-7		-5
SC	-7	-15	-17	-26
NC	8	-27	2	-25
SH	42	-4	20	-22
NH	43	-9	43	-9
CR	62	3	76	10
Top Chord		-42		-51
Span		-15		-11

b. Test 2

Reading Location	End of Backfill	
	Vertical (mm)	Horizontal (mm)
SS		3
NS		4
SC	-19	-33
NC	-10	-4
SH	-19	-39
NH	27	12
CR	53	20
Top Chord		-37
Span		7

NOTES:
1. Positive horizontal displacement = outward movement of structure
2. Positive vertical displacement = upward movement of structure (i.e., peaking)
3. All displacements are measured from initial (before Test 1 backfill) conditions
4. Horizontal displacement of crown is positive towards north
5. Readings are adjusted for footing settlements
6. 1 in. = 25.4 mm

tions of the metal culvert for both tests and for all positions of the live-load vehicle. The maximum displacement of the metal culvert occurred between the wheels of the live-load vehicle (Figure B-13, Test 1).

For all soil covers, and for both tests, the concrete culvert experienced less than 1.5 mm (0.06 in.) of deflection.

TABLE B-5 Comparison of concrete culvert backfilling deformations (tape extensometer)

Reading Location	3.05 m (10ft) of Backfill		End of Backfill	
	Vertical (mm)	Horizontal (mm)	Vertical (mm)	Horizontal (mm)
SS		0.2		0.3
NS		0.4		0.4
SC	0.4	0.1	0.3	0.7
NC	0.7	2.3	0.0	0.4
SH	-0.1	-0.2	-0.7	-0.5
NH	-0.5	0.5	-0.8	0.1
CR	-0.2	-4.6	-0.2	1.7
Top Chord		1.3*		0.4*
Span		0.6		0.7

NOTES:
1. Sign conventions same as Table B-4
2. *Average of readings taken between the shoulders and curvature locations
3. 1 in. = 25.4 mm

Long-Term Deformations

Metal and concrete culvert deformations under constant earth load were monitored over a period of about 9 months with tape, soil, and structural extensometers. The results of these measurements are presented by Webb et al. (1998). In summary, the measuring locations on the metal culvert continued to show downward movements during the monitoring period, although these movements essentially stabilized 27 weeks after construction finished. The most movement occurred at the crown [total of about 9 mm (0.35 in.)] followed by the shoulders [total of about 5 mm (0.2 in.)] with little movement at the curvatures. There were no visual signs of long-term footing settlements; however, this movement was not monitored for the 9-month period. The top chord and span dimensions increased during the first two monitoring periods (consistent with the trends observed at the crown and shoulder locations) with less change (slight extension) thereafter. The concrete culvert experienced small downward movements at the reading locations during the first two monitoring periods, after which it showed very little change. Some of these movements may be the result of footing settlements.

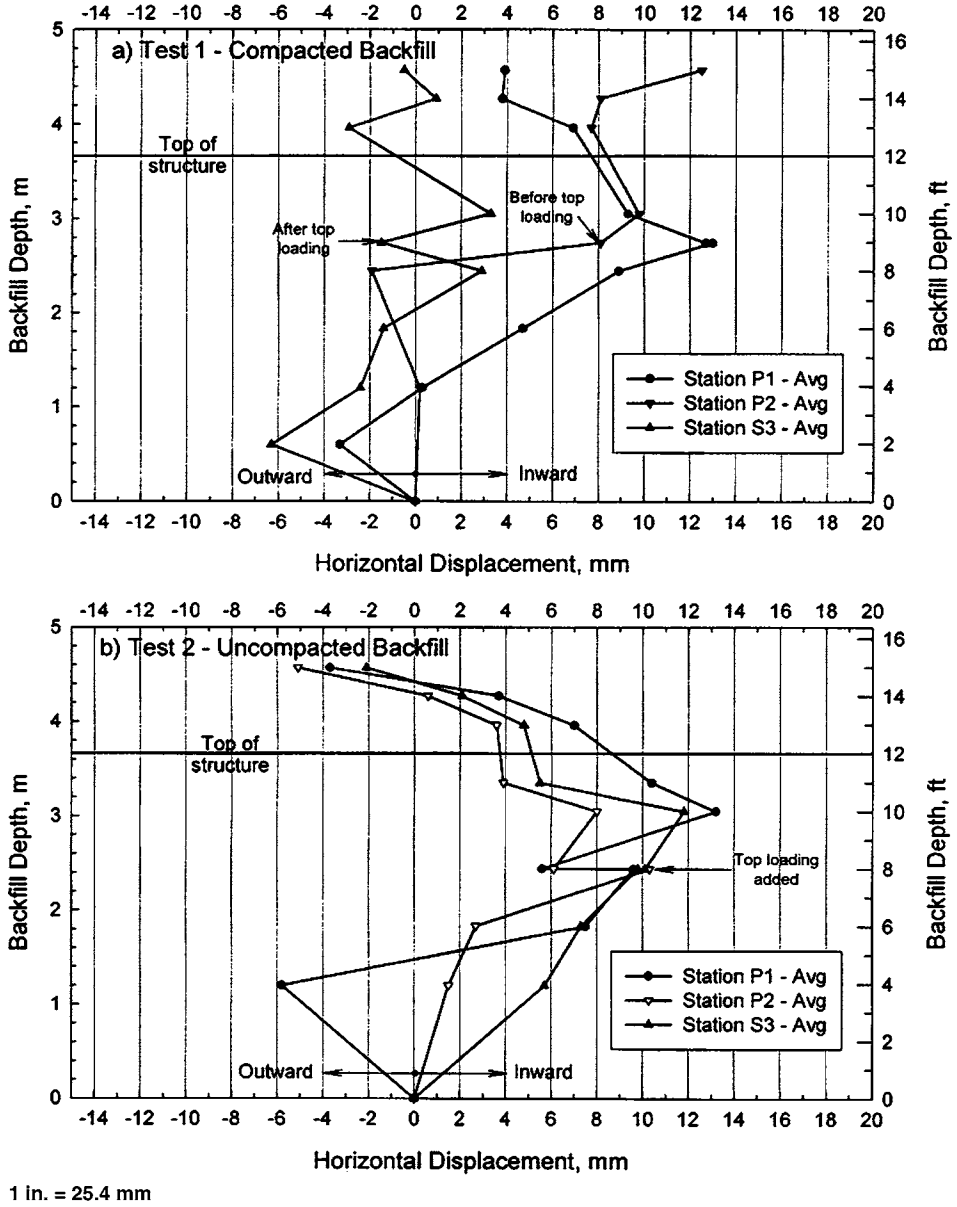

Figure B-10. Average horizontal springline displacements during backfilling.

Thrusts and Bending Moments

During Backfilling

Sets of four weldable electrical resistance strain gauges were installed at each of 25 locations (Figure B-15) on the inside wall of the metal culvert (circumferential and longitudinal directions on inside crest and valley locations). However, the thrust strains were small and are believed to be in error [explained in detail by Webb et al. (1998)]. The computed bending moments are believed to be correct and, therefore, only bending moments are reported here. Wall thrusts were estimated from measured radial pressures as shown later.

The variation in bending moment during backfilling is shown in Figures B-16 and B-17 for Tests 1 and 2, respectively. Positive bending moment corresponds to tension on the inside fiber. These figures indicate similar trends for both tests with the largest bending moments developing at the crown. The smallest bending moments developed at the shoulders. The effect of top loading is smaller for Test 1 with compacted backfill than for Test 2 with loosely placed backfill.

Hoop thrust was computed from measured radial pressures based on the ring compression theory (White and Layer 1960) in which thrust in the conduit wall is equal to the radius of curvature of the plates times the radial pressure ($T = pR$). Computed thrusts using this theory and average bending moments

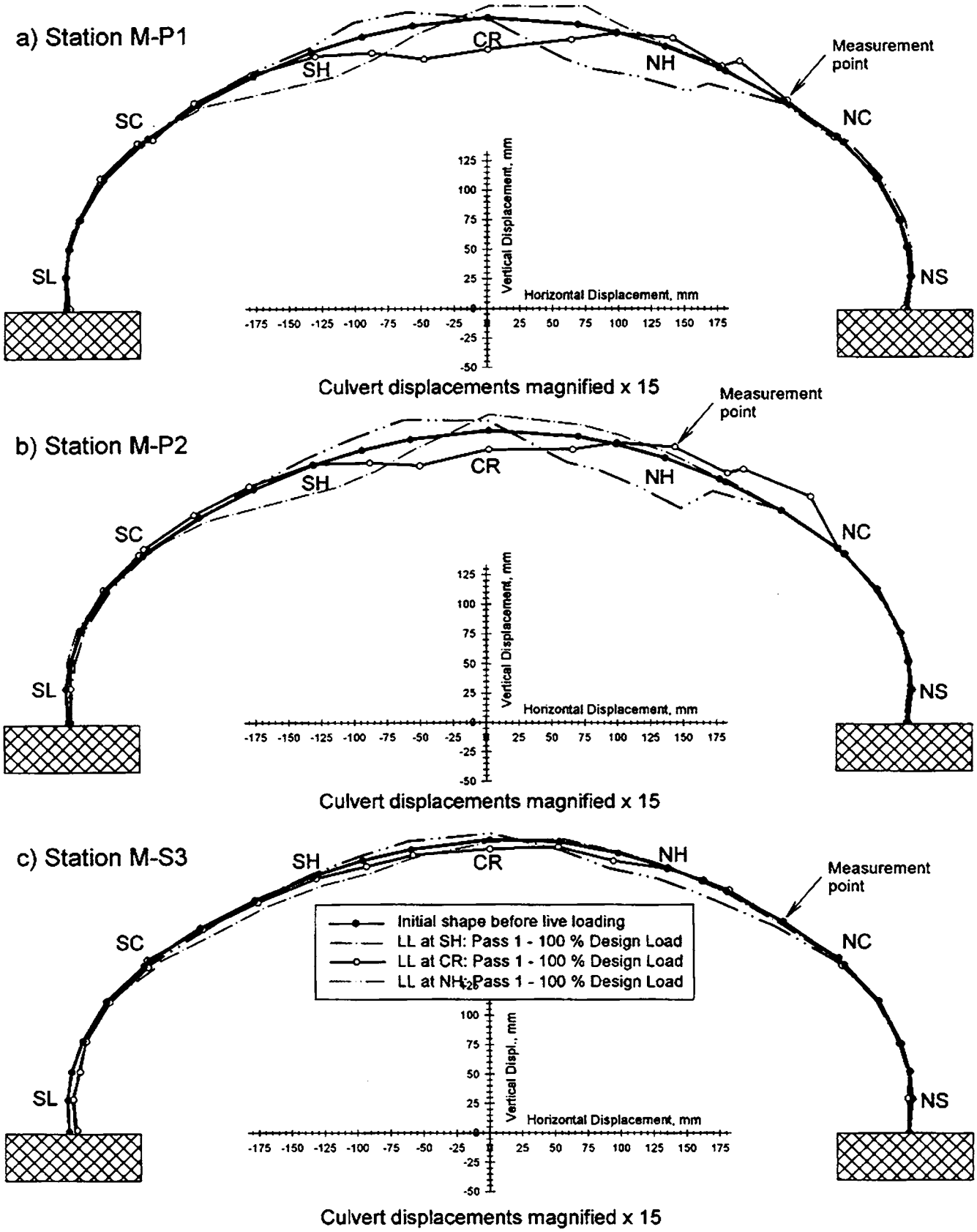

1 in. = 25.4 mm; 1 ft = 0.31 m

Figure B-11. Metal culvert live-load displacements: Test 1, 0.3-m cover.

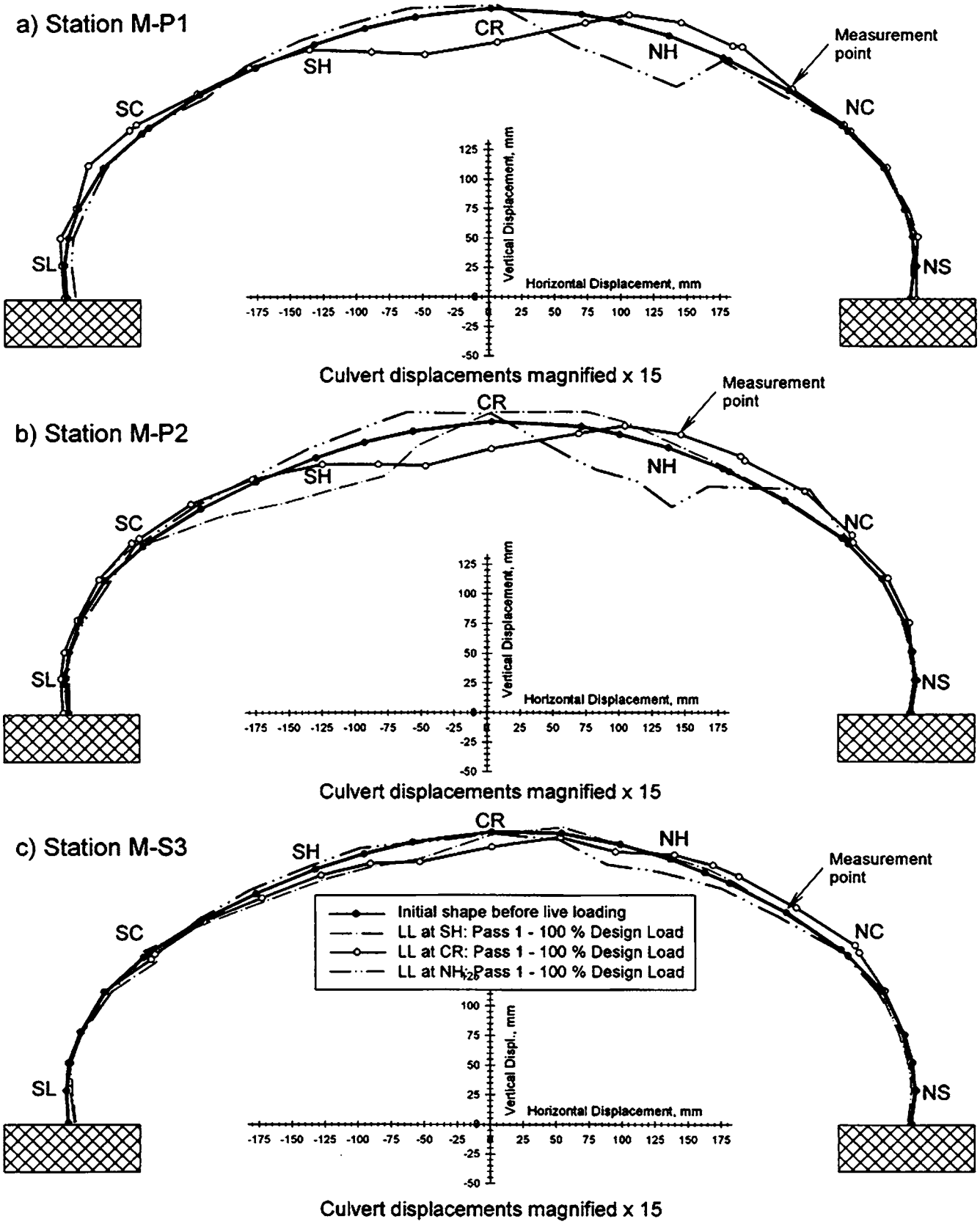

1 in. = 25.4 mm; 1 ft = 0.31 m

Figure B-12. Metal culvert live-load displacements: Test 2, 0.3-m cover.

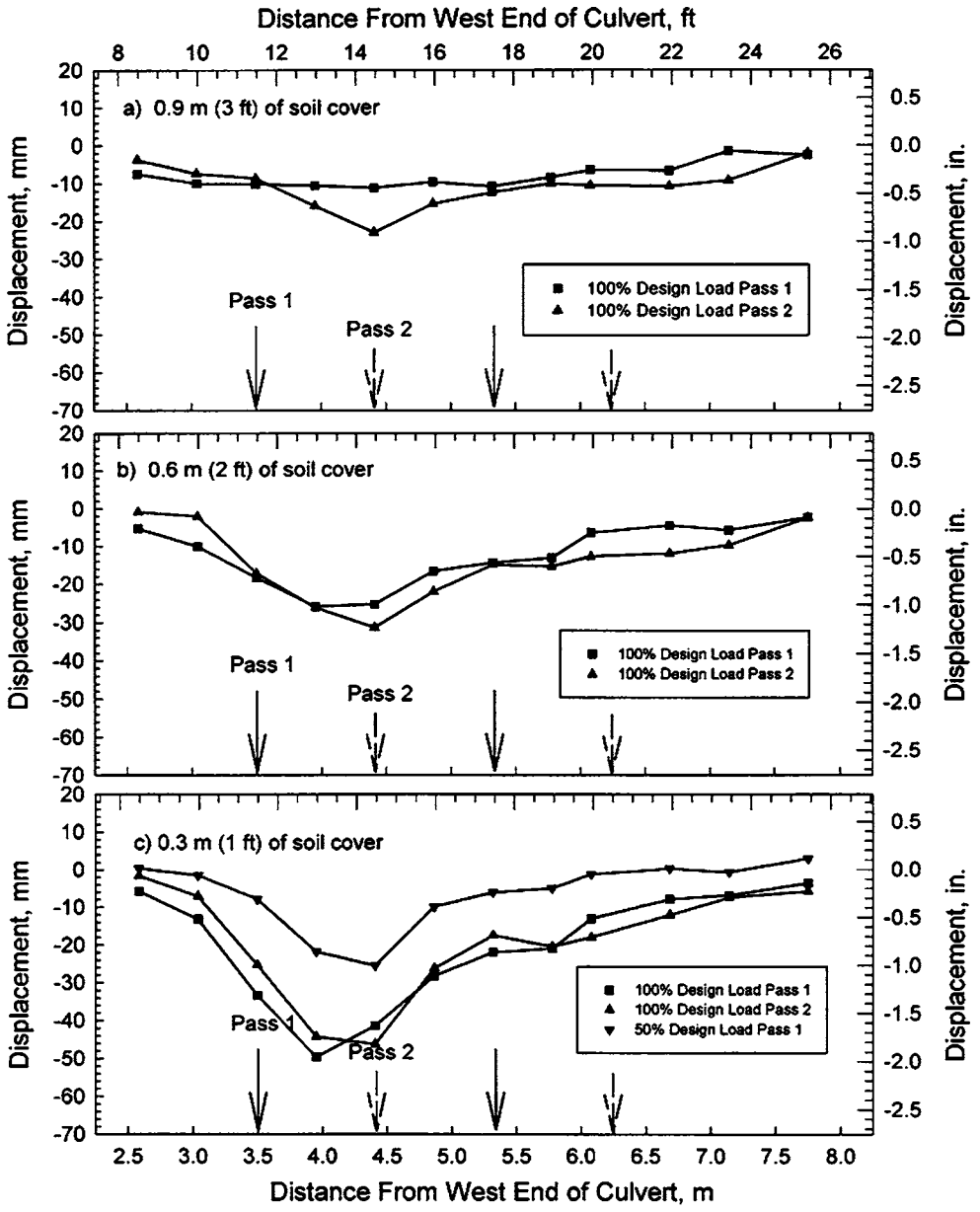

Notes: 1. Positive displacement is upward movement
2. Displacements are computed relative to end of backfilling condition at 0.9m of soil cover (displacements are zeroed at 0.9m of cover)

Figure B-13. Longitudinal deflection profile at metal culvert crown: Test 1.

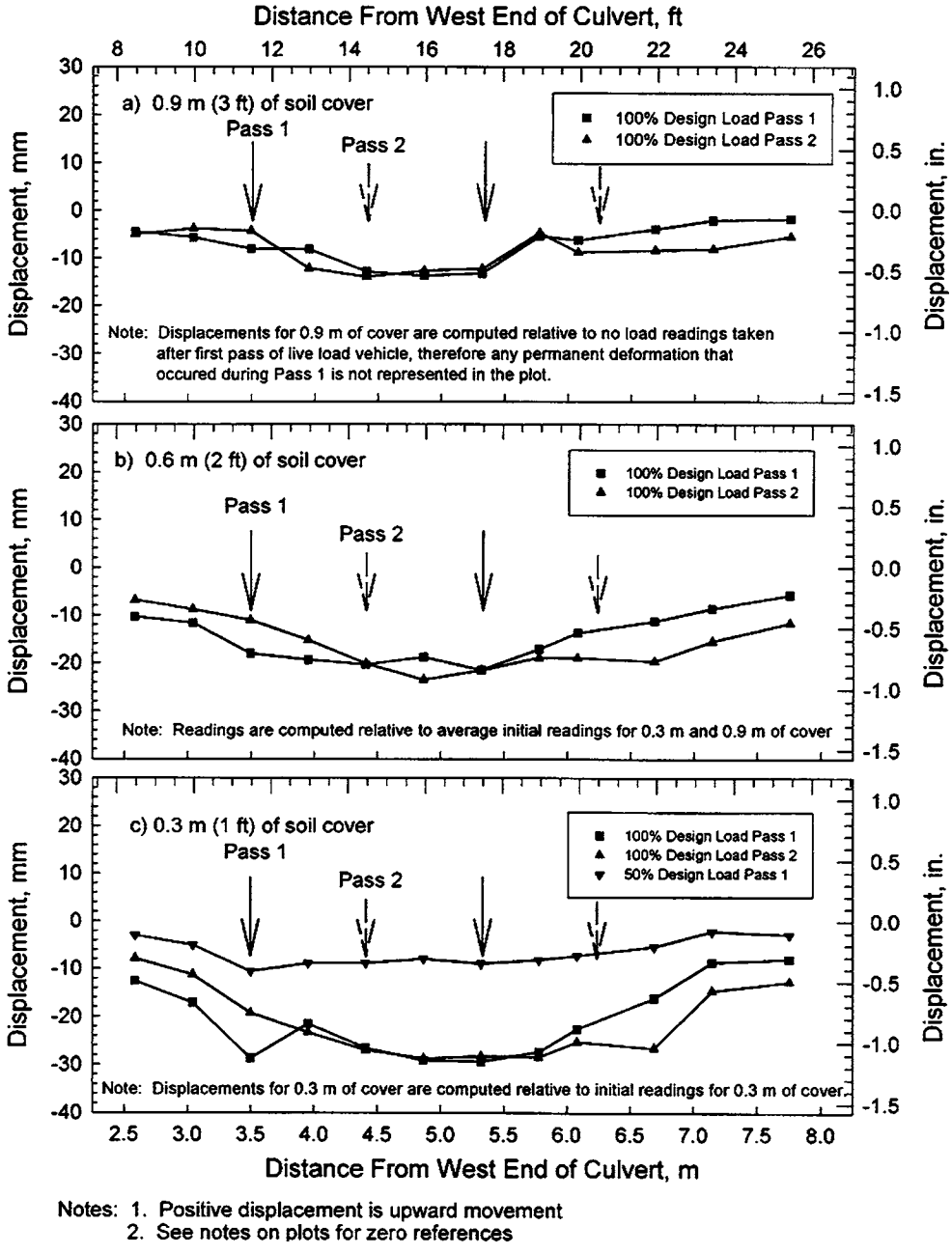

Notes: 1. Positive displacement is upward movement
2. See notes on plots for zero references

Figure B-14. Longitudinal deflection profile at metal culvert crown: Test 2.

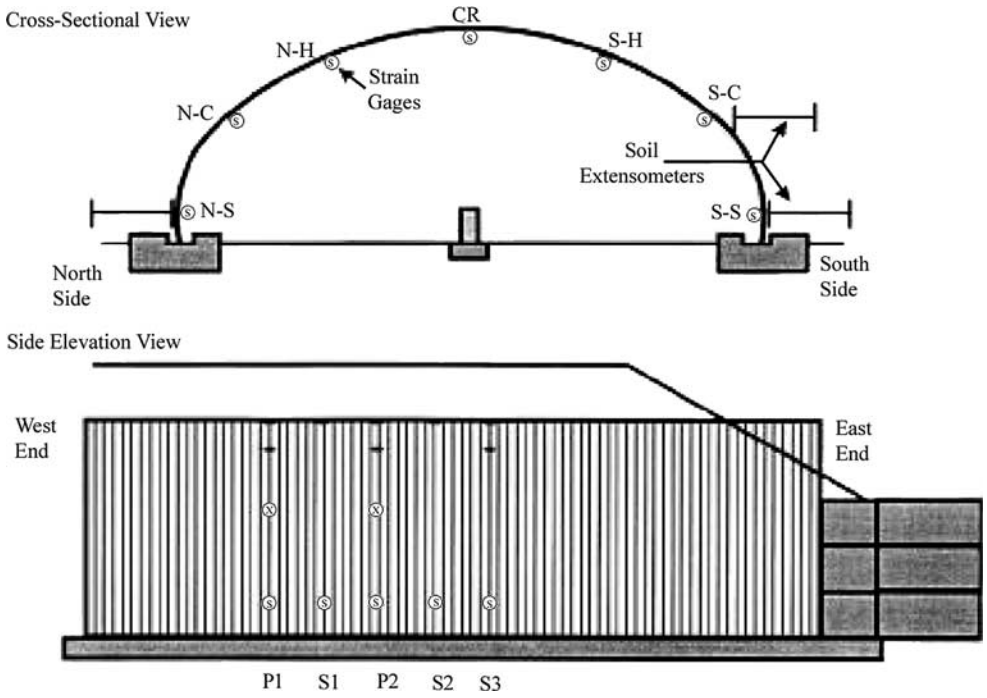

Figure B-15. Strain measurement locations in metal culvert.

are shown in Figure B-18 for Test 1 and Figure B-19 for Test 2. The resulting thrust distribution is fairly uniform in magnitude (as would be expected). In addition to computing thrusts from the measured radial pressures, additional strain gauges were installed just before removal of the backfill at the centroidal axis of the wall section at seven locations around the culvert circumference. These locations included the culvert springlines, curvatures, shoulders, and crown of Station P2. Measurements included both circumferential and longitudinal strains. After the centroidal strain gauges were added, the structures were uncovered, and the load on the metal culvert could thus be obtained from unloading, as shown in Figure B-19a. Thrusts computed from unloading the culvert using the measured radial pressures and the strain gauges installed at the centroid are in good agreement. The bending moment distributions are reasonably symmetric with negative moments at the crown and springline locations (inside fiber in compression) and positive moments at the curvature changes (moments are plotted on tension side of structure). The bending moment distributions are similar for the two tests, except that larger moments developed at the springlines of Test 2.

During Live-Load Testing

Bending moments with the live-load vehicle over the crown during Pass 1 are plotted in Figure B-20 for Test 1 and in Figure B-21 for Test 2. Moment is plotted on the tension side of the structure. Three depths of soil cover and five measurement stations are included. The figures indicate that the peak live-load bending moments at the shoulders and crown increase substantially as cover depth decreases. No significant moments developed at the springline and point of curvature changes from the live-load vehicle. The crown moment measured between the wheel paths (Station S1) is larger than that measured underneath the wheel paths (Stations P1 and P2), which implies that the maximum bending moment and thus deflection of the structure occurred between the wheel paths. Longitudinal crown deflection profiles shown in Figures B-13 and B-14 support this. The effect of the weight of the front axle of the live-load vehicle is noted in the slightly larger bending moments at the stations under the wheel paths of the live-load vehicle (Stations P1 and P2) of the north shoulders compared with those of the south shoulders. Bending moments for both tests are similar.

The distribution of the bending moment due to the tandem axles of the live-load vehicle positioned over the south shoulder during Pass 1 is plotted in Figure B-22 for Test 1. Moment distribution and magnitude were similar for Test 2 and are not presented. Figure B-22 shows increasing moments with decreasing depth of fill. Peak negative live-load bending moments at the south curvature changes and the crown are similar in magnitude. Positive moments at the shoulder are smaller in magnitude than the negative moments. No significant moments developed at the springlines or at the north curvature changes from the live-load vehicle. Bending moments with the live-load vehicle placed over the springline were small and are not presented.

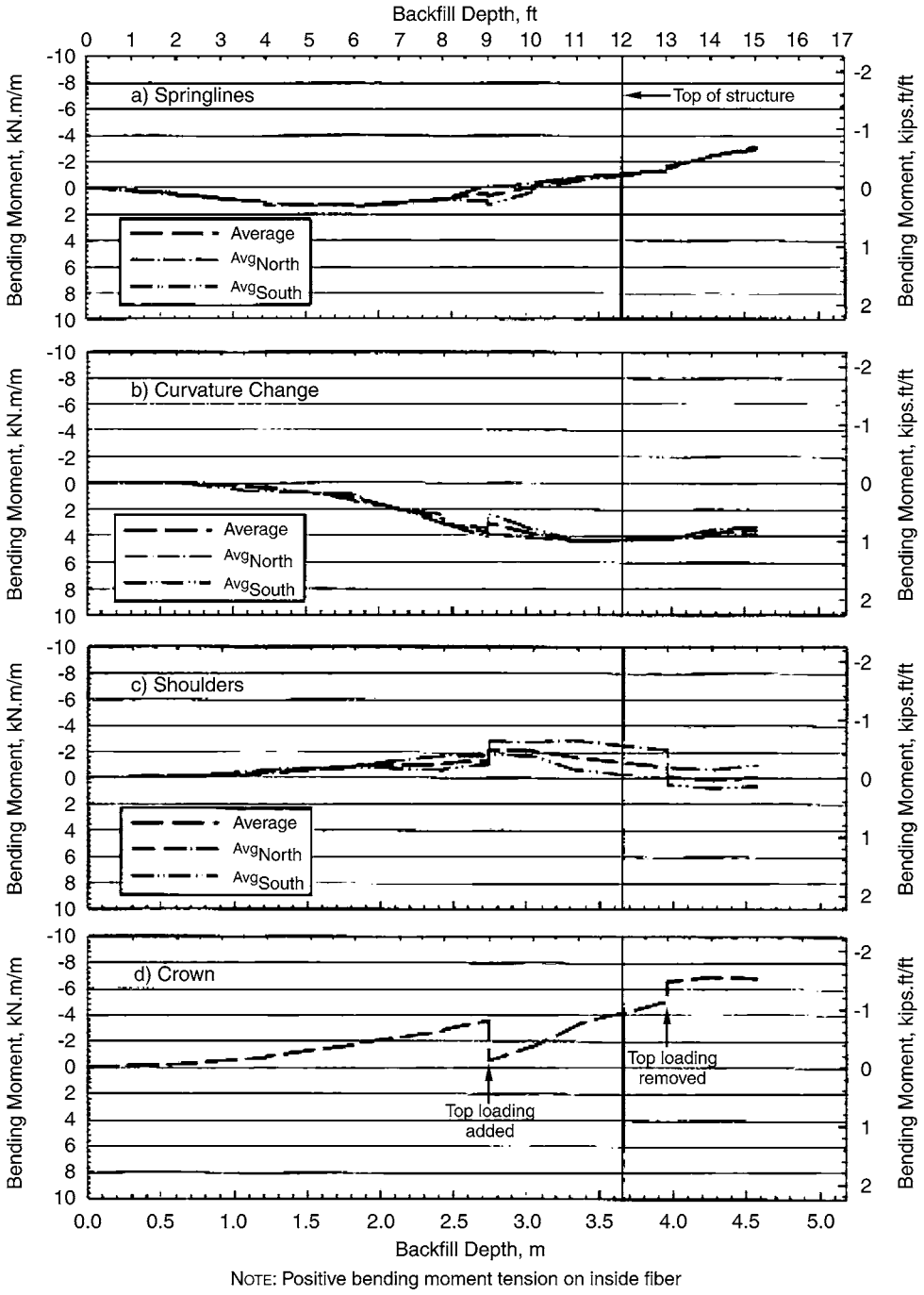

Figure B-16. Variation in bending moment during backfilling: Test 1.

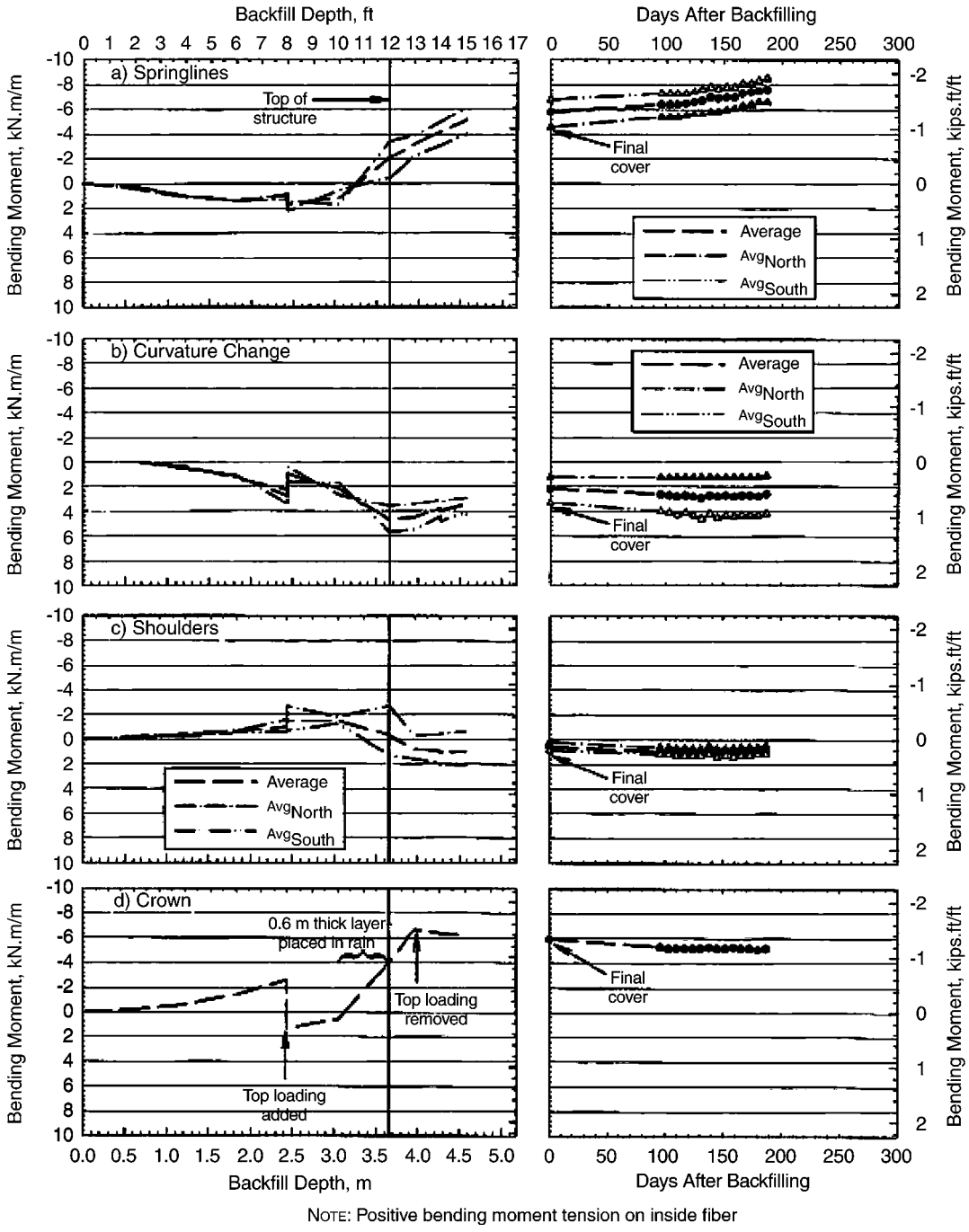

Figure B-17. Variation in bending moment during backfilling: Test 2.

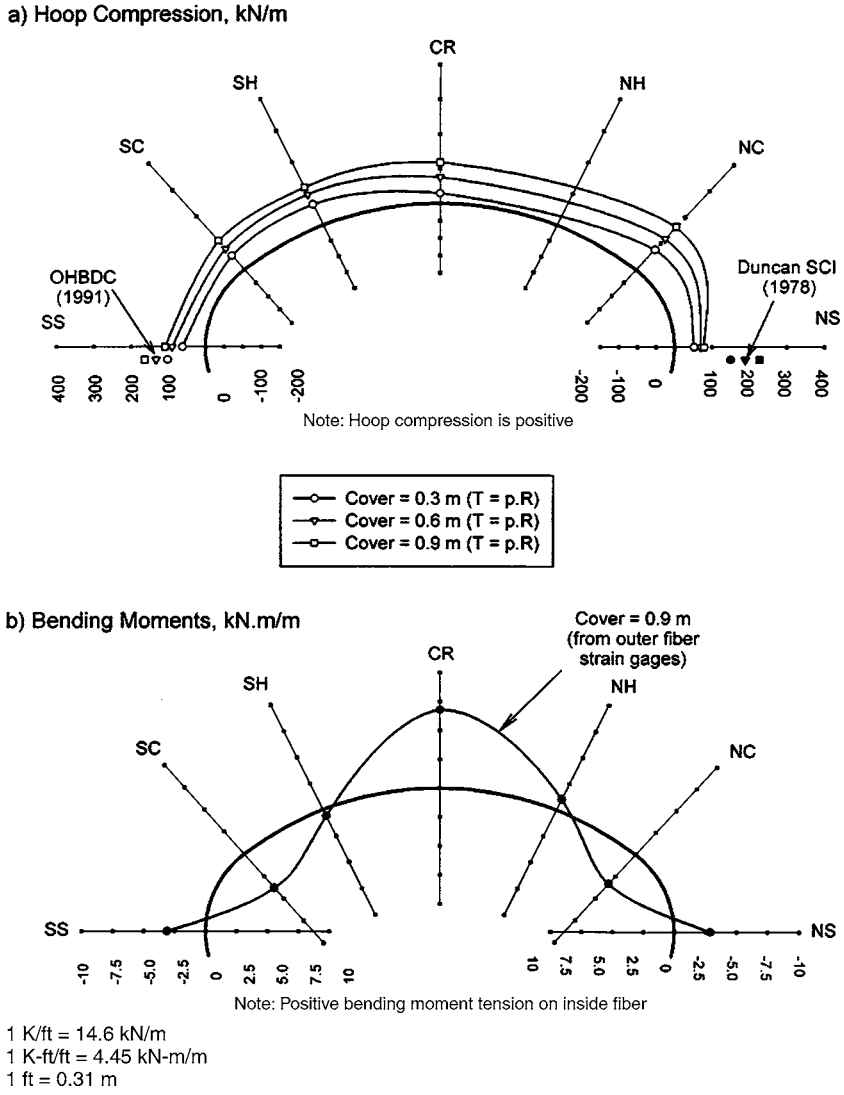

Figure B-18. Hoop compression and bending moment during backfilling: Test 1.

Because of concerns about the accuracy of the measurements, wall thrusts during live-load testing are not presented.

Long-Term Monitoring

After live-load testing was complete, the depth of fill over the crown was increased to 1.4 m (4.5 ft), and the culvert performance was monitored for about 9 months. The bending moments in the metal culvert continued to increase for the first 6 months (Webb et al. 1998). The total increase was about 2 kN-m/m (0.45 k-ft/ft). Small increases in moments also occurred at the curvature and shoulder locations.

Radial Pressures

The transverse and longitudinal locations of installed earth pressure cells around the metal and concrete culverts are shown in Figures B-23 and B-24, respectively. Sixteen earth pressure cells were installed around each culvert.

During Backfilling

Average interface radial pressures around the concrete culvert with increasing backfill depth are shown in Figure B-25 for both tests. The cells installed lower down on the culvert experienced the largest pressures. The biggest differences between the two tests are the much lower pressures at the curvatures for Test 2 compared with Test 1.

Average interface radial pressures around the metal culvert are shown in Figure B-26 for both tests. All cells for Test 2 developed higher pressures than those for Test 1. Final cover produced higher pressures than end of backfilling at 0.9 m (3 ft) of cover (Figure B-25b).

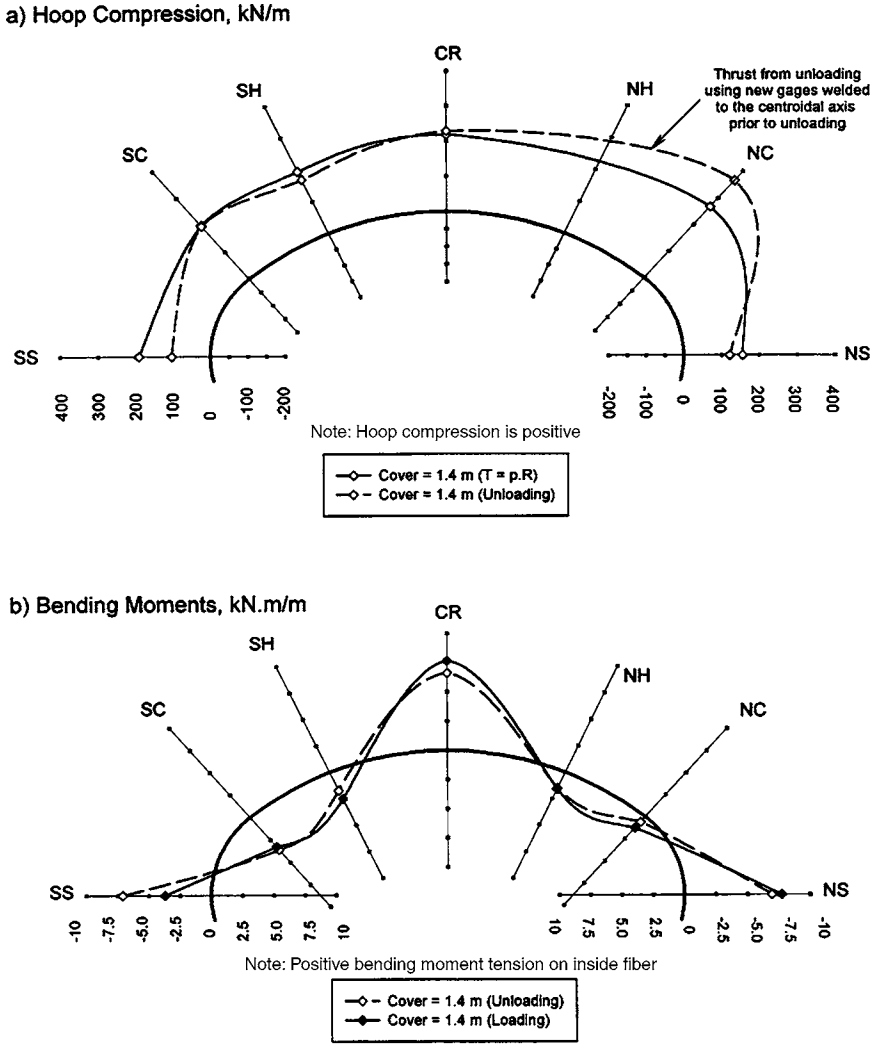

1 K/ft = 14.6 kN/m
1 K-ft/ft = 4.45 kN-m/m
1 ft = 0.31 m

Figure B-19. Hoop compression and bending moment during backfilling: Test 2.

During Live-Load Testing: Concrete Culvert

Changes in interface pressures around the concrete culvert due to different positions of the live-load vehicle are presented in Figure B-27 for 0.9 m (3 ft) of soil cover. See Figure B-3 for positions of vehicle relative to location of gauges. Measured pressures are presented in both a longitudinal direction (looking down the length of the structure) and a transverse direction (cross-sectional view of the structure with positions of the tandem axles of the live-load vehicle). The longitudinal plots of the figure (Figure B-3a to d) show the superimposed pressures from the two passes of the live-load vehicle—i.e., Pass 2 has been shifted to coincide with Pass 1 and, therefore, the centerline of the two rear wheel groups for both passes are located at axis positions 4.6 and 6.4 m (15 and 21 ft).

For all wheel positions and gauge locations, the peak pressures are never greater than about 50 kPa (7.3 psi), which is small relative to the tire inflation pressure of about 620 kPa (90 psi). The gauges located at the south top (ST) locations (Figure B-27a) show pressures with the tandem axles of the vehicle positioned over the south shoulder and crown locations. The pressures measured between the vehicle centerline and 0.3 m (3 ft) outside wheel positions 5.5 and 7.3 m (18 and 24 ft) are much less than those under the wheels because of longitudinal spreading. South top pressures for other vehicle positions were negligible.

Pressures at the crown (Figure B-27b) are largest for the tandem axles of the vehicle positioned over the crown. Next largest are those with the tandem axles of the vehicle positioned over the south springline because of the weight of the front

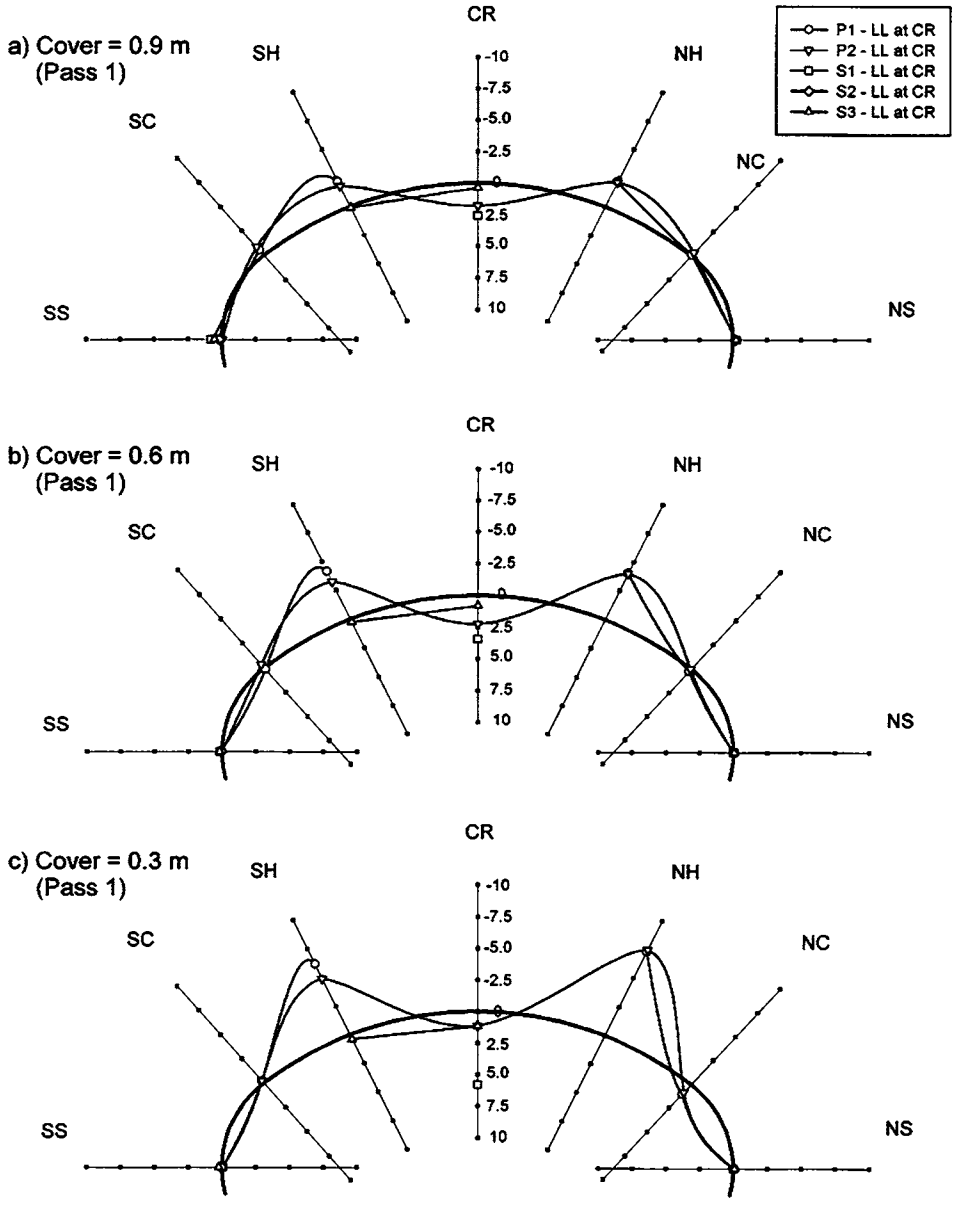

Note: Positive bending moment tension on inside fiber (Units of kN-m/m)

1 K/ft = 14.6 kN/m
1 K-ft/ft = 4.45 kN-m/m
1 ft = 0.31 m

Figure B-20. Live-load bending moments at crown: Test 1.

axle over the crown (see Figure B-3). Again, pressures drop substantially in the longitudinal direction when the gauges are not directly under the wheel groups. Crown pressures for other positions of the vehicle were negligible. Pressures at the shoulders are largest for the tandem axles of the vehicle positioned over the shoulder (Figure B-27c and d). Furthermore, the magnitudes of these pressures are less and the distribution is more uniform than at the crown and top locations because of the deeper soil cover above the gauges and thus more load attenuation and spreading. The greater angle of installation of the shoulder gauges than the crown and top gauges is also likely a factor in the pressure reduction. The live-load pressures at the curvature gauges have not been plotted.

The transverse plots of Figure B-27e to h present measured pressures of the gauges installed in the upper regions of the culvert (no curvature gauges are shown) of Stations P1 and P2 (Stations S2 and S3 are not shown) and for all positions of the live-load vehicle. At the crown gauge of Station P1 and Pass 1

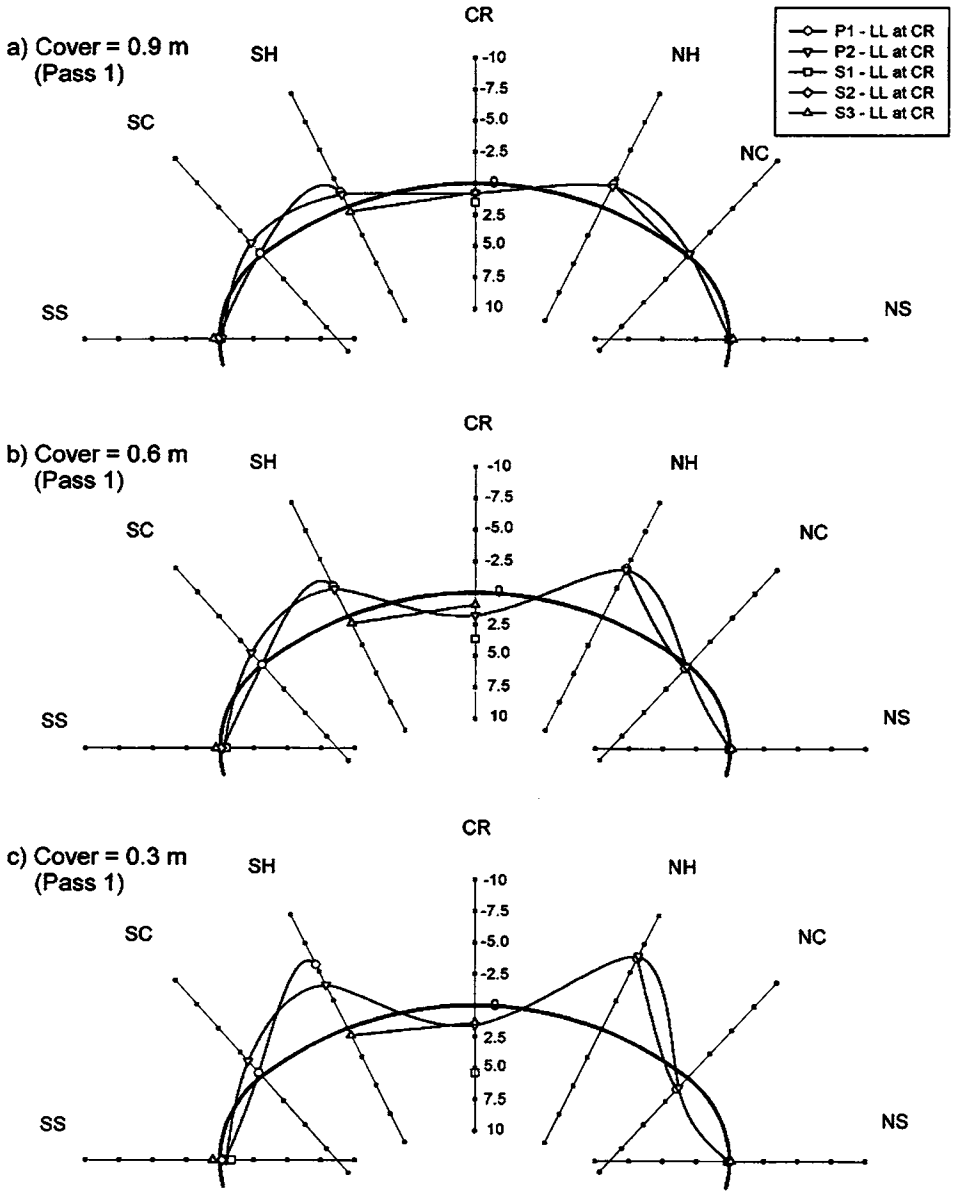

Note: Positive bending moment tension on inside fiber (Units of kN-m/m)

1 K/ft = 14.6 kN/m
1 K-ft/ft = 4.45 kN-m/m
1 ft = 0.31 m

Figure B-21. Live-load bending moments at crown: Test 2.

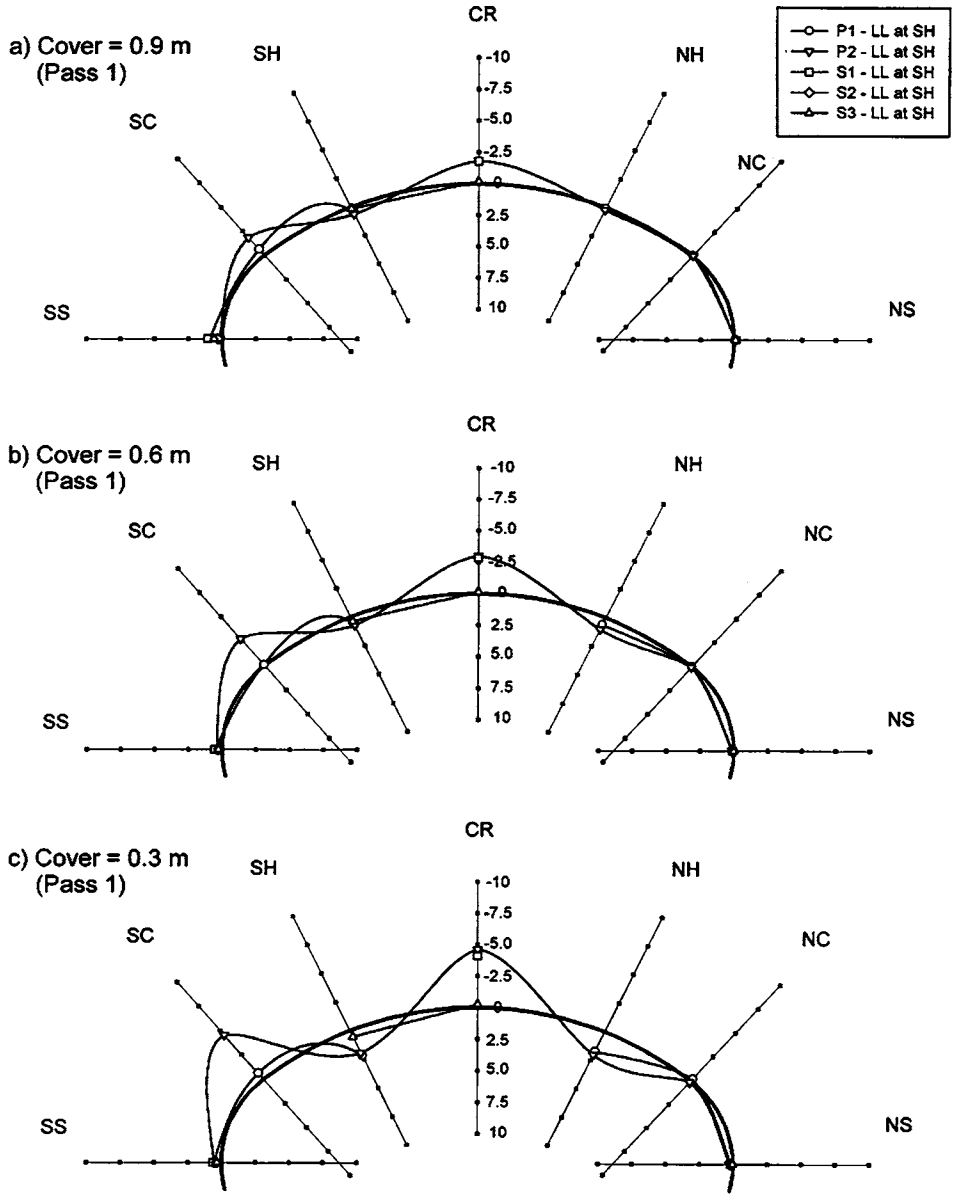

Note: Positive bending moment tension on inside fiber (Units of kN-m/m)

1 K/ft = 14.6 kN/m
1 K-ft/ft = 4.45 kN-m/m
1 ft = 0.31 m

Figure B-22. Live-load bending moments at crown: Test 1.

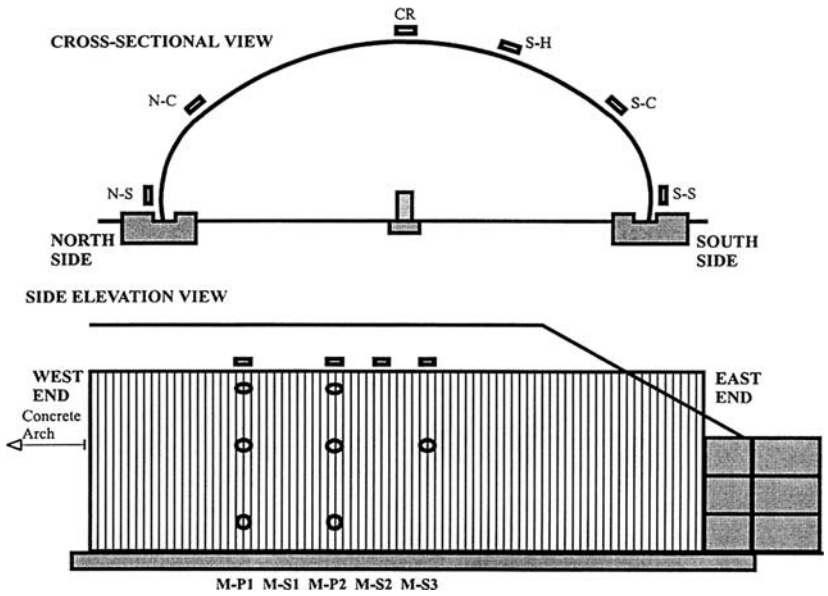

Figure B-23. Interface pressure cells for metal culvert.

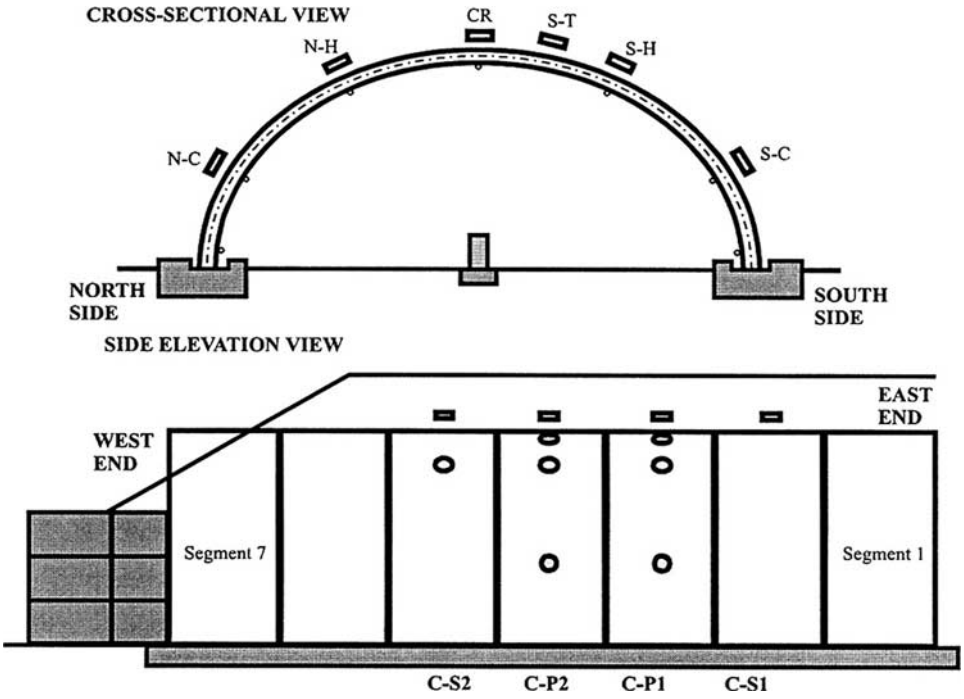

Figure B-24. Interface pressure cells for reinforced concrete culvert.

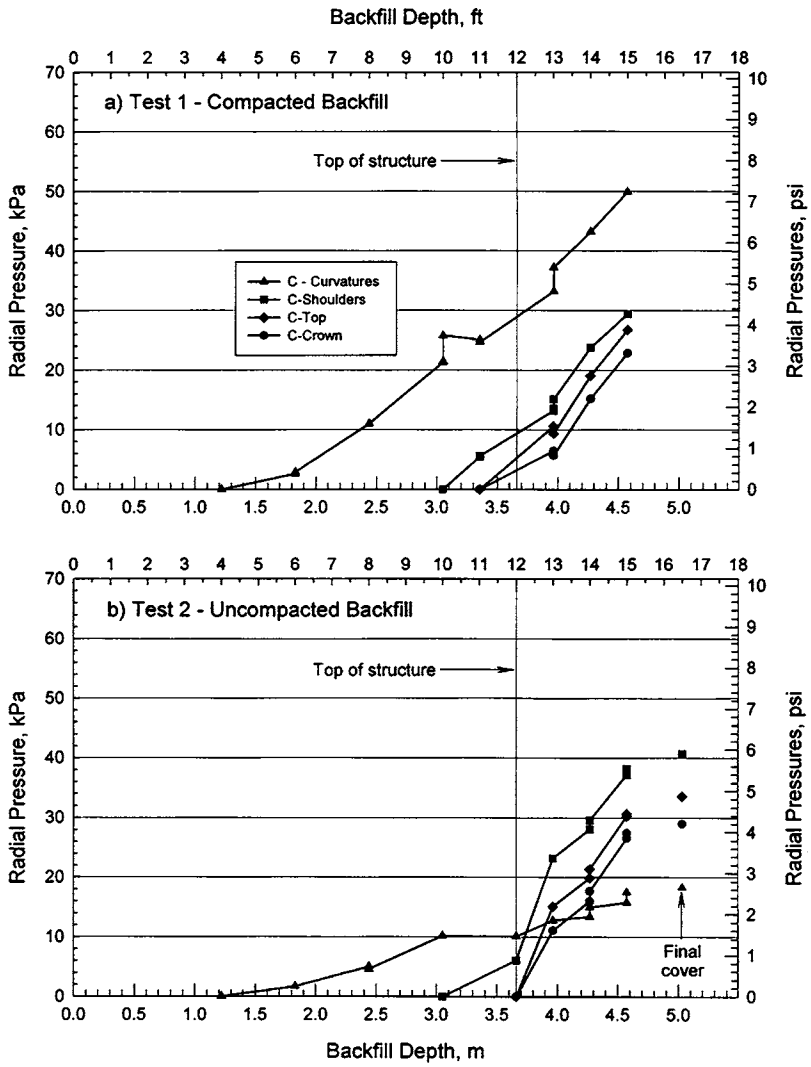

Figure B-25. Average radial pressures on concrete culvert during backfilling.

(Figure B-27e), the pressure increased when the tandem axles of the vehicle were positioned over the south springline (due to the weight of the front axle), then decreased when the tandem axles of the vehicle were positioned over the south shoulder, and then increased again considerably when the tandem axles of the vehicle were positioned over the crown, after which it dropped essentially to zero for other positions of the vehicle. A similar procedure can be followed for other gauges to explain the trends. Figure B-27e and f indicate good agreement between similar transverse gauge locations. Figure B-27g and h present almost a mirror image of Figure B-27e and f but with a reduced scale due to load spreading in the longitudinal direction.

Similarly, for 0.3 m (1 ft) of soil cover, pressures plotted in the longitudinal and transverse directions are presented in Figure B-28 [see Webb et al. (1998) for 0.6 m of cover and more discussion]. Comparison of Figure B-27a with Figure B-28a shows significantly increased pressures with decreasing soil cover. Figures B-27b and B-28b show that the crown pressures actually decrease with decreasing cover with the tandem axles of the vehicle positioned over the crown, because the rear wheels are straddling the crown and the effect of load spreading in the longitudinal direction diminishes with decreasing soil cover.

During Live-Load Testing: Metal Culvert

Changes in interface pressures around the metal culvert during live-load testing for different positions of the vehicle are presented in longitudinal format in Figure B-29 for 0.9 m (3 ft) of soil cover. Pressures measured at each gauge position after superimposing the two vehicle passes, as for the concrete culvert, are presented separately in the figure. The live-load vehicle wheel group positions are located at axis positions 3.4 and 5.2 m (11 and 17 ft) in Figure B-3.

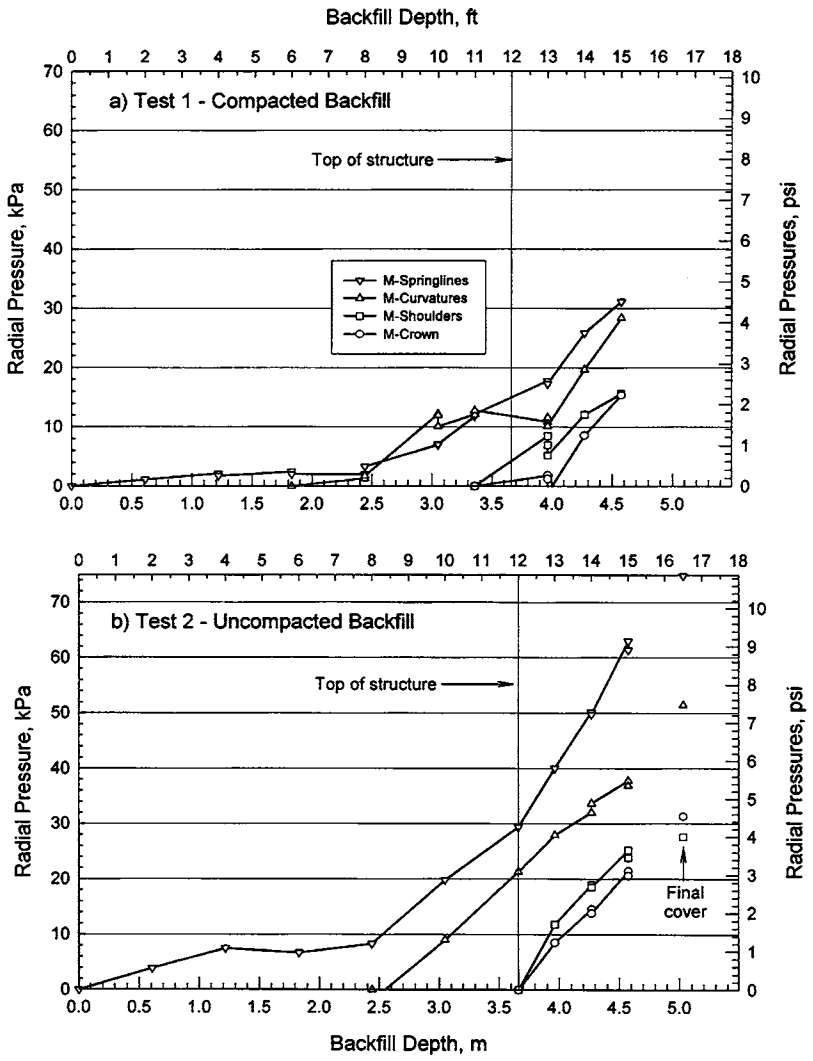

Figure B-26. Average radial pressures on metal culvert during backfilling.

Highest pressures at the south shoulders developed with the tandem axles of the vehicle positioned over the crown followed by the tandem axles of the vehicle positioned over the south shoulder (Figure B-29a). The pressure distributions in the longitudinal direction are fairly uniform and smaller in magnitude than those of the concrete culvert.

Highest pressures at the crown developed with the tandem axles of the vehicle positioned over the crown (Figure B-29b). The effect of the front axle on crown pressure can also be seen when the tandem axles of the vehicle are positioned over the south springline.

Pressures measured at the springlines are fairly uniform and similar for the two sides of the structure, with the highest pressures developing with the tandem axles of the vehicle positioned over the shoulder followed by the tandem axles positioned over the springline on each side (Figure B-29c and d). Pressures at the change in curvature were highest with the tandem axles of the vehicle positioned over the shoulder and crown locations (Figure B-29e and f). Radial pressures on the metal culvert during live-load testing at 0.3 m (1 ft) of cover are presented in Figure B-30 [see Webb et al. (1998) for more discussion and plots]. Measured trends appear to be similar to those at deeper soil cover, with the exception of higher springline pressures developing at reduced soil cover (Figure B-30c and d). As for the concrete structure, the effect of the rear wheels straddling the crown gauges is more significant at shallow cover because less load spreading occurs.

Relative Concrete Segment Movement

Nine gauges were installed on the concrete culvert between segments at the shoulder and crown locations to measure vertical movement between adjacent segments during the live-load tests. Three gauges were installed (one each at the crown and both shoulders) at the joint between Stations S1 and P1

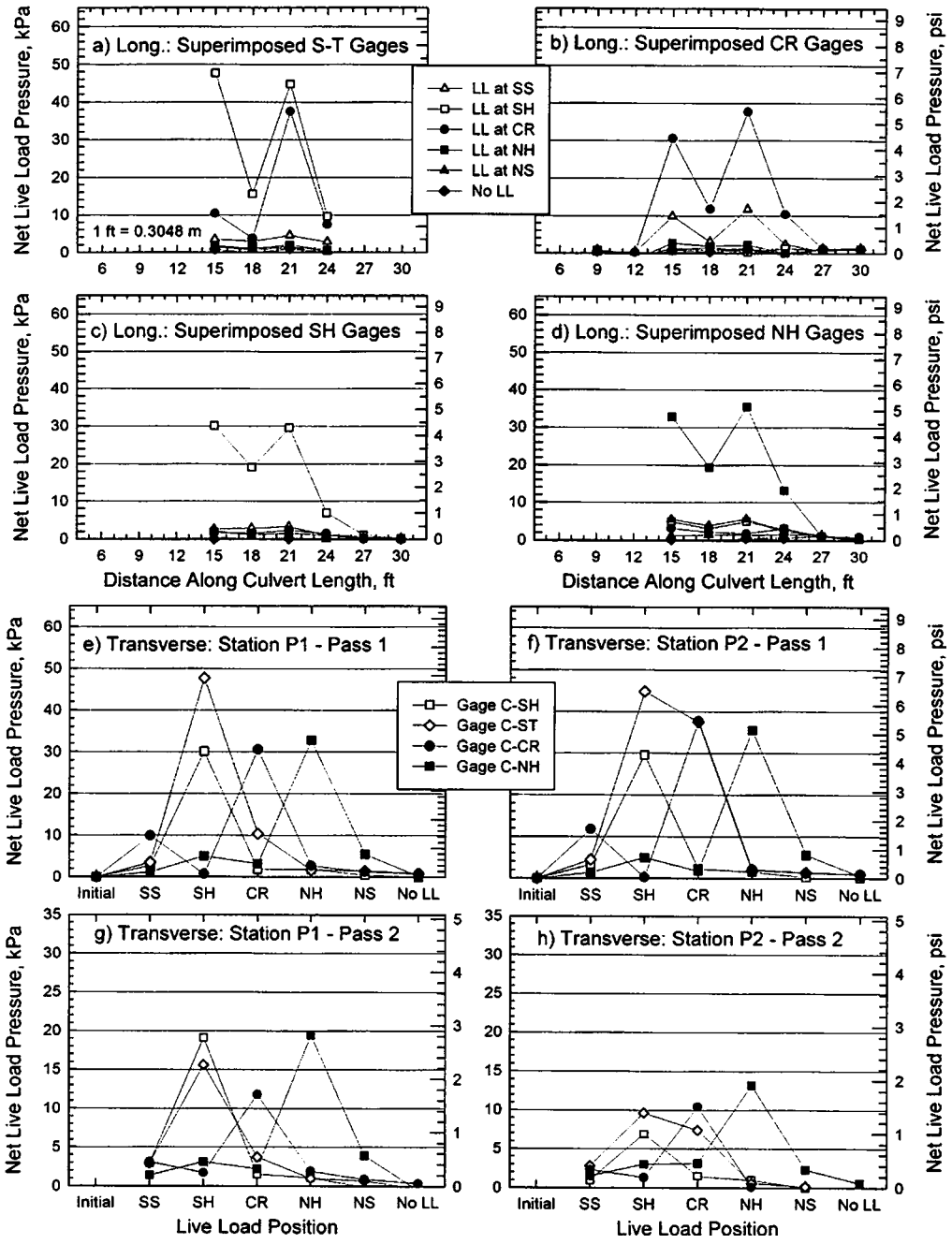

Figure B-27. Live-load pressures on concrete culvert at 0.9 m of soil: Test 1.

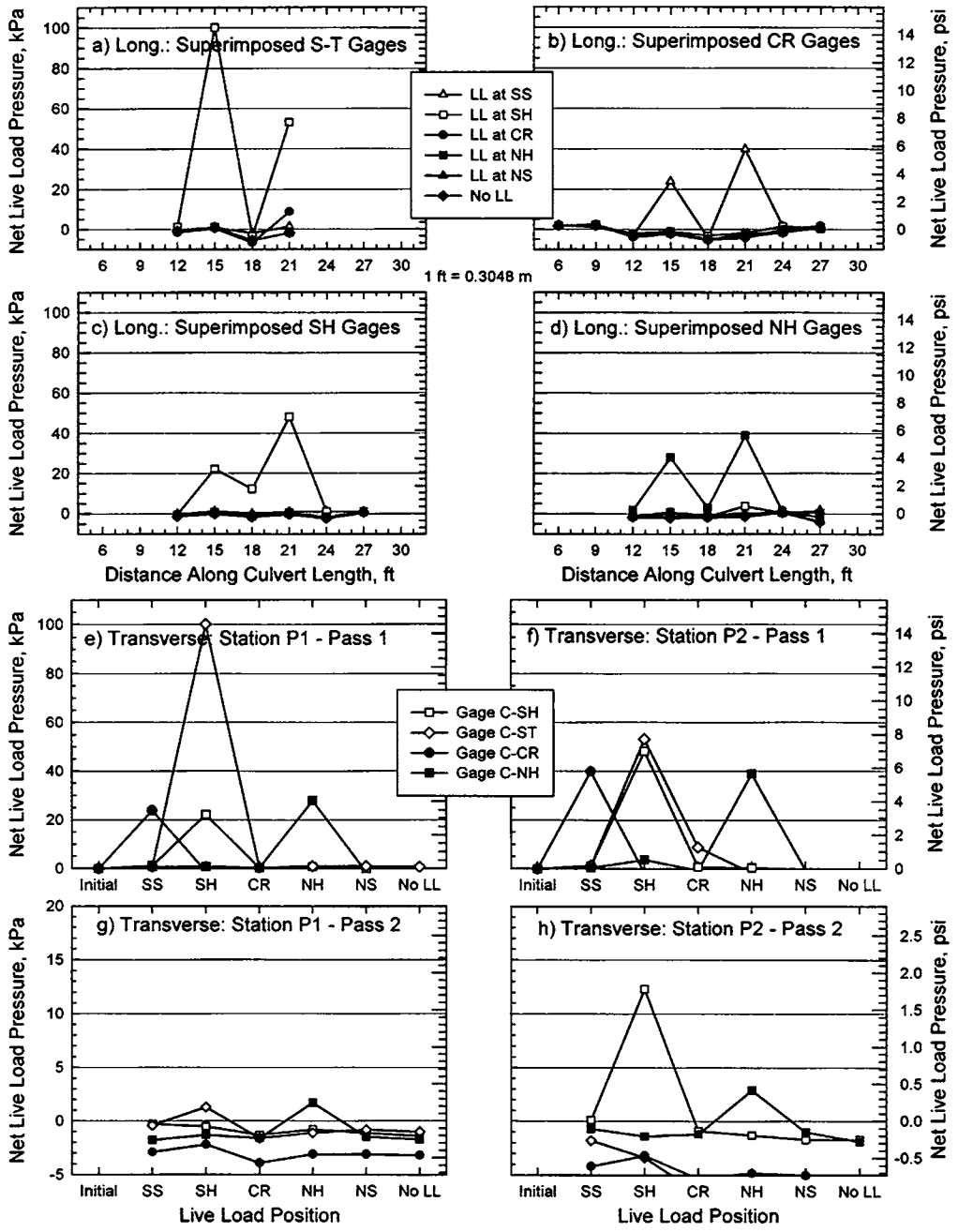

Figure B-28. Live-load pressures on concrete culvert at 0.3 m of soil: Test 1.

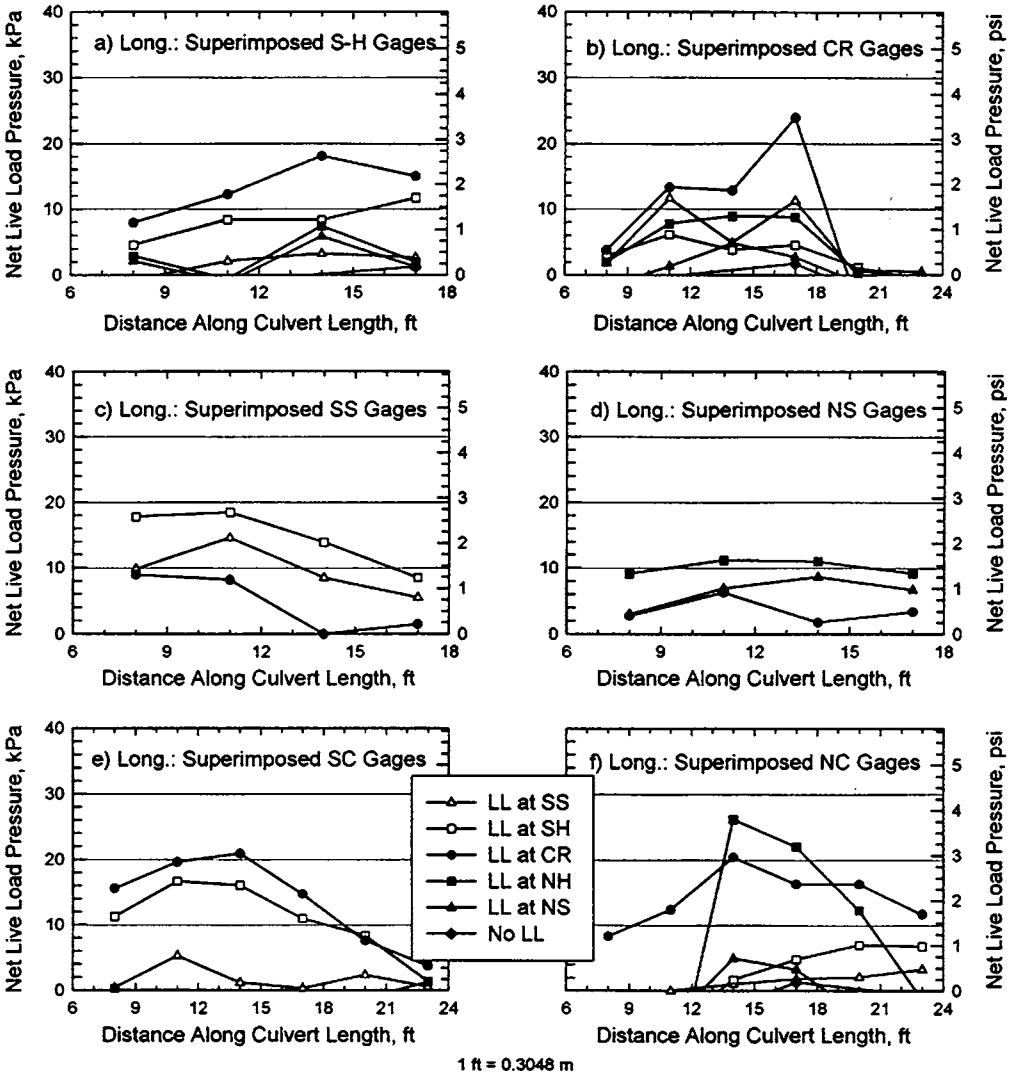

Figure B-29. Live-load pressures on metal culvert at 0.9 m of soil: Test 1.

(Segments 2 and 3). Two gauges were installed (one each at the south shoulder and crown) between Stations P1-P2, P2-S2, and S2-Segment 6. For Test 1, essentially zero relative movement occurred during backfilling, and a maximum movement of about 1.5 mm occurred during live-load testing at 0.3 m (1 ft) of soil cover at Stations S1-P1 and P2-S2 with the tandem axles of the vehicle positioned over the crown. Similarly, for Test 2, almost zero relative movement occurred during backfilling, but, during live-load testing, maximum relative movements of about 2 mm were measured at the crown with 0.3 m (1 ft) of soil cover and the tandem axles of the vehicle positioned over the crown.

Concrete Cracks

Development of new cracks and widening and lengthening of existing cracks on the concrete culvert were monitored during testing. Most of the cracks on the precast concrete segments developed before installation at the test site. These cracks were typically visible on the underside of the culvert near the crown, numbering between seven and nine per segment. Crack widths were measured after the culverts were backfilled and typically varied between 0.10 and 0.13 mm (0.004 and 0.005 in.). The maximum observed crack widths were 0.18–0.20 mm (0.007–0.008 in.) as reported by LaFave (1998).

During the first set of live-load tests, the maximum crack widths developed with the tandem axles of the live-load vehicle positioned over the culvert crown. Live-load testing at 0.3 m (1 ft) of soil cover for this position of the live-load vehicle produced average crack widths of 0.18–0.20 mm (0.007–0.008 in.), with maximum crack widths of 0.25–0.28 mm (0.010–0.011 in.). After the culverts were uncovered, the concrete segments were inspected, and no new cracks had developed on the outside surface of the segments.

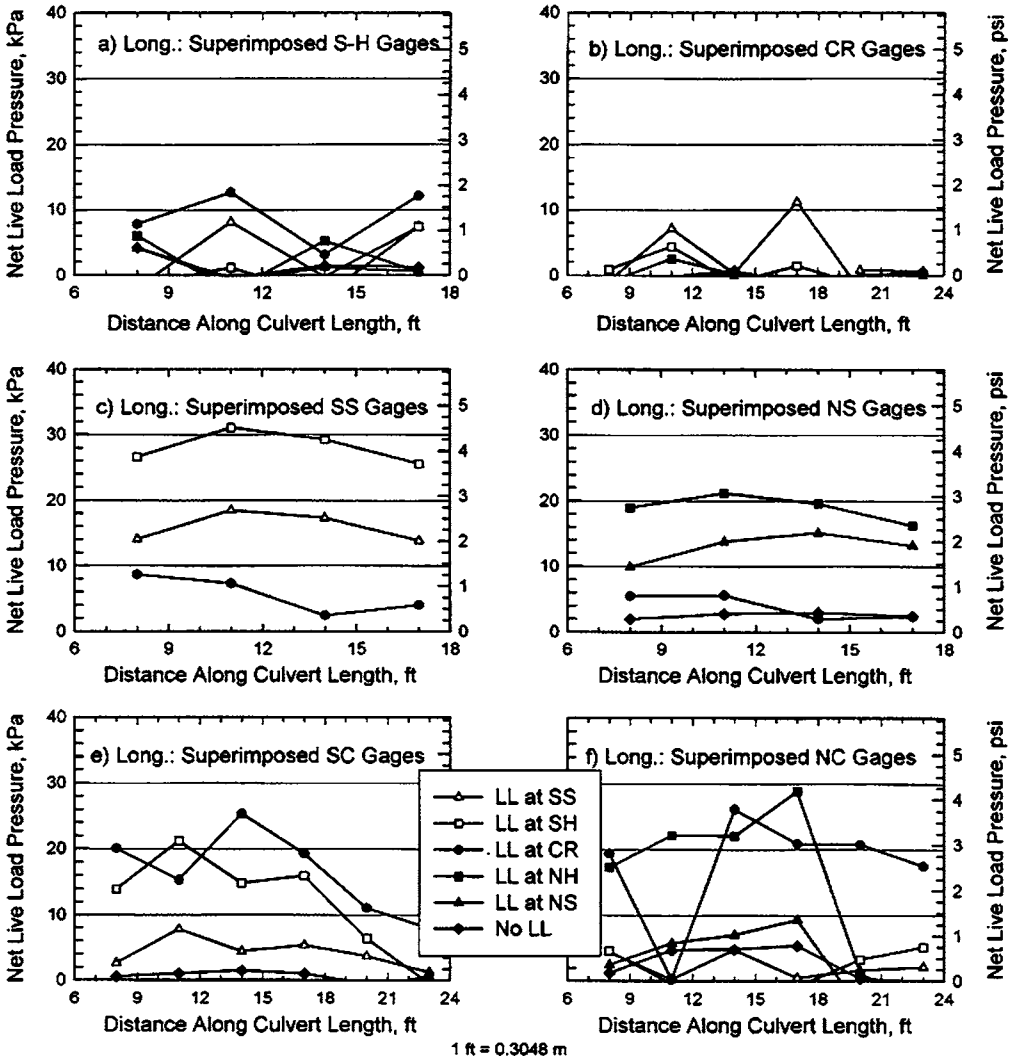

Figure B-30. Live-load pressures on metal culvert at 0.3 m of soil: Test 1.

During the second set of live-load tests, a couple of new cracks developed on the underside of some concrete segments at 0.6 and 0.3 m (2 and 1 ft) of soil cover; however, average and maximum crack widths were similar to those of Test 1.

Additional concrete culvert measurements, including thrusts and moments computed from measured surface and embedded strain gauges, are given by LaFave (1998).

Foundation Movements

The culvert foundations were instrumented to monitor rotations and settlements at various locations along the length on each side of the structure. No rotations of the foundations occurred for either test. Settlements were uniform along the length of each structure and the same for both footings. For Test 1, the footings settled 4–4.5 mm measured at the end of backfilling with virtually no change during live-load testing. About 1–1.5 mm (0.06 in.) of rebound occurred after the structures were uncovered to begin Test 2. Test 2 then produced about 2 mm of additional settlement due to the earth load; once again, there was no change due to live loads.

Backfill Displacement

Six soil extensometers were installed in the backfill soil to measure displacement of the structural backfill during backfilling and live-load testing. Four of these extensometers were installed at the springline elevation on both sides of the metal culvert, and the other two were installed at the change of curvature on both sides. Gauges at the springlines showed inward movement of the sides of the metal structure until about 2.4 m (8 ft) of backfill was placed, at which point outward movement occurred at a reduced rate. More outward movement of

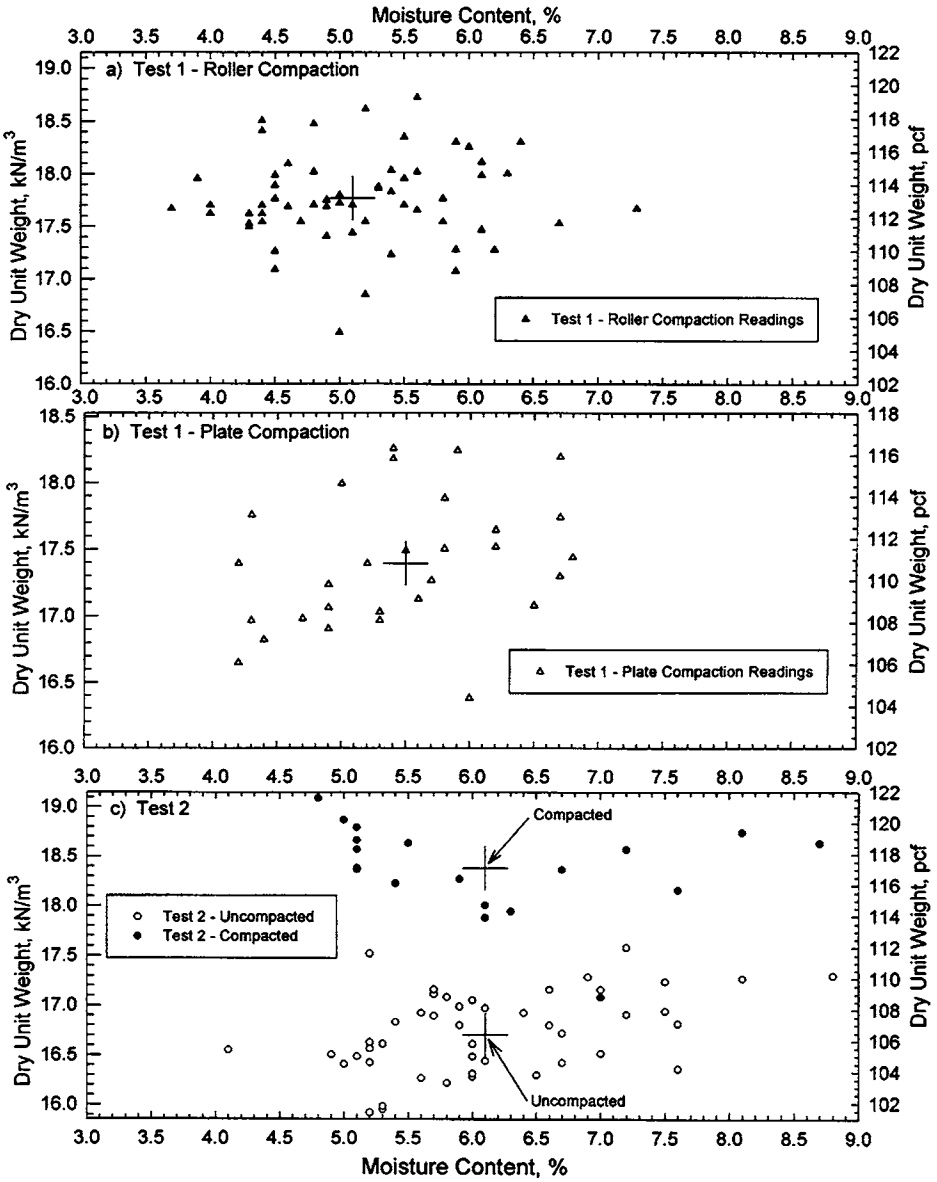

Figure B-31. Dry unit weight and moisture content of backfill.

the sides of the structure occurred in Test 2 than in Test 1 because of the less stiff backfill material for the second test. The trends higher up on the structure at the curvature elevation were less evident. Structural backfill displacements during live-load testing are summarized by Webb et al. (1998).

Backfill Compaction

Dry unit weight and moisture content of the backfill soil as measured with the nuclear density gauge are plotted in Figure B-31 for both tests and different compaction techniques. The average dry unit weight and moisture content for each test and each compaction technique are also shown in the figure. The compacted densities shown in Figure B-31 for Test 2 were measured in the compacted soil cover. The compacted density for Test 1 backfill ranged from about 17.2 to 18.5 kN/m^3 (90–95 percent standard Proctor). The average uncompacted and compacted densities of Test 2 backfill were about 16.7 and 18.4 kN/m^3 (87 and 96 percent standard Proctor), respectively. On average, the roller compactor produced higher soil unit weight than the vibratory plate compactor, which in turn produced higher soil unit weight than backfill placed without compaction during Test 2.

APPENDIX C

COMPUTER MODELING OF FIELD TESTS

CONTENTS

INTRODUCTION

This Appendix presents the results of finite element analyses conducted before and after testing of the large-span metal and reinforced concrete arch culverts (Appendix B). Both two-dimensional and three-dimensional finite element procedures are used to estimate culvert response. A new soil-plasticity-based procedure to model the effect of compaction during construction is described.

A number of two-dimensional finite element procedures were developed in the 1970s (Kay and Abel 1976, Katona 1978, Duncan 1979) to evaluate structural response, and they were substantial improvements over the semi-empirical culvert design tools they replaced (Marston and Anderson 1913, Spangler 1956). These finite element procedures used linear and nonlinear elastic soil models and were capable of modeling the construction process and two-dimensional vehicle loads (ones that were uniform in the direction of the culvert axis) under working loads. Although the procedures have been used successfully to develop culvert design procedures [e.g., by Duncan (1979) and Moore (1988)], they have two significant limitations. First, earth-load analysis has been affected by problems in assessing the impact of soil compaction on culvert response, and the nonlinear elastic soil models are unable to correctly predict soil response after shear failure. Second, live-load modeling has been constrained by the approximations used to convert three-dimensional loads to equivalent "line" loads (approximations typically based on applications of Boussinesq or trapezoidal stress distribution theories).

This study explores the ability of two different finite element procedures to predict culvert behavior. First, analysis is conducted with elastic-plastic soil models (Moore 1985, El Sawy et al. 1997), which should better predict culvert response beyond "working" loads when significant zones of backfill soil have experienced shear failure. Second, passage of vehicles (live load) over long-span metal and concrete culverts induces a three-dimensional structural response, and the performance of the three-dimensional finite element procedure of Moore and Brachman (1994) is assessed.

Use of computer analyses during the culvert design process requires confirmation that successful analysis is not conditional on knowing the culvert response to be predicted. Therefore, the study includes an assessment of the ability of the finite element analysis to predict culvert response in advance (instead of after the test results are known, when parameter fitting might be used to "best fit" analysis to measured values). "Class A" predictions were documented before the field tests (Moore et al. 1997). These predictions are included in comparisons of calculated values with field measurements.

The finite element procedures are reviewed, the test structures are defined, and the soil parameters are discussed. Calculations for the corrugated metal culvert response to earth load and live load are presented, including those made before the field tests were conducted. Comparisons are made with measurements of culvert deflection and bending moment as

well as earth pressure. A new procedure to model the influence of compaction on the culvert is used in the earth-load calculations. The relative performance of two-dimensional and three-dimensional live-load predictions is then investigated. The section on metal culvert analysis then concludes with specific recommendations about the two methods of analysis to be used in parametric studies for culvert response to earth and live load reported in Appendix D.

Results for the concrete arch test culvert are then presented. Calculated values of earth pressures around the culvert are compared with measured values. The implications of the performance of the computer analyses are discussed in relation to the parametric study reported in Appendix D.

GEOMETRY AND LOAD HISTORY FOR TEST CULVERTS

Figure C-1 shows a cross section of the metal culvert and the principal dimensions. Details for the 9.1-m (30-ft) span reinforced concrete arch culvert with 3.5-m (11.5-ft) rise were similar and are presented in Appendix B. The test structures were placed end to end in a trench and backfilled to depths of 0.3 m (1 ft), 0.6 m (2 ft), 0.9 m (3 ft), and finally 1.2 m (4 ft). Appendix B provides full details of the field testing.

Some of the key steps in the construction and testing sequence are as follows:

- The structures were erected on reinforced-concrete footings.
- Granular backfill was placed in 0.6-m (2-ft) lifts, with the level of backfill soil on one side of the structure never placed more than 0.3 m (1 ft) above the opposite side.
- Two tests were planned and executed, one with well-compacted backfill and the other with backfill placed loosely around the structure. The first field test featured backfill soil with a density of 92 percent of maximum standard Proctor. The second test had soil densification limited to the effect of the machine used to spread the material, and a density of 87 percent resulted. However, the top layer of soil for this second test was compacted to a density of 96 percent so that the loaded test vehicle could be successfully driven across the structure.

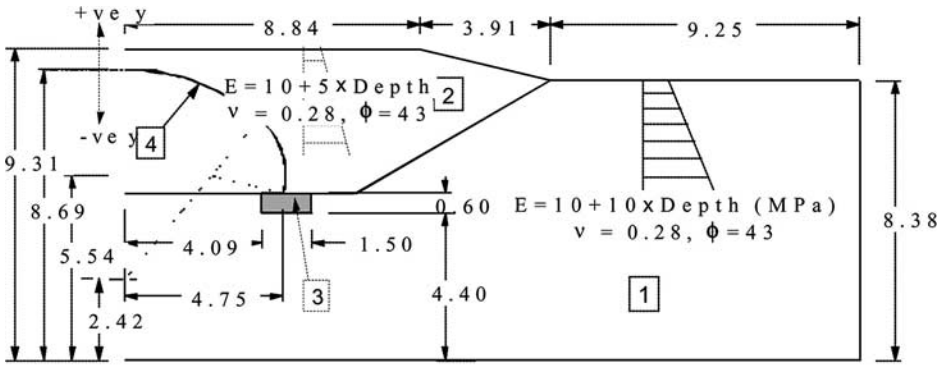

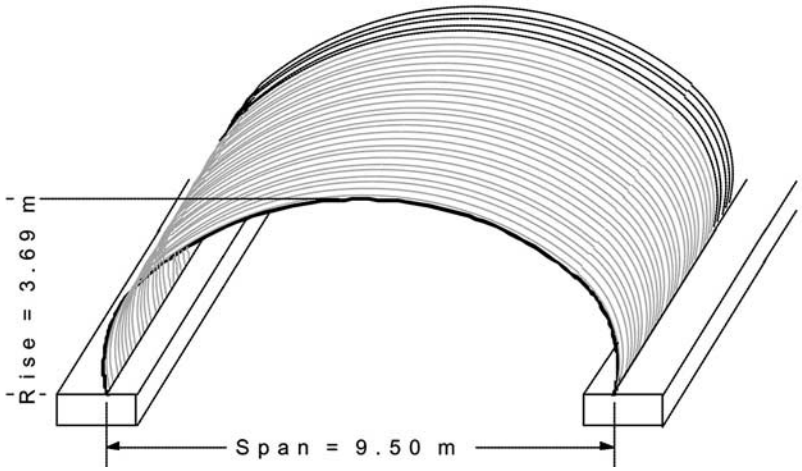

Figure C-1. Geometry of low-profile metal arch culvert.

- The structure was instrumented with strain gauges at crown, shoulders, and springlines. Gauges were placed on the inside and outside surfaces of the corrugated plate. Additional gauges were added at the neutral axis of the plate, toward the end of the test program. Strains are in the elastic range of the steel plate, which permits bending moment and thrust to be inferred (see Appendix B).
- Various techniques were used to monitor the metal culvert deformations, leading to measurements of crown, shoulder, and springline movement throughout the construction sequence. Some more general profiles were also recorded, giving a more complete picture of structural deformations around the arch culvert.
- The reinforced concrete structure was instrumented with strain gauges at the shoulders to measure stress resultants. These measurements were reported and analyzed by LaFave (1998) to provide estimates of thrust and bending moment.
- Appendix B shows the circumferential location of each of the earth pressure cells used to monitor soil stresses during backfilling and under the influence of vehicle live load:
  – SC: midway between the south footing and the shoulder of the culvert,
  – SH: the south shoulder of the culvert,
  – ST: midway between the shoulder and crown on the south side of the structure,
  – CR: at the crown of the structure,
  – NT: midway between the shoulder and crown on the north side of the structure,
  – NH: the north shoulder of the culvert, and
  – NC: midway between the north footing and the shoulder of the culvert.
- During the field test, the metal culvert experienced significant upward movement during placement of sidefill. To limit this phenomenon, blocks of concrete were added on the top of this culvert when the backfill material was at a height of 2.4 m (7.9 ft) and 2.7 m (9.9 ft) for the tests with densities of 87 and 92 percent, respectively.
- A three-axle test vehicle of total weight 370 kN (83,200 lb) was used in the tests. Specific axle weights are given in Appendix B. Measurements were made for culvert at burial depths of 0.3 m (1 ft), 0.6 m (2 ft), and 0.9 m (3 ft). Further measurements were made at burial depths of 1.2 m (4 ft) and 0.6 m (2 ft) after placement of additional gauges to better interpret metal culvert thrusts. During each pass of the test vehicle, it was located at a number of different lateral positions:
  – SS: the midpoint between the two rear axles placed over the springline on the south side of the structure,
  – SC: the midpoint between the two rear axles placed midway between springline and crown on the south side of the structure, and
  – CR: the midpoint between the two rear axles placed directly over the crown of the structure.
- Tests were also conducted with the test vehicle positioned on the north side of the test culvert. These are not included in this document, because measurements and analysis of culvert response with vehicle at SS, SC, and CR are considered sufficient for this evaluation of prediction quality.

METHODS OF ANALYSIS

Two-Dimensional Earth-Load Analysis

The finite element procedure AFENA (modified from Carter 1992) used to undertake the two-dimensional finite element analysis of culvert response to earth load has the following features (Figure C-2):

1. Elastic-plastic soil models were used to characterize soil response before and after shear failure:

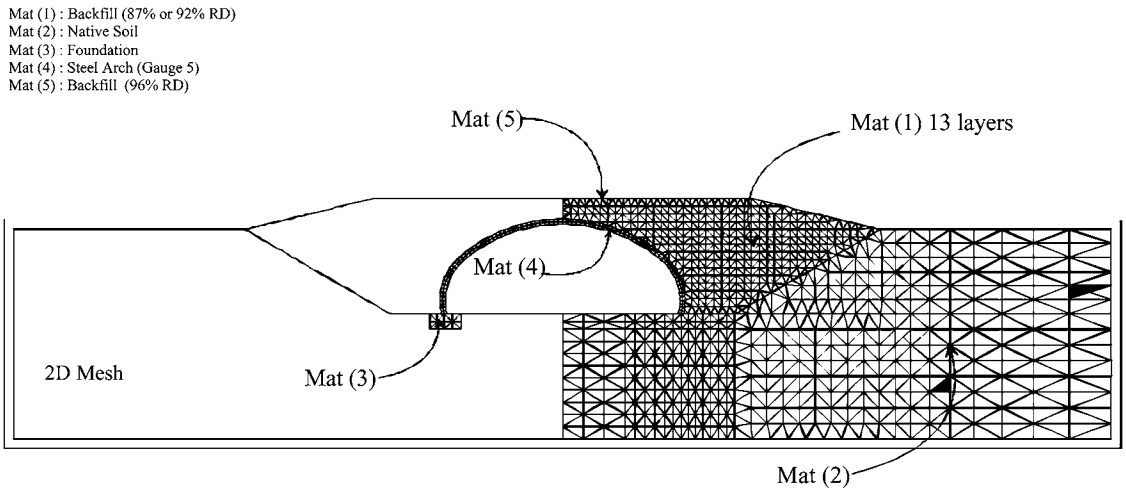

Figure C-2. Two-dimensional finite element mesh: metal culvert.

- Shear strength is modeled by using the Mohr-Coulomb failure criterion with friction angle ϕ' and cohesion c'; results were obtained assuming an associated flow rule (dilation angle equal to friction angle).
- A linear variation of elastic soil modulus with depth is modeled within any given soil zone; modulus is set equal to $E_0 + mz$, where E_0 is the surface value and m is the gradient with depth z.
- Unit weight γ_s is modeled as uniform with depth within each soil material.
- Pore water pressures are assumed to be zero.
- Culvert construction is modeled to simulate the progressive placement of 15 layers of backfill soil.
- Top loading of the culvert during construction was numerically simulated by applying, and later removing, forces to the top of the culvert (this was modeled in the post-test analyses only).
- Increases in soil stiffness were modeled through changes to the reference position of the linearly varying backfill modulus (it was kept at the top surface of the backfill material at each specific stage).

Triaxial test results from Sussmann at UMass were used to estimate elastic soil properties and shear strength for the soil materials. Her four modulus measurements were fitted to the stress-dependent modulus function of Janbu (1963), using Janbu parameter values for typical backfill materials described by Selig (1990). A geostatic stress condition was then used to infer modulus variations with depth. Finally, those modulus profiles were approximated as linear modulus functions.

$$E(z) = E_0 + mz \qquad \text{(C-1)}$$

Two density conditions were initially envisaged for the field tests, 85 and 95 percent density, corresponding to uncompacted and well-compacted backfill soils. Actual field construction resulted in the uncompacted backfill used in the second test having a density of 87 percent, whereas the compacted soil in the first test had a density of 92 percent. The layer of soil at the ground surface in Test 2 was compacted to a density of 96 percent.

Parameters estimated for each of the soil density conditions are presented in Table C-1. Values used in the Class A (i.e., pretest) predictions are shown, as are values revised for the actual field densities. Revisions included unit weights actually measured in the field as well as a slight reduction in Poisson's ratio. The strength and stiffness parameters increase monotonically with density, with the exception of the surface layer properties for the 96-percent density soil. These have parameters reduced somewhat so they better represent strength and stiffness close to the ground surface instead of at greater depths. Values for the native soil at the test site are also shown. This was the same granular soil as that used to backfill the structure for a density estimated as 95 percent.

2. The structural elements used to characterize the corrugated steel plate are those of Bathe and Bolourchi (1980):

   - The structural element represents the corrugated plate as a series of rectangular layers of given width and thickness. Table C-2 presents details of the layer geometry for the 5.5-mm (0.213-in.) thick, 250 × 50 mm (6 × 2 in.) corrugated plate.
   - The structural element models the progressive development of yield through the corrugated metal plate.
   - Parameters used to characterize the material were elastic modulus E of 200 GPa, Poisson's ratio n of 0.2, yield modulus σ_y of 233 MPa, and post-yield modulus E_h of 2 GPa.

The behavior of flexible buried structures can be significantly influenced by the stresses and deformations produced during soil compaction. Various approaches to modeling compaction have been adopted in the past. Katona (1978) proposed a model in which layers of material placed during the analysis were loaded and then unloaded by artificial surcharge pressures. This can induce some of the global effects of compaction on flexible metal culverts, such as peaking during placement of the sidefill, but the procedure relies on an empirical evaluation of the surcharge pressures and is unable to produce correct results for rigid culverts. Seed and Duncan (1983) developed a complex semi-empirical procedure to incorporate the stress path associated with soil compaction within their nonlinear elastic soil model. This proce-

TABLE C-1 Parameters used to model the backfill and native soils

		Percent of Maximum Standard Proctor						
		85%	87%	92%	95%	96%		
Parameters	Native Soil	Loose Class A Material	Loose Material (Test 2)	Dense Material (Test 1)	Dense Class A Material	Surface Material (Test 2)	Concrete Culvert Class A	Concrete Culvert Post-Test
E_o MPa	20.0	6.7	8.0	14.3	20.0	17.0	3×10^4	2.7×10^4
m MPa/m	3.8	0.4	1.1	2.4	3.8	3.5	N/A	N/A
ν	0.28	0.3	0.28	0.28	0.3	0.28	0.2[1]	0.17[1]
c' kPa	0.0	0.0	0.0	0.0	0.0	0.0	N/A	N/A
ϕ'	43.0	34.0	34.5	38.5	43.0	41.5	N/A	N/A
γ kN/cu m	20.0	20.0	17.5	18.5	20.0	19.3	N/A	N/A

1. Poisson's ratio of zero is used in all three-dimensional analysis of the concrete culvert
2. 1 MPa = 145 psi; 1 MPa/m = 3.7 psi/in.; 1 kPa = 0.14 psi; 1 kN/cu m = 6.37 lb/cu ft

TABLE C-2 Geometry of the multilayer plate model

Element	Width (mm/m)	Depth (mm)
1	160.3	8.2
2	104.0	39.9
3	160.3	8.2

1 mm = 0.039 in.; 1 mm/m = 0.001 in./in.

dure, however, has proved difficult to apply and cannot be used for elastic-plastic soil models.

It is unreasonable to expect accurate simulation of compaction effects, because they involve the vagaries of the construction environment. A reasonable objective, however, is to seek a procedure that gives bounds to the effects of construction. Such a procedure is proposed here. A brief description is provided; further details are given by Taleb (2000).

Figure C-3a shows the cross section of an elliptical culvert during the construction process, where placement of one specific layer of soil is taking place on the right-hand side of the structure.

One limit to behavior is where the effects of compaction on the culvert are assumed to be zero. This corresponds to soil placement with stresses and strains resulting from no other action but the self-weight of the newly placed soil.

The other limit can be ascertained if the maximum possible effect of compaction loads on the newly placed soil layer is estimated. Compaction of soil during construction of an embankment generates residual horizontal earth pressures once the compaction process is completed. For compaction of sidefill adjacent to a culvert, this compaction will induce one of the following:

- Increased horizontal pressures if the culvert is rigid and the newly placed soil is constrained against all horizontal deformation;
- Tensile horizontal strains if the side of the culvert is free to displace away from the new soil layer; or
- Some degree of additional horizontal stress and tensile horizontal strain if the culvert provides partial restraint against lateral movement.

The procedure adopted here is to impose additional horizontal stresses within the newly placed soil layer, like those induced by compaction on soil with full lateral constraint (Figure C-3b). The finite element procedure then enforces total equilibrium, considering the stiffness of the soil-structure system. This leads to release of all or part of these horizontal stresses, depending on the stiffness of the soil envelope and the side of the culvert at that location. Rigid culverts will experience little deformation, and the additional lateral pressures will remain in the soil and will change the thrusts and moments in the structure (Figure C-3c). Flexible metal culverts will deform laterally to release most of the imposed stresses. Therefore, the deformations often seen in the field when sidefill is compacted adjacent to a flexible metal culvert result (Figure C-3d). Bending moments are also affected. Thrusts do not change significantly, because the additional earth pressures have been released.

The state of passive earth pressure corresponds to soil with fully mobilized shear strength and represents the largest values of horizontal stress that can be induced during compaction. Therefore, these passive earth pressures are used to provide the "upper bound" compaction prediction.

Three-Dimensional Live-Load Analysis

The finite element procedure of Moore and Brachman (1994) was used to assess the impact of vehicle live loads. This semi-analytic procedure is based on the use of a two-dimensional finite element mesh and Fourier integrals to treat the variations in load and response in the axial direction. This approach leads to a harmonic decomposition in the axial direction and is computationally efficient compared with conventional three-dimensional formulations. However, the method is based on the principle of superposition and requires linear material behavior. Furthermore, the Fourier integrals imply modeling of the culvert as infinitely long.

The original formulation of Moore and Brachman (1994) has been modified to incorporate orthotropic shell elements. These are based on the harmonic axi-symmetric shell elements of Rotter and Jumikis (1988) but have been modified in two ways. First, the harmonic formulation was redeveloped within a Cartesian coordinate system, permitting use in problems with prismatic geometry, like the metal culvert. Second, the harmonic formulation was adapted for use in Fourier integral analysis rather than Fourier series analysis. This permits consideration of just one set of applied loads in the axial direction of the culvert (i.e., one truck) instead of periodic loading, like that required when Fourier series are used.

The equations used to determine the orthotropic properties of the corrugated metal plate are presented with the material parameters in Table C-3, based on the work of Ansourian (1981). The reinforced concrete structure was modeled with uniform thickness of 250 mm (10 in.) and modulus chosen to represent the combined effect of steel and concrete. The analysis cannot explicitly model the effect of the separate segments of the precast concrete arch structure. This assumption of continuity and full transfer of thrust and moment between segments is an important issue discussed later in this appendix.

The three-dimensional analysis features explicit modeling of the wheel loads of the test truck. All analyses had the forces applied by the wheels at the end of each axle distributed over a 0.65×0.3 m (2.1×1 ft) area. The axle length between wheel loads is 0.9 m (3 ft).

TWO-DIMENSIONAL FINITE ELEMENT PREDICTIONS FOR THE METAL CULVERT

The pretest and post-test calculations for the large-span metal culvert response under earth load are presented in this section and compared with field measurements.

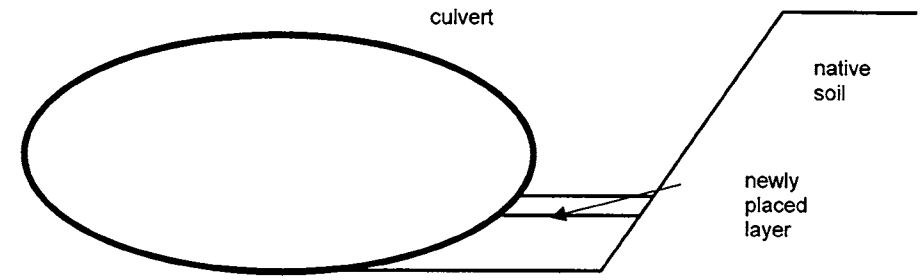

a. Location of the New Layer of Soil

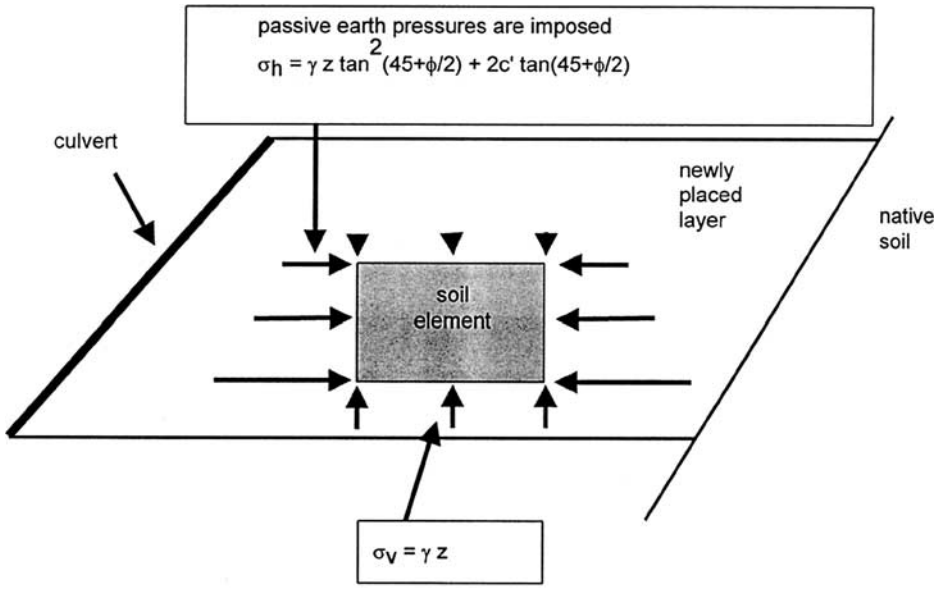

b. Passive Earth Pressures Imposed on Soil Layer

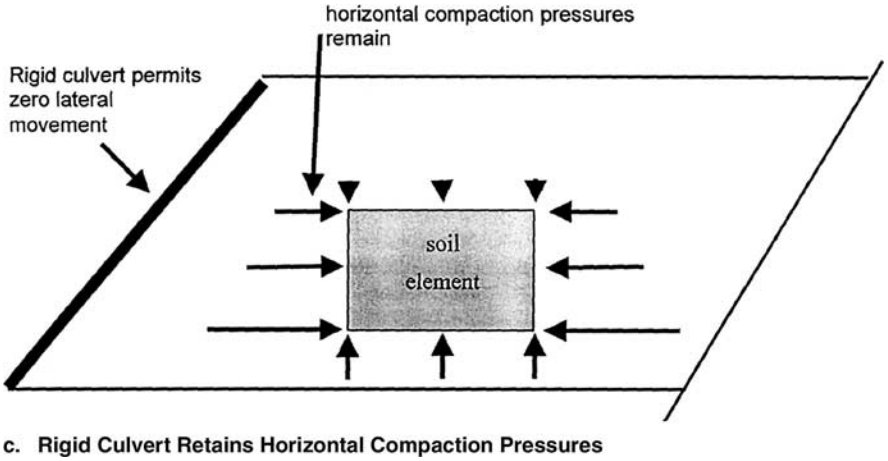

c. Rigid Culvert Retains Horizontal Compaction Pressures

Figure C-3. Introduction to compaction model.

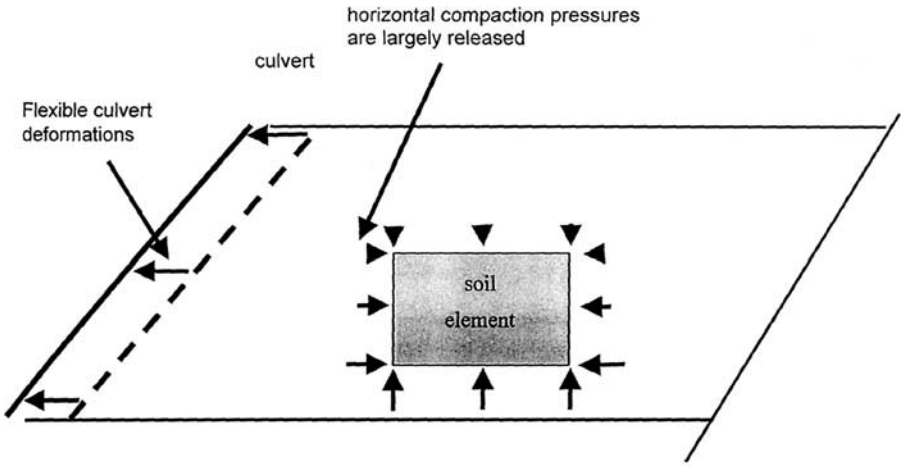

d. Flexible Culvert Deformations Release Most of the Horizontal Compaction Pressures

Figure C-3. (Continued)

Deformations

Figure C-4 shows calculations of the response of the culvert crown and changes in chord length from shoulder to shoulder during earth placement to a cover depth of 0.9 m (3 ft).

- Figure C-4a and b show crown deflections for the culverts in well-compacted and uncompacted backfill, respectively.
- Figure C-4c and d show changes in shoulder-to-shoulder distance for the culverts in well-compacted and uncompacted backfill, respectively.

Each figure shows measured values (Appendix B) as well as the pretest and post-test calculations. Pretest predictions are for the "design" backfills of density 95 and 85 percent. Two post-test calculations are given, one without modeling of compaction stresses and one considering the imposition

TABLE C-3 Parameters for the orthotropic plate model

Parameter and Direction	Membrane or Bending	Expression for Plate Property[1]	Value
Equivalent Thickness T mm	membrane & bending	$d\sqrt{\frac{3}{2\left(1+\frac{\pi^2 d^2}{4b^2}\right)}}$	56.02
E MPa	membrane	$\frac{Et}{d}\sqrt{\frac{2}{3}\left(1+\frac{\pi^2 d^2}{4b^2}\right)^3}$	25,144.6
meridional	bending	$\frac{3}{2}\left(1+\frac{\pi^2 d^2}{8b^2}\right)\frac{Et}{d}\left[\frac{2}{3}\left(1+\frac{\pi^2 d^2}{4b^2}\right)\right]^{3/2}$	28,823.4
E MPa	membrane	$\frac{2}{3}E\left(\frac{t}{d}\right)^3\sqrt{\frac{2}{3}\left(1+\frac{\pi^2 d^2}{4b^2}\right)^3}$	142.4
axial	bending	$\frac{2}{3}E\left(\frac{t}{d}\right)^3\sqrt{\frac{2}{3}\left(1+\frac{\pi^2 d^2}{4b^2}\right)^3}$	142.4
G	membrane	$\frac{Gt}{d}\sqrt{\frac{2}{3\left(1+\frac{\pi^2 d^2}{4b^2}\right)}}$	7,524.5
MPa	bending	$G\left(\frac{t}{d}\right)^3\left(\frac{2}{3}\right)^{3/2}\left(1+\frac{\pi^2 d^2}{4b^2}\right)^{5/2}$	119.0
ν	membrane		0.0
	bending		0.0

1. Ansourian (1981)
2. 1 MPa = 145 psi; 1 mm = 0.039 in.

b = Half wavelength of corrugation
d = Depth of corrugation
E = Young's modulus
G = Shear modulus
T = Thickness of the corrugated plate

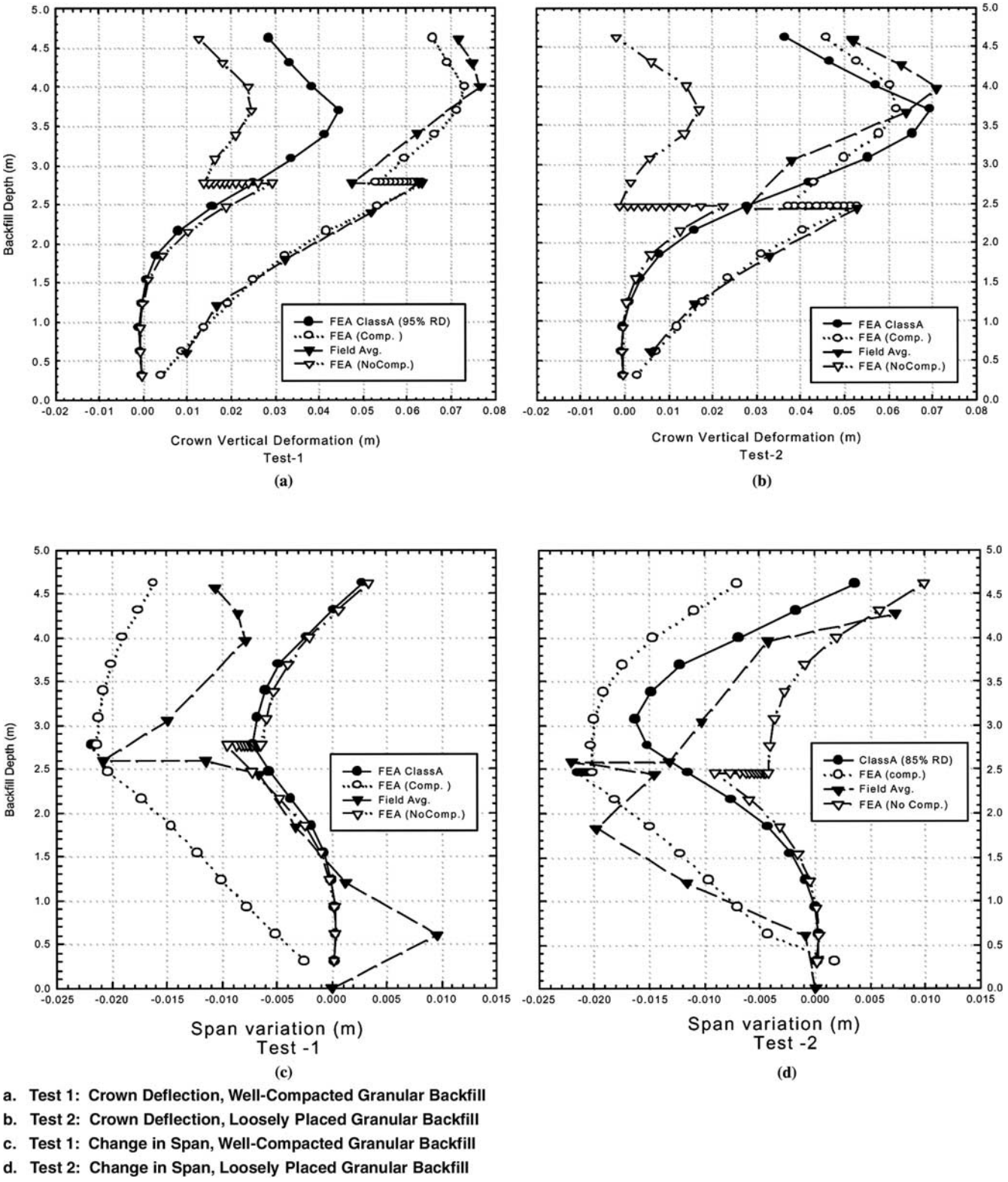

a. Test 1: Crown Deflection, Well-Compacted Granular Backfill
b. Test 2: Crown Deflection, Loosely Placed Granular Backfill
c. Test 1: Change in Span, Well-Compacted Granular Backfill
d. Test 2: Change in Span, Loosely Placed Granular Backfill

Figure C-4. Culvert deformations during culvert burial: measured response, pretest prediction, post-test predictions with and without compaction simulation.

and subsequent release of "upper bound" (full passive) compaction stresses.

As the fill is placed adjacent to the structure, the crown of the culvert moves upward ("peaking" deflections). Calculations of crown movement based on compaction modeling provided excellent calculations of crown movement for both low-density ("uncompacted") and high-density ("well-compacted") backfills. Crown deformations are largely unaffected after placement of the first 2 m (6.6 ft) of sidefill, and the analysis without compaction modeling produced incremental response that was also very satisfactory. However, predictions with and without the compaction model are significantly different during placement of the first 2 m (6.6 ft) of backfill. Little crown movement is calculated if compaction is not modeled during placement of the first 1 m (3.3 ft) of that soil, whereas measured response and analysis with compaction featured significant crown uplift.

Calculations of the impact of concrete top loads were reasonable, further evidence that the finite element analysis is successfully modeling the stiffness of the soil-structure system. Excessive downward movement is calculated for the soil with 87 percent density, whereas the prediction for the denser soil was close to that observed in the field. It appears that the parameters chosen for the lower density soil are somewhat low, given the soil density actually achieved in the field.

It is interesting that these results imply that the test structure with uncompacted backfill of low density was actually partially compacted in the field. This may have resulted as the dozer worked to spread the soil during placement of the backfill and is consistent with the soil density measured for this uncompacted soil. In fact, differences between dense and loose materials were only 5 percent in the field, whereas an absolute difference in density of 10 percent had been envisaged based on laboratory compaction tests.

Table C-4 summarizes the calculated and measured response of the crown using values of total uplift movement to the point where backfill reaches the crown and the subsequent downward movement as the earth is placed up to 0.9 m (3 ft) above the culvert. Again, these demonstrate that the calculated values are similar in nature to the deformations measured in the tests.

Calculations of span variation for both test cases are made with almost equal success (Figure C-4c and d). Span changes during the two tests show some variations in field measurements that are difficult to explain but are likely a result of the measurement technique used and construction over more than one day. However, the measurements generally lie between the two post-test calculations.

TABLE C-4 Comparison of calculated and measured displacements: metal arch culvert at two different densities, uplift of crown, and subsequent downward movement

Backfill Density	Measured	Predicted
Up 92%	76 mm	73 mm
Down 92%	-6 mm	-9 mm
Up 87%	71 mm	70 mm
Down 87%	-19 mm	-16 mm

1 mm = 0.039 in.

Class A predictions for culvert deformation are essentially the same as the post-test calculations made without modeling of compaction-induced earth pressures. The only significant difference lies in the absence of top loading from the pretest load path. In general, the pretest deformation estimates are good, particularly beyond the first 2 m (6.6 ft) of sidefill placement (where compaction effects were found to become negligible).

Thrusts

The finite element calculations for crown and shoulder thrust are shown in Figure C-5. Field test measurements for thrust were not accurate during backfilling and are not included. Calculations are in accordance with a conventional understanding of metal culvert response. Compaction has almost no impact on thrust, and the pre- and post-test predictions are very similar.

Moments

Bending moments at the crown and shoulders are illustrated in Figure C-6. Table C-5 summarizes the calculated and measured results. Calculations at other locations were also reviewed and yield similar trends. Peak negative moments occur at the crown, as a result of lateral earth pressures and compaction-induced deformation during placement.

These results indicate that the measured moments lie between the moment calculations with and without soil compaction. Up to a backfill depth of 2 m (6.6 ft), measurements at the crown are close to those predictions obtained with the "upper-bound" compaction model. Beyond that point, the measured values move somewhat closer to the "no-compaction" estimates. Values at the shoulders are consistently closer to the no-compaction calculations. In general, the analysis provides good estimates of rate of change of bending moment with culvert burial depth. The compaction and no-compaction analyses act as reasonable bounds to the culvert response.

Ignoring the impact of the top loading used to reduce upward crown movement during construction, moment magnitudes increase monotonically until backfill reaches the crown. After the crown is buried, the trends are reversed, as further soil material is placed over the structure. Both the magnitude and pattern of moment development appear to be correctly simulated by the finite element analysis. Backfill densities have only a minimal effect on the measured and calculated values of bending moment.

Results obtained with the compaction model provide conservative bending moments for this shallow buried structure. Bending moments would eventually change sign as the structure was buried further. From that point on, the no-compaction analysis would yield conservative values of bending moments.

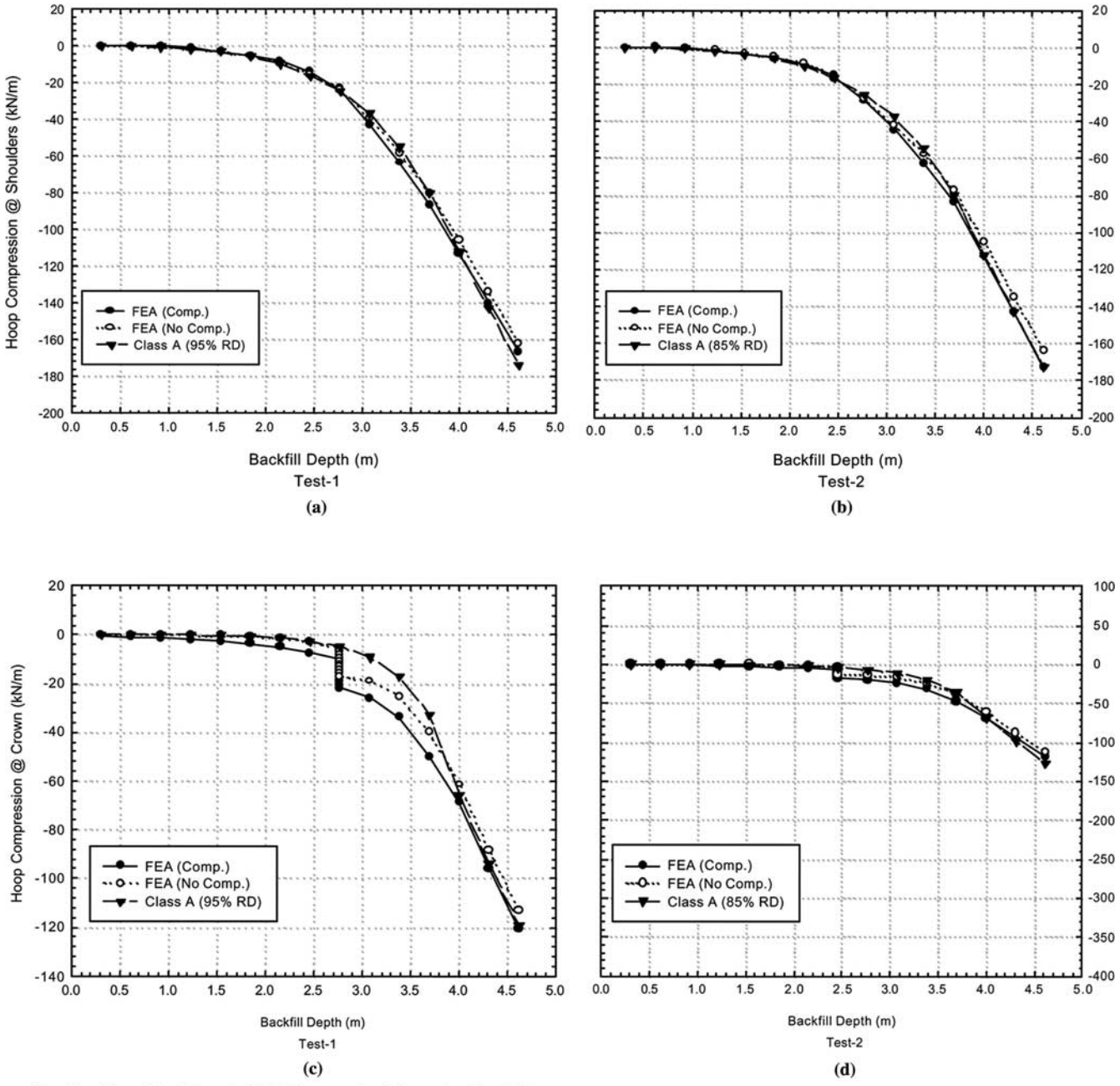

a. Test 1: Shoulder Thrust, Well-Compacted Granular Backfill
b. Test 2: Shoulder Thrust, Loosely Placed Granular Backfill
c. Test 1: Crown Thrust, Well-Compacted Granular Backfill
d. Test 2: Crown Thrust, Loosely Placed Granular Backfill

Figure C-5. Culvert thrusts during culvert burial: pretest prediction, post-test calculations with and without compaction simulation.

Soil Stresses

To further examine the effect of earth loads, soil stresses normal to the culvert at the crown and springline are plotted in Figure C-7 for both tests. The calculations are again compared with the measured results reported in Appendix B. The results are in good agreement, except at the springline during Field Test 1. Stress readings for that test at that location indicate little response from the stress cell through the middle stage of culvert burial. Analysis reveals that the compaction model has little effect on stress predictions. The analysis releases these additional stresses, as the flexible culvert deforms. Com-

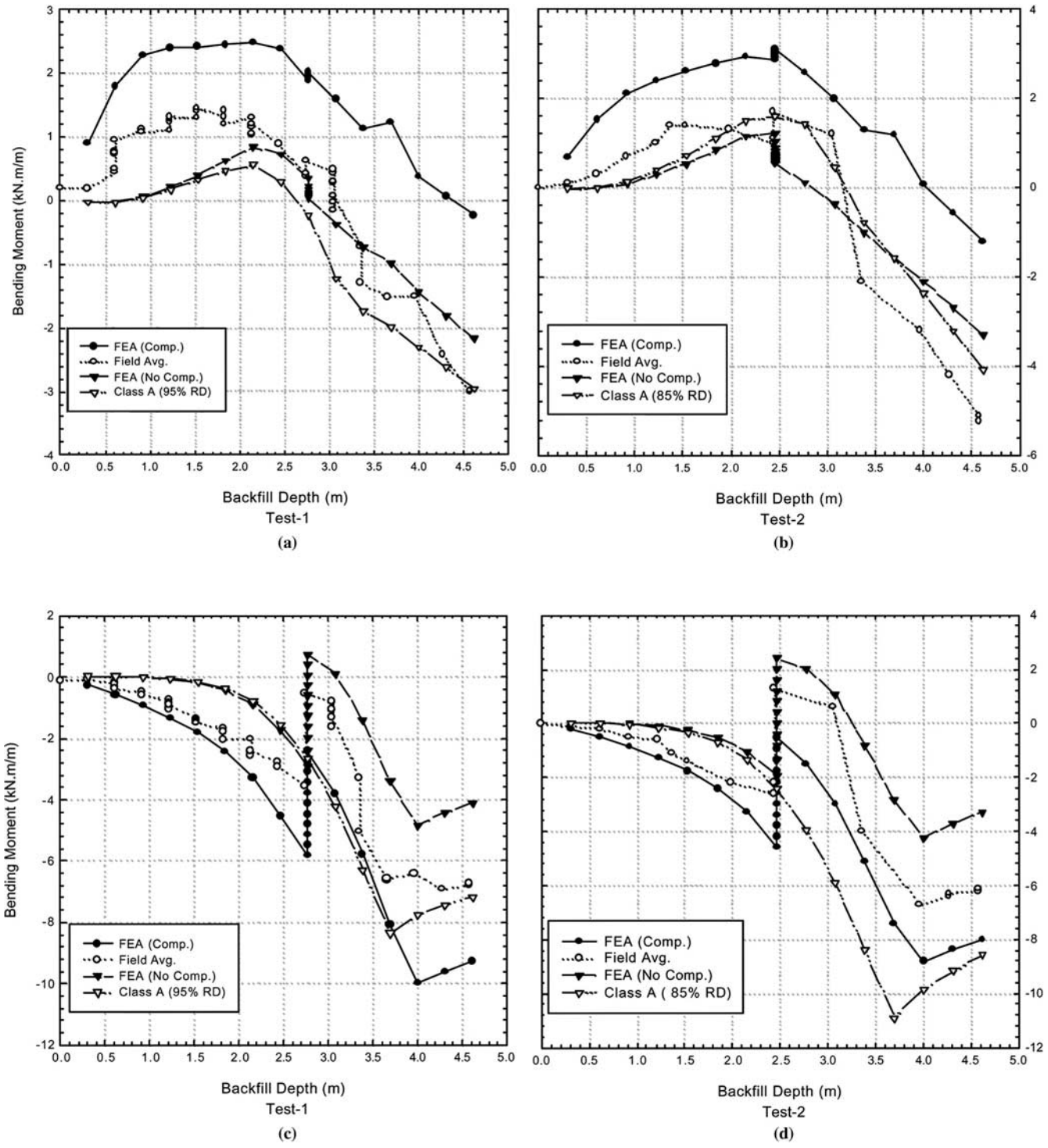

a. Test 1: Crown Moment, Well-Compacted Granular Backfill
b. Test 2: Crown Moment, Loosely Placed Granular Backfill
c. Test 1: Shoulder Moment, Well-Compacted Granular Backfill
d. Test 2: Shoulder Moment, Loosely Placed Granular Backfill

Figure C-6. Culvert moments during culvert burial: measured response, pretest prediction, post-test calculations with and without compaction simulation.

TABLE C-5 Comparison of calculated and measured moments: metal arch culvert

	Backfill Density	Location and Test	Measured kN-m/m	Predicted kN-m/m
Minimum	92%	Crown Test 1	-3.0	-0.2 to -2.2
		Shoulder Test 1	-6.8	-4.9 to -10.0
	87%	Crown Test 2	-5.2	-1.2 to -3.3
		Shoulder Test 2	-6.8	-4.3 to -8.9
Maximum	92%	Crown Test 1	1.4	0.8 to 2.5
	87%	Crown Test 2	2.7	1.2 to 3.2

1 kN = 225 lbs

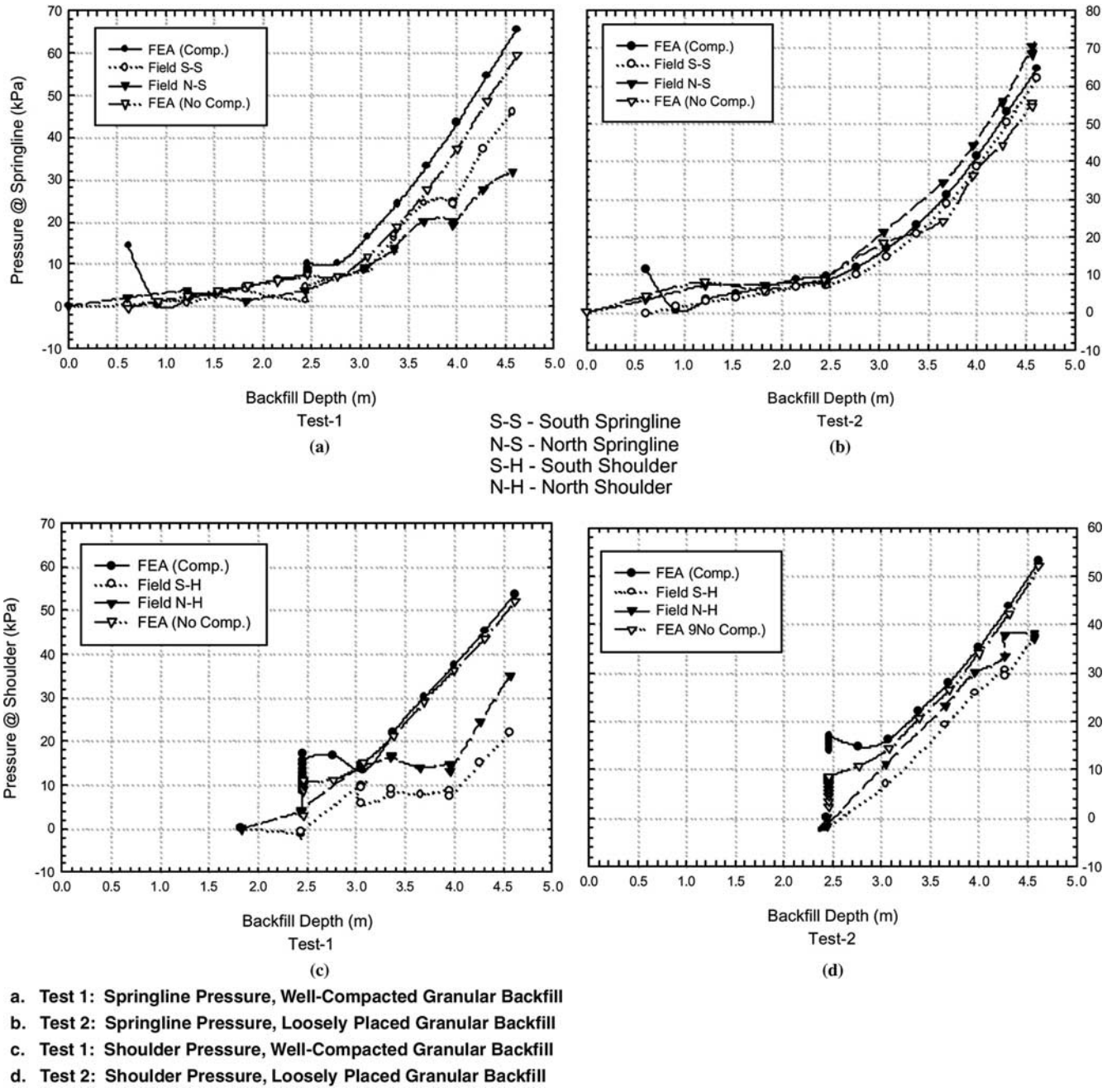

a. **Test 1: Springline Pressure, Well-Compacted Granular Backfill**
b. **Test 2: Springline Pressure, Loosely Placed Granular Backfill**
c. **Test 1: Shoulder Pressure, Well-Compacted Granular Backfill**
d. **Test 2: Shoulder Pressure, Loosely Placed Granular Backfill**

Figure C-7. Radial pressures during culvert burial: measured response, pretest prediction, post-test calculations with and without compaction simulation, N–S north shoulder, S–S south shoulder.

paction therefore affects deflection and moment but not thrust and soil pressure.

Plastic Zones

Analysis of culvert response to earth load leads to shear failure in the backfill soil. Figure C-8 shows zones of plastic soil material (soil that has fully mobilized shear strength) at various points through the construction process. Clearly, nonlinear soil response has occurred, and the structures are affected by shear failure in the soil adjacent to the structure. These zones of plastic material eventually reduce because, as fill over the culvert crown increases earth stresses, strength also increases in this frictional soil.

THREE-DIMENSIONAL METAL CULVERT ANALYSIS FOR VEHICLE LOAD

Culvert testing featured essentially static surface live loading with a test vehicle of weight 370 kN (83,200 lb) on three axles, 310 kN (70,000 lb) on the tandem rear axles, at shallow to very shallow covers—namely, 1.2 m (4 ft), 0.9 m (3 ft), 0.6 m (2 ft), and 0.3 m (1 ft). This vehicle represents an AASHTO design tandem increased for impact. This truck, at very shallow covers, represents culvert testing well beyond conventional service conditions.

Performance of the three-dimensional elastic finite element analysis is reviewed in this section. Key considerations include distribution of deflection, thrust, and moment along the culvert axis and evaluation of culvert response at live loads above conventional vehicle weights. Most calculations presented here are for the "worst" burial case—namely, cover of 0.3 m (1 ft). Calculations presented for thrust are for a burial depth of 0.6 m (2 ft), because these load tests were conducted after modification of the field instrumentation to provide reliable thrust measurements.

Figure C-9 shows half the mesh used in the three-dimensional finite element calculations (both sides of the structure were discretized because the culvert response to truck load is not symmetric).

Culvert Deformations

Calculations and measurements of incremental culvert deformation are presented in Figure C-10. Culvert responses for Test 1 are shown in Figure C-10a and b for locations directly under the wheel loads and 2.8 m (9.2 ft) from the axle centerline. Figure C-10c and d show similar results for Test 2

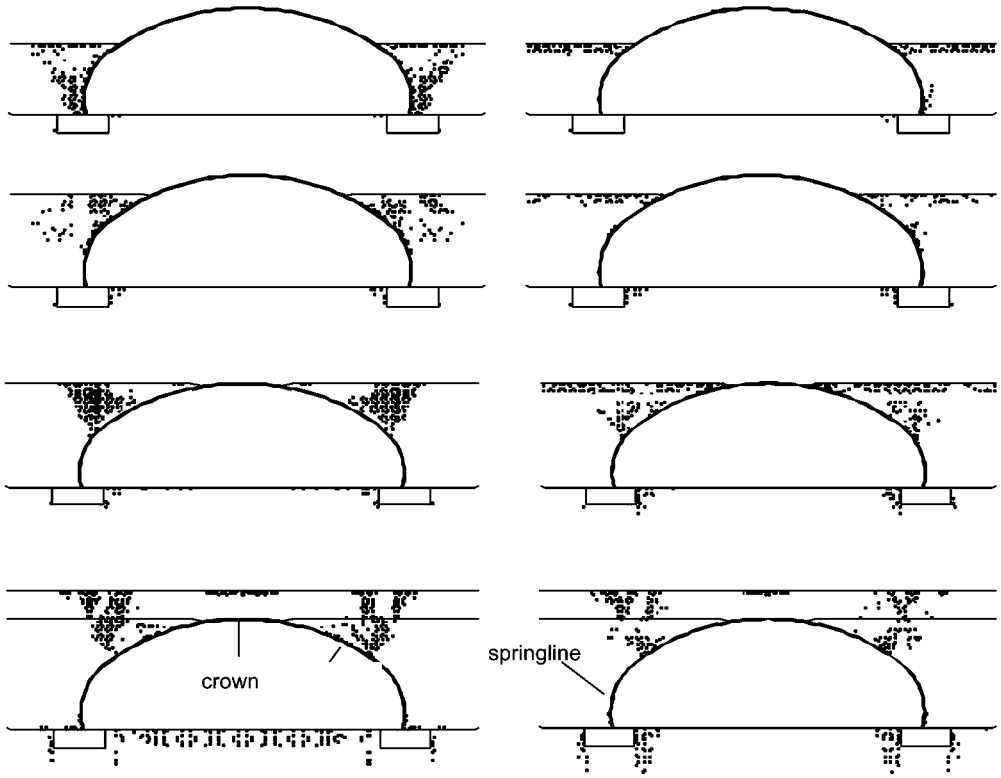

Figure C-8. Development of plastic zones around culvert.

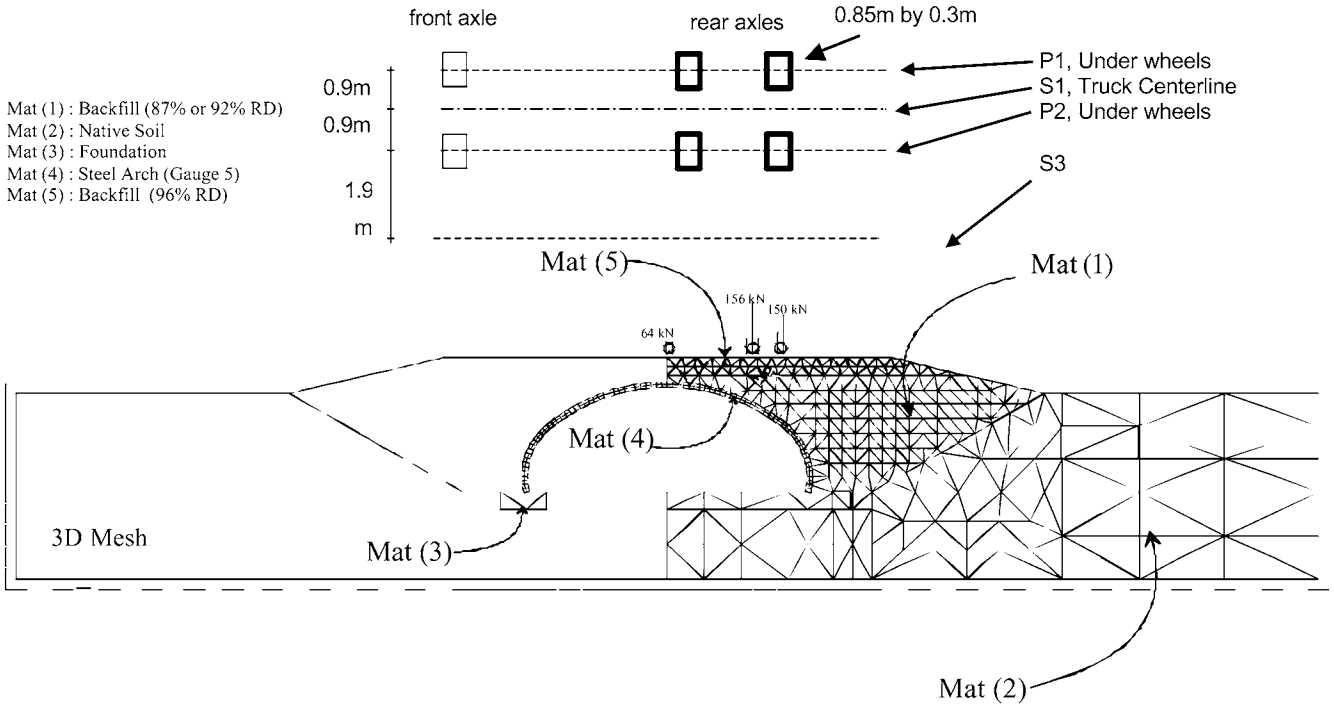

Figure C-9. Three-dimensional finite element mesh and vehicle axle loads: rear axles shown located over south shoulder; plan view of wheel footprint also shown together with axial locations for instruments (P1, P2, S1, and S3).

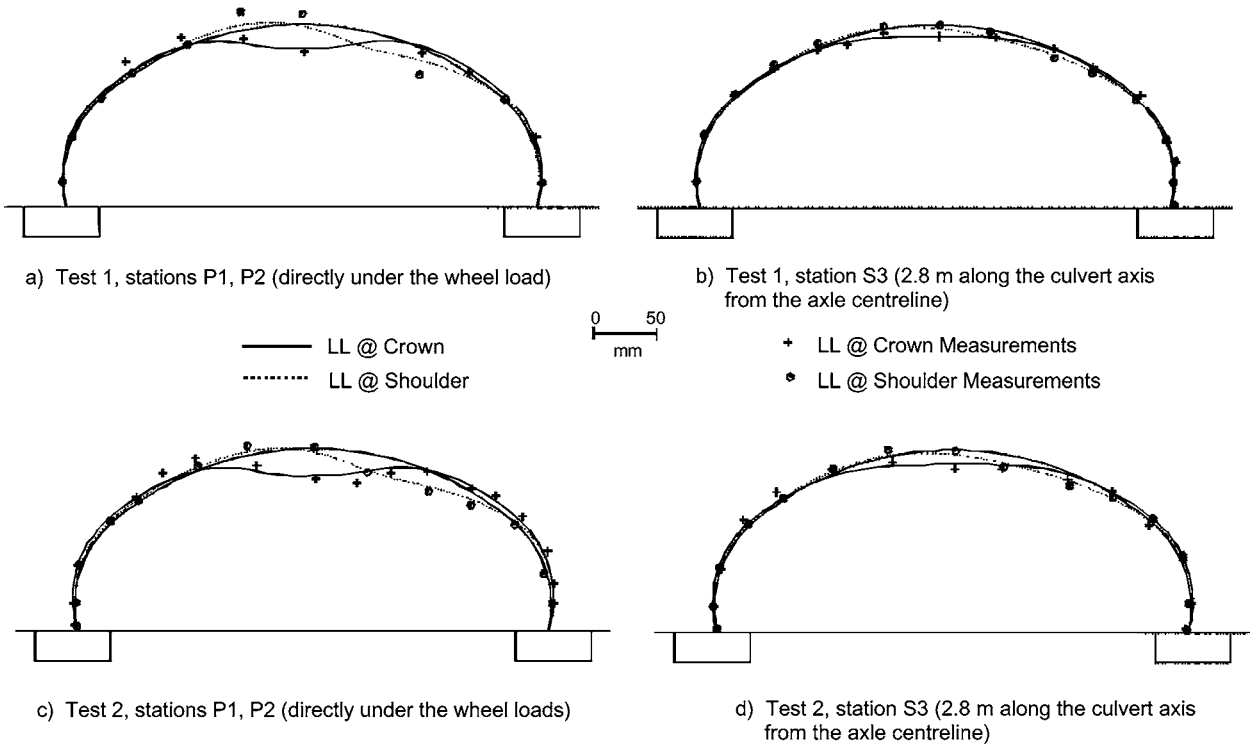

Figure C-10. Live-load deformations for culvert under 370-kN (83,000-lb) vehicle: rear axles centered at crown and south shoulder, 0.3-m (1-ft) cover.

(the culvert with lower density backfill). Each figure presents results for the tandem rear axles of the test vehicle centered over the shoulder and then over the crown.

The analysis provides the correct deflection patterns and largely the right magnitudes of deformation. Calculations for axles centered at the crown are particularly effective, with errors of 20 percent or less in deflection magnitude.

Only one set of calculations have magnitude that varies significantly from those measured in the field. These are directly under the wheel loads during Test 1 (the culvert with compacted backfill), specifically at axial position P1 (directly under the wheels). Measured deflections in that one case are approximately double those calculated.

Thrusts

Calculations and measurements of incremental culvert thrusts are presented in Figure C-11. These results reveal that the measured thrusts resulting from the action of the test vehicle exceed those calculated by three-dimensional analysis. The largest value of thrust, both measured and calculated, occurs when the tandem axles of the test vehicle are centered at the crown. This is at an axial location under the wheel loads. Measured thrust is 50 percent greater than the value calculated at that location.

Thrust values measured 2.8 m (9.2 ft) from the truck centerline are closer to the thrust predictions at that location. The pattern of compressive and tensile thrust increments is correctly calculated, and magnitudes are within 30 percent of field measurements.

Moments

Calculations and measurements of incremental culvert moments are presented in Figure C-12. Bending moment patterns are successfully calculated, although the magnitudes of the calculated moments are not as satisfactory. Magnitudes directly under the wheels appear to be 50 to 70 percent of the measured values, whereas calculations at a distance of 2.8 m (9.2 ft) from axle centerline have values about double those measured.

These discrepancies probably result because the elastic analysis ignores the potential for shear failure in the soil. Shear failure will reduce the ability of the "arch" of soil across the crown to carry loads away from the location of the wheel loads. Higher moments therefore result directly under vehicle wheels, and lower moments occur in the structure at other axial positions.

The analysis also suggests that complex moment distributions can be expected in the structure at such shallow cover heights. The calculations infer that the crown is not the most critical location. Instead, large peaks occur a short distance on either side of the crown. The crown value is about 20 percent of those peak values. These two moment peaks coalesce into one once there is more soil between wheel and structure. This was apparent for analyses performed at greater cover depth [for example, 0.9 m (3 ft)] and can also be seen when eccentric placement of the test truck increases distance between load and culvert (shown in Figure C-12 for P1, P2 solutions where axles are centered over the culvert shoulder).

Two-Dimensional Versus Three-Dimensional Live-Load Calculations

The conventional approach to undertaking finite element calculations for live-load response is to use two-dimensional "plane strain" analysis, with vehicles represented as equivalent line loads. Such two-dimensional calculations can employ nonlinear soil models like the elastic-plastic formulation used

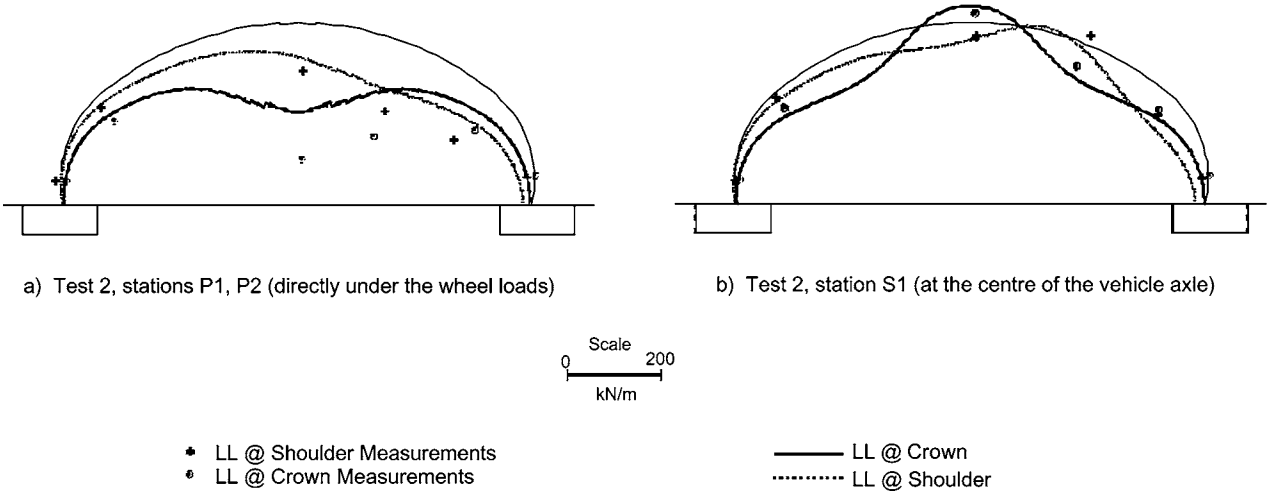

Figure C-11. Live-load thrusts for culvert under 370-kN (83,000-lb) vehicle: rear axles centered at crown and south shoulder, 0.6-m (2-ft) cover.

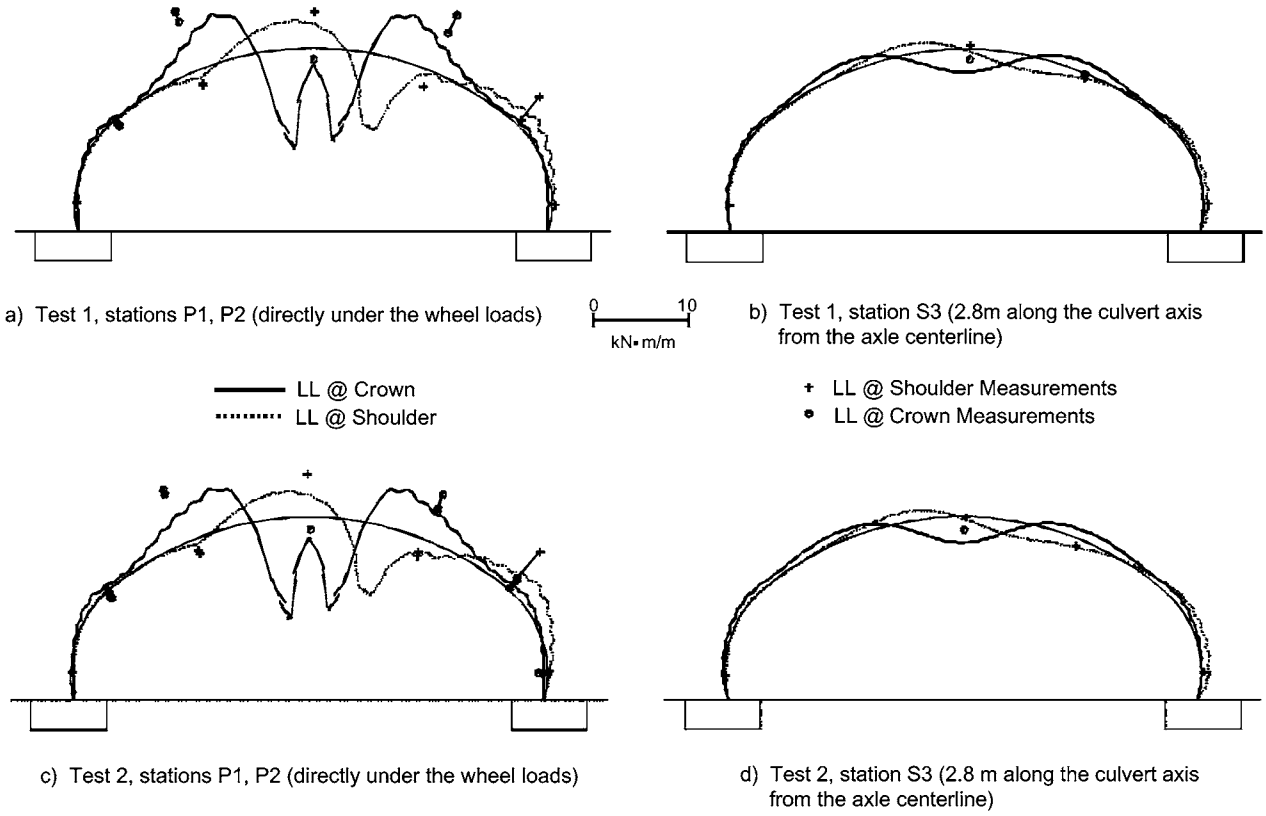

Figure C-12. Live-load moments for culvert under 370-kN (83,000-lb) vehicle: rear axles centered at crown and south shoulder, 0.3-m (1-ft) cover.

earlier in this appendix, which can be valuable when the intention is to predict culvert response during extreme load events. However, they rely on approximate techniques for calculation of equivalent line load. The relative effectiveness of two- and three-dimensional analyses is now investigated.

The two-dimensional calculations presented here were part of the pretest calculation exercise conducted by Moore et al. (1997). Calculations were for the test culvert within an envelope of loosely placed backfill, the 85-percent density parameters given in Table C-1. A total vehicle load of 30 kN/m (2,100 lb/ft) was divided equally between the two rear vehicle axles. The first stage of the analysis featured construction simulation to obtain an estimate of the earth-load condition around the metal culvert. The vehicle was then numerically "driven" across the culvert to the crown by the procedure outlined by El Sawy et al. (1997).

Table C-6 presents results of three-dimensional and two-dimensional analyses as well as field test measurements reported in Appendix B. The table gives values of deflection, thrust, and moment at the culvert crown for the rear axles of the test vehicle centered over the culvert crown. Values of deflection and moment are for very shallow cover—namely, 0.3 m (1 ft). Values of thrust are for 0.6 m (2 ft) of backfill placed over the crown.

These comparisons reveal how two-dimensional and three-dimensional modeling of surface live-load attenuation with depth result in significant differences in calculations of deflection, moment, and thrust:

TABLE C-6 Response for vehicle live load: rear axles centered over crown, low-density backfill, crown values

		Deflection mm Cover 0.3 m		Moment kN-m/m Cover 0.3 m		Thrust kN/m Cover 0.6 m	
Source of Data	Load	under Wheel Load	2.8 m from Axle cL	under Wheel Load	2.8 m from Axle cL	under Wheel Load	at Axle cL
3D elastic	370 kN	-22.2	-11.7	-2.1	-1.5	-180	34
2D elastic-plastic	30 kN/m	-23.2		-5.7		-32	
Webb et al (1998)	370 kN	-26.8	-11.7	-1.6	-1.4	-277	38

1 kN = 225 lbs; 1 kN/m = 69 lb/fr; 1 m = 39.4 in.; 1 mm = 0.039 in.; 1 kN-m/m = 2,670 in.-lb/ft

- Measurements of crown deflection are reported in Appendix B at the two different axial locations shown in the table [under the wheel loads and 2.8 m (9.2 ft) from the axle centerline]. These deflections are close to the three-dimensional predictions shown in Figure C-10. Only one two-dimensional value is shown, because the two-dimensional analysis does not model variations in the axial direction. That value is close to deflection measured under the wheel loads.
- Crown moments measured in the field are close to those calculated by the three-dimensional procedure. The two-dimensional estimates are more than three times the field measurements.
- Thrusts measured for the culvert at 0.6 m (2 ft) cover depth are again similar in form to those resulting from the three-dimensional analysis. This time, the two-dimensional calculations are very low, in fact about one-ninth of the field measurements.

It is clear that use of nonlinear analysis with two-dimensional line-load equivalents produces results that differ significantly from those that are measured. The three-dimensional elastic calculations are much closer to the observed field values. It is clearly important to have explicit modeling of the three-dimensional attenuation of load with depth, and this attenuation appears to have a very different impact on deflection, thrust, and moment. This likely results from the fundamental differences in the nature of these quantities. Thrust in a thin elastic structure is proportional to the first derivative of the in-plane deformations, whereas moment is proportional to the second derivative of the out-of-plane deformations. Variations in load thus produce different gradients of deflection, moment, and thrust. Two-dimensional analysis requires use of different line loads for calculations of deflection, thrust, and moment.

The principle attraction of using two-dimensional analysis to calculate live-load response is its inclusion of nonlinear models for soil and structure. As the choice of line load is unclear—depending as it does on whether deflection, thrust, or moment is being sought—the ability of the procedure to correctly deduce the impact of nonlinearity is questionable. Therefore, it is concluded that the three-dimensional elastic culvert analysis is the more effective computational approach.

METAL CULVERT ANALYSIS: DISCUSSION AND CONCLUSIONS

Influence of Soil Compaction

A new procedure was introduced to provide information on the likely effects of soil compaction: horizontal earth pressures, like those expected to remain after compaction is imposed, and equilibrium calculations undertaken to calculate the extent of culvert deformation and horizontal stress release. The procedure was implemented to provide an upper bound to the expected response through the use of residual earth pressures associated with shear failure in the soil and the passive stress state. Analysis without consideration of compaction represents a lower bound. Comparisons with measured response revealed that these analyses did provide effective bounds on the culvert response.

Upward crown movements like those experienced in the field were calculated by the construction analysis. Calculations obtained with the upper-bound compaction model matched the measured culvert response closely. Calculations made without considering compaction underestimated culvert deformations and bending moments for the first 2 m (6.6 ft) of backfill placement (the sidefill material).

Moment calculations for earth loading were generally successful, with measured response lying between calculations without compaction modeling and those with imposition of horizontal compaction pressures. The compaction model provides conservative calculations of culvert moment for shallow burial. Conservative estimates of moment in deeply buried structures will require the effects of compaction to be neglected.

Calculations of radial earth pressures are also reasonably close to the field measurements. As might be expected for a flexible metal culvert of this type, compaction of the sidefill influenced culvert deformations and changed the bending moment instead of the final soil stresses or values of thrust.

Class A Predictions

Pretest (Class A) predictions did not include the effects of the top loading conducted during the field tests to limit crown deformations during sidefilling, nor did they feature use of the upper-bound compaction model. Like the post-test calculations made without consideration of compaction, they provided excellent estimates of changes in moment and deformation after placement of the first 2 m (6.6 ft) of backfill soil. They demonstrate that the two-dimensional elastic-plastic finite element model is capable of predicting culvert response in advance with a reasonable degree of accuracy.

The success of this aspect of the project can be attributed to both the effectiveness of the analysis and the quality of the soil parameters chosen for use in the study. That choice was based on simple geostatic earth pressures and a small number of triaxial test measurements of elastic soil modulus. It is important to note that parameter choices were made in this study with the intention of producing the best estimates for the measured field response. Design calculations require use of conservative (generally lower bound) soil parameters and would be handled in a different fashion.

Live-Load Predictions

Calculations for culvert response under live load were generally successful. Most estimates of culvert deformation

were close to those measured in the field. The elastic finite element procedure appears to underestimate live-load thrusts and moments directly under the wheel loads, probably as it neglects shear failure in the soil (overestimating the extent to which the soil lying over the culvert can transfer load around and along the culvert).

The calculated response is much closer than that provided by conventional plane strain analyses, which use two-dimensional (line-load) equivalents. Comparisons between two-dimensional and three-dimensional finite element analyses revealed the importance of explicitly modeling the three-dimensional vehicle load. A line load, which provides reasonable estimates of crown deflection, was found to produce moments that exceed measured values by a factor of 3 but thrusts that were nine times too small.

TWO-DIMENSIONAL EARTH-LOAD PREDICTIONS FOR REINFORCED CONCRETE CULVERT

Figure C-13 shows the reinforced concrete culvert and the instrumentation used to monitor radial earth pressures around the circumference. Figure C-14 shows the two-dimensional and three-dimensional finite element meshes used in all calculations. Both the two-dimensional and three-dimensional methods of analysis were described in an earlier section of this Appendix.

Soil Stresses

The effect of earth loads on soil stresses normal to the culvert at crown and springline are plotted in Figure C-15a to d for Test 1 and in Figure C-16a to d for Test 2. These post-test calculations are compared with the measured results reported in Appendix B.

Table C-7 summarizes measurements and calculations at 0.9 m (3 ft) depth. From all these data, it appears that

- Earth pressure readings at symmetric locations on north and south sides of the test culvert are very similar (i.e., values at SC resemble those at NC, and those at SH resemble those at NH);
- The two-dimensional finite element calculations are similar to the field measurements;
- Calculations further from the crown are consistently close to measured values—these more deeply buried locations do reveal discrepancies in the initial rates of change in pressure with depth, but these are resolved on further burial so the overall trend is excellent; and
- Calculations near the crown lie somewhat below measured values—it may be that these discrepancies would disappear if further burial had taken place in the field (these readings are discussed further below).

In general, the finite element analysis provided good-quality calculations for this first field burial case.

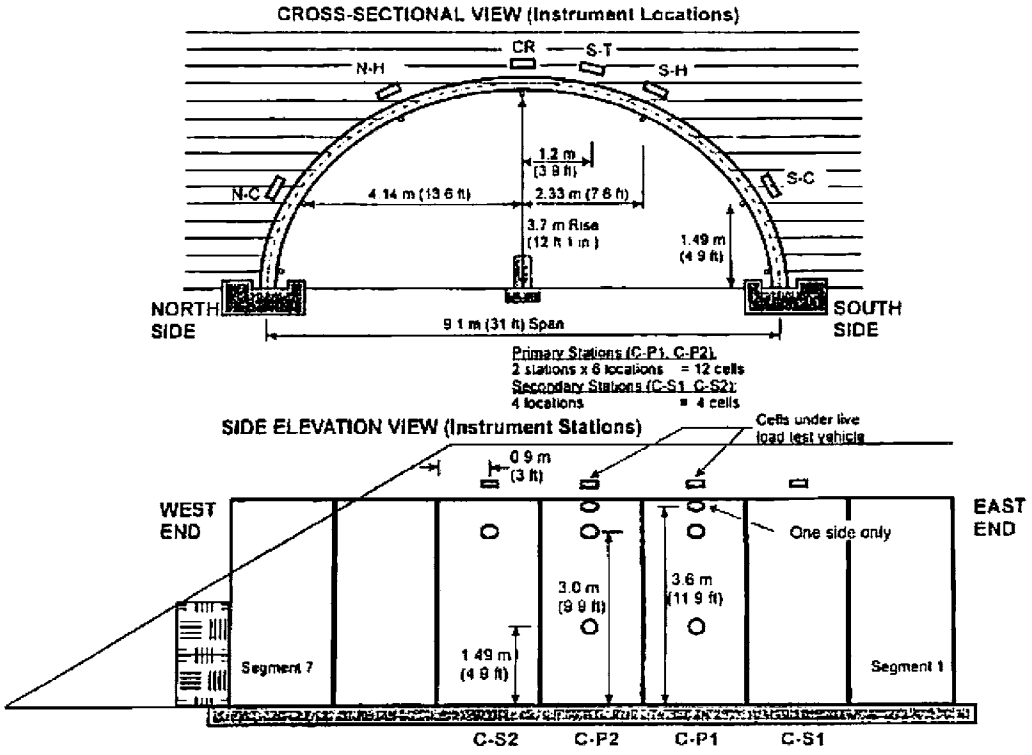

Figure C-13. Earth pressure cell locations around concrete culvert.

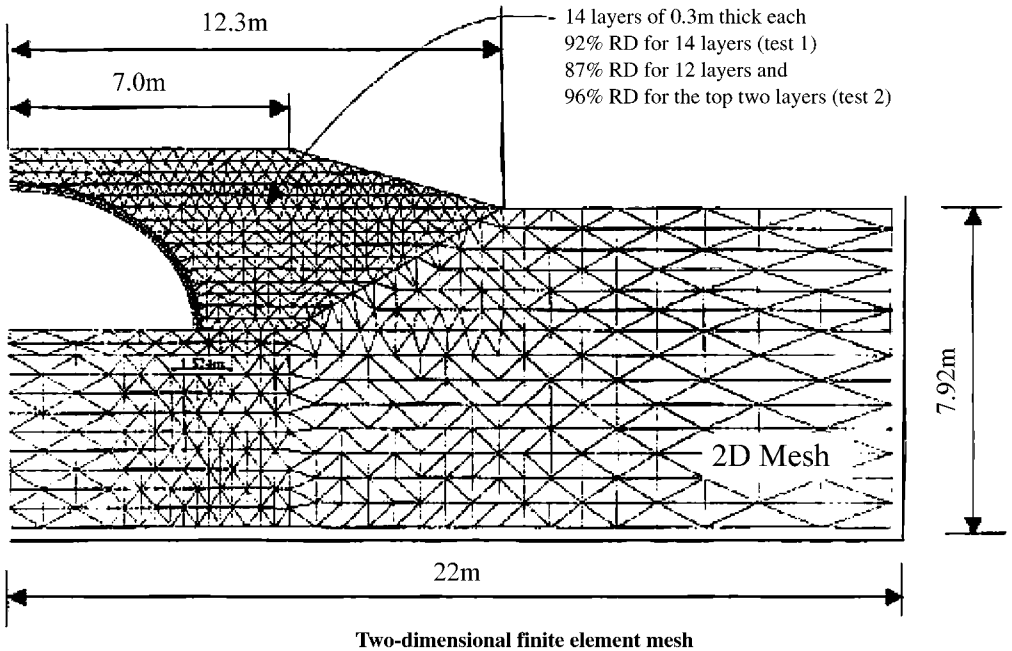

Two-dimensional finite element mesh

(a)

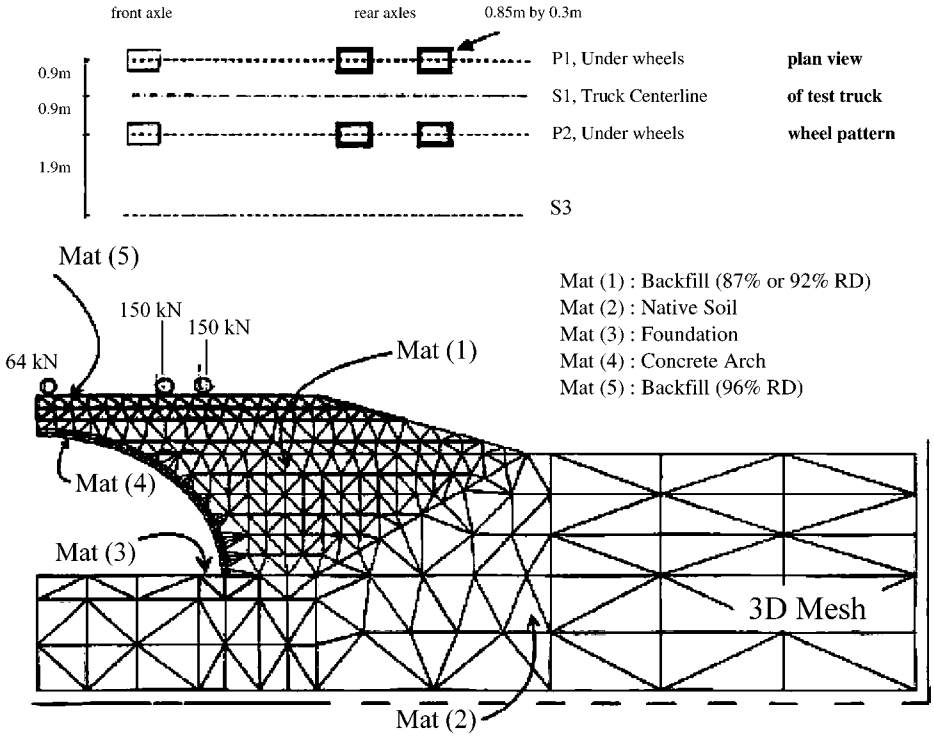

Three-dimensional finite element mesh

(b)

Figure C-14. Finite element meshes used for analysis of concrete culvert.

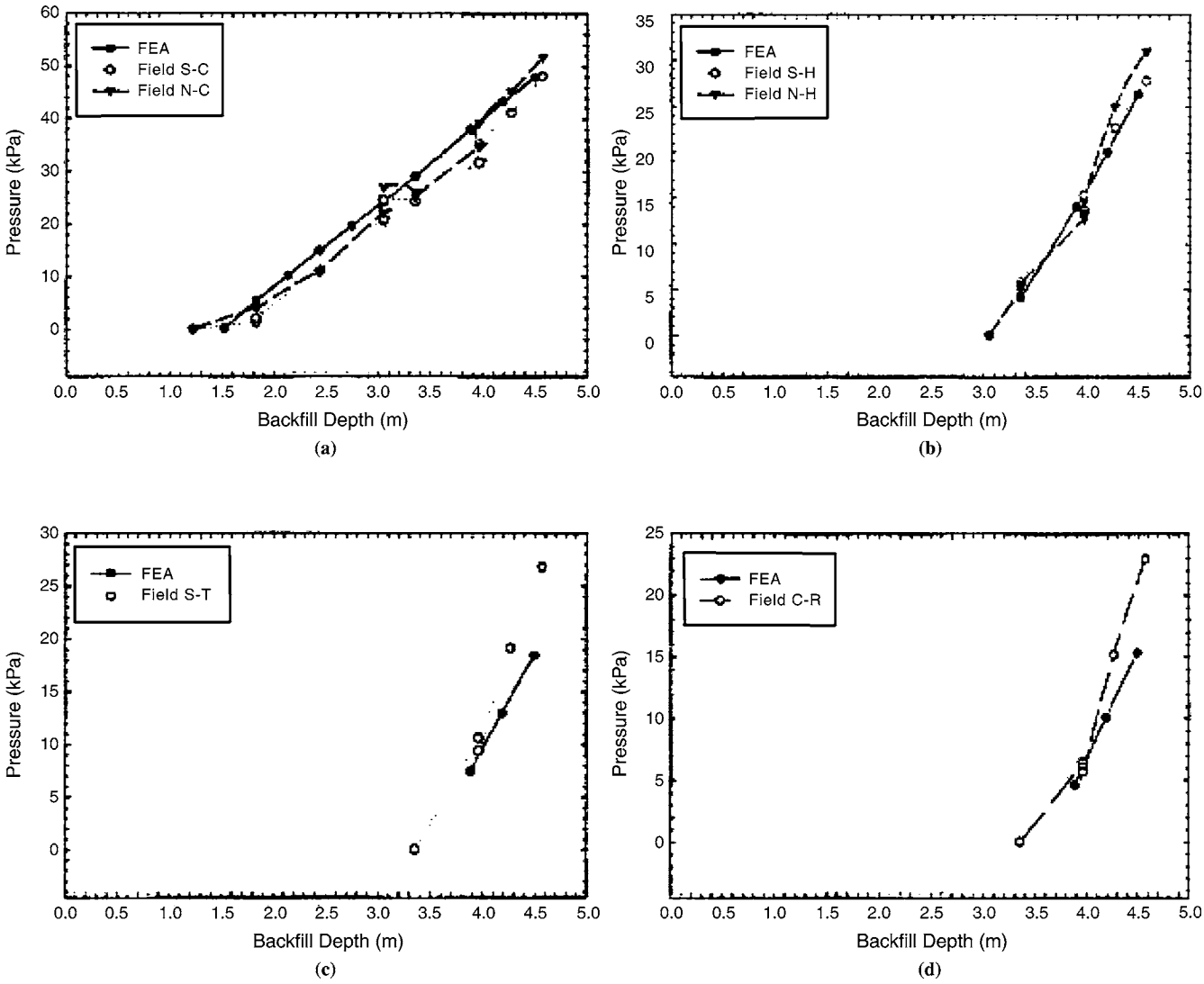

Figure C-15. Comparison of field-measured and predicted normal earth-load soil stresses around concrete culvert during backfilling: Test 1.

Figure C-16 shows estimates of earth pressures for the second field burial case. With the exception of Figure C-16a (earth pressures at the furthest distance from the crown), the finite element calculations are close to the field measurements. With the exception of locations SC and NC, the measurements and calculations for Test 2 are close to those for Test 1. Soil density appears to have little influence on the earth pressures for this structure.

The finite element calculations are large relative to the measurements at SC and NC (Figure C-16a). The measurements at SC and NC also differ from each other. The source of these discrepancies is unclear. It appears that some physical condi-

TABLE C-7 Pre- and post-test calculations and measurements of soil pressures due to earth loads

		Earth Pressures kPa							
		Test 1				Test 2			
		SC-NC	SH-NH	ST	CR	SC-NC	SH-NH	ST	CR
Measured	North	52	31	–	–	22	–	–	–
	South	48	28	27	23	11	41	30	27
Calculated	Pre-Test	24	–	–	–	21	–	–	–
	Post-Test	52	26	18	16	44	25	19	18

1 kPa = 0.14 psi

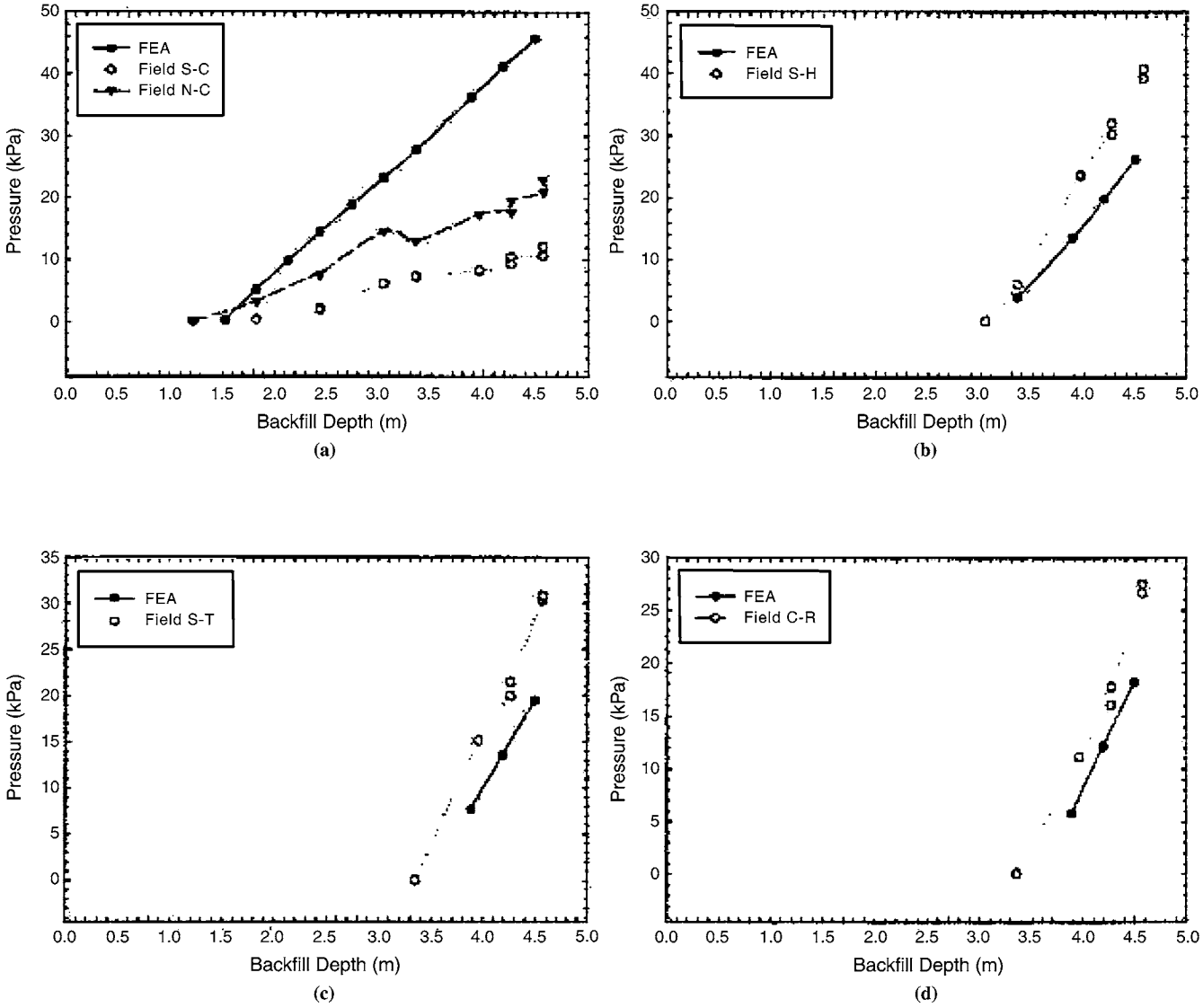

Figure C-16. Comparison of field-measured and predicted normal earth-load soil stresses around concrete culvert during backfilling: Test 2.

tion resulted during Test 2, a condition that affected each side of the culvert differently; perhaps a change in the soil placement technique at these locations resulted in increases in earth pressures elsewhere (some increase in pressure can be seen at SH relative to those for Test 1).

Two sets of earth pressure calculations are given in Table C-7. The pretest predictions reported by Moore et al. (1997) are given as well as the post-test calculations described above. The pretest predictions are approximately half the field measurements (with the exception of the values for Test 2 at the shoulders) and are consistently lower than those made after the field tests were completed. Two possible explanations for this are the revised geometry relative to that assumed in the pretest analyses or modeling of the concrete culvert with two-noded structural elements in the post-test predictions and eight-noded continuum elements in the pretest calculations. Eight-noded continuum elements can produce overstiff (or "locking") behavior in some situations, although how this could have influenced the earth pressures in this manner is unclear. Two-noded structural elements were used in all subsequent analysis for this project.

These comparisons also highlight an important discrepancy between measurement and calculation near the culvert crown. The soil at this location likely experiences a vertical earth pressure distribution close to geostatic values. Using a bulk unit weight of 20 kN/m^3 (128 pcf) implies vertical stress of 18 kPa (2.6 psi) at 0.9 m (3 ft) depth. This is consistent with the finite element calculations and implies that either the stress distribution at the crown is not geostatic or, more likely, that the stress cells overestimate earth pressures when the stress is low.

Stress Resultants

The finite element calculations for thrust and moment distribution around the culvert perimeter are shown in Figure C-17 for both Test 1 and Test 2.

Figure C-17a shows the distribution in thrust, together with field thrust values reported by LaFave (1998) near the footings (denoted the "base") and at the shoulder (SH). Measurements to permit stress resultant estimates were taken immediately after construction and some time later (3 days before live loading), with significant changes in magnitude noted. In both cases, the differences between springline and shoulder values are close to the differences calculated by the finite element method. However, the overall magnitudes at the end of construction appear high compared with the computer calculations.

Moment calculations for Test 1 are shown in Figure C-17b. Shoulder moment estimates after construction and 3 days before live loading are almost identical and are reasonably close to the calculations at this location. Unfortunately, moment is close to zero at this point, and the effectiveness of this component of the analysis is difficult to judge without measurements of moment at CR or SC (points where moments reach a maximum).

Figure C-17c and d contain thrust and moment distributions calculated for Test 2. In this case, thrust values at

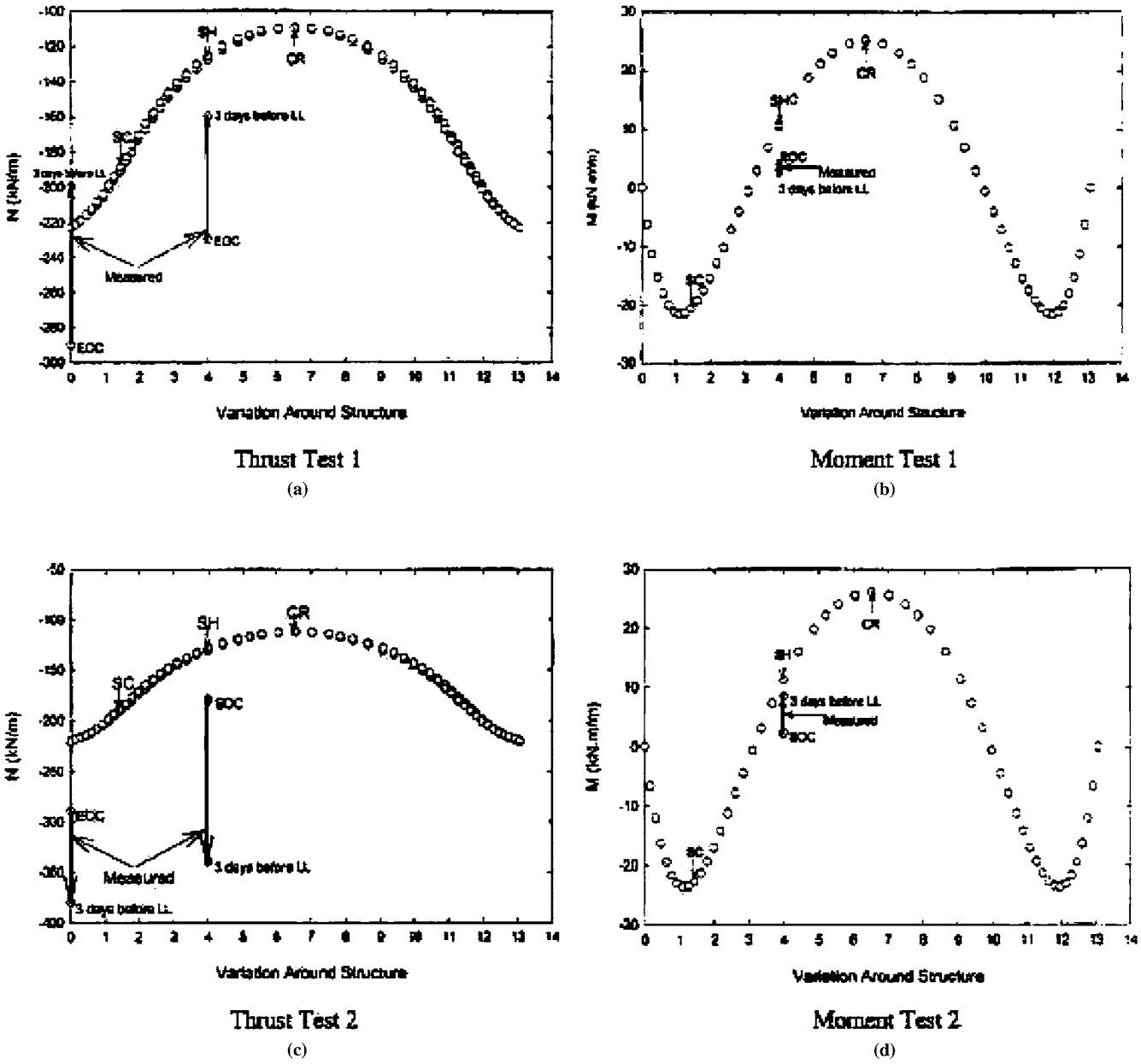

Figure C-17. Thrust and moment in concrete culvert.

springline and crown again differ by amounts close to calculated values. The absolute magnitude of the thrusts is close to the values calculated at the end of construction. Increases in thrust were then observed over time, attributed to footing movement by LaFave (1998).

Moment is again measured at shoulder (SH), a location with moment close to zero. Field measurements imply that moments move closer to the predicted values before live-load testing.

THREE-DIMENSIONAL LIVE-LOAD PREDICTIONS FOR REINFORCED CONCRETE CULVERT

Live-load test results are examined for the reinforced concrete test structure only for the Test 2 condition; that is, for backfill placed loosely around most of the structure and soil directly at the ground surface compacted to provide strength adequate to support the test vehicle. This test feature measured values of earth pressure of larger magnitude than most of those obtained in Test 1 because of the axial position of the test vehicle. These larger values imply better resolution [the stress cells are unlikely to be as accurate when measured stress is less than 10 kPa (1.5 psi)] and are also of greater significance with respect to culvert design and performance.

Figures C-18 through C-21 compare measured and calculated earth pressures for burial depths 0.3 m (1 ft) and 0.9 m (3 ft). Each figure includes one set of finite element estimates as well as earth pressures measured at two different axial positions (locations that are identical in terms of the axial position of the pressure cell relative to the wheel loads). The axial live-load position *Z* is indicated on the horizontal axis of each figure. The figures correspond to the following:

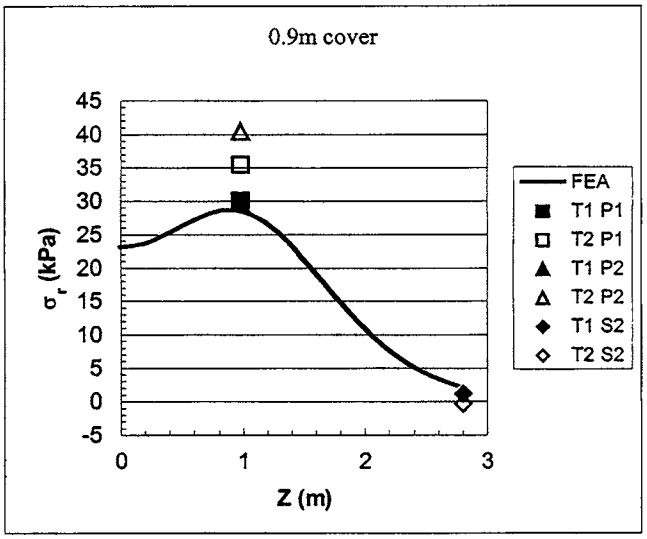

Figure C-19. Radial pressures along SH–LL vehicle above SH: 0.9-m (3-ft) cover.

- Stresses along SH, with LL vehicle located above SH and 0.3 m (1 ft) of cover (Figure C-18);
- Stresses along SH, with LL vehicle located above SH and 0.9 m (3 ft) of cover (Figure C-19);
- Stresses along ST, with LL vehicle located above SH and 0.3 m (1 ft) of cover (Figure C-20); and
- Stresses along ST, with LL vehicle located above SH and 0.9 m (3 ft) of cover (Figure C-21).

Figures C-18 and C-19 have measured data plotted at two axial locations: at P1/P2 (which are at identical distances from the axles) and at S2. Figures C-20 and C-21 have data available at only one location: P1/P2.

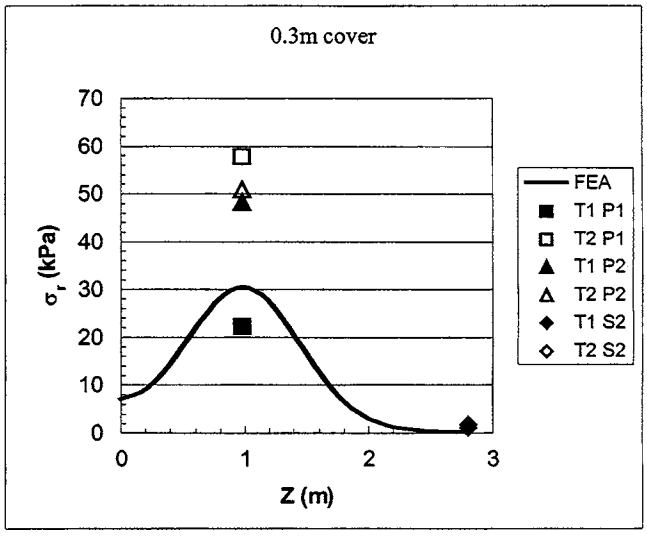

Figure C-18. Radial pressures along SH–LL vehicle above SH: 0.3-m (1-ft) cover.

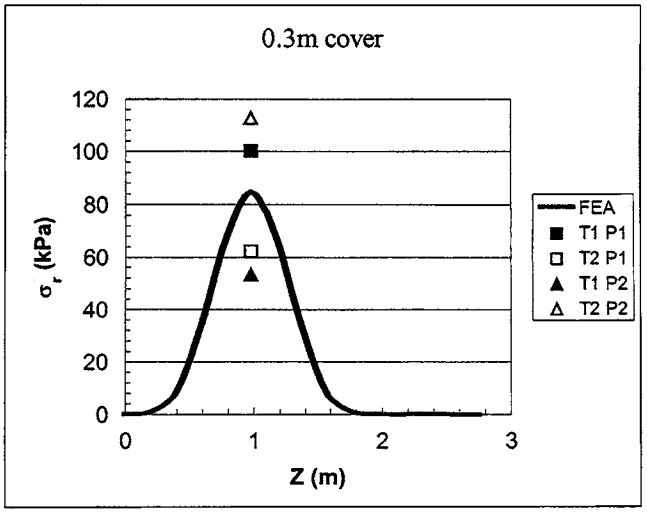

Figure C-20. Radial pressures along ST–LL vehicle above SH: 0.3-m (1-ft) cover.

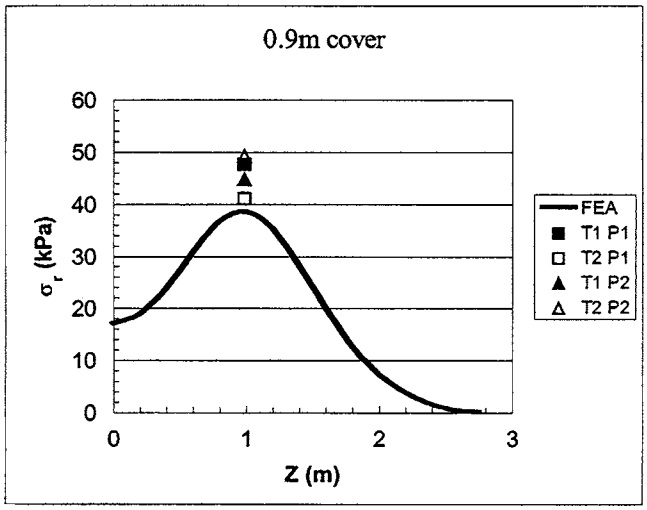

Figure C-21. Radial pressures along ST–LL vehicle above SH: 0.9-m (3-ft) cover.

Consideration of these results indicates the following:

- The two measured values generally exhibit the same trends, peaking when specific wheel loads lie directly over or almost over the pressure cell. The earth pressure measurements differ by between 20 and 60 percent relative to their mean value. This is an indication of the inconsistency of the measurements, resulting from the instruments themselves, and variations in the backfilling and truck-loading conditions.
- The three-dimensional elastic finite element calculations generally show the same trend as the test vehicle location changes over the structure. Those calculations generally lie between the field measurements, although in the case of 0.3 m (1 ft) of cover calculated values of peak pressure along SH and ST are less than either of the peaks measured in the field. Overall, there is a reasonable match between measured and calculated changes in earth pressure, particularly given the large differences observed in each set of field measurements. This discrepancy may be caused by the fact that, at 0.3 m (1 ft) of cover, there had already been precompaction during testing at 0.9-m (3-ft) and 0.6-m (2-ft) cover depths.

Figures C-22 through C-27 compare measured and calculated earth pressure distributions around the circumference for burial depths of 0.3 m (1 ft) and 0.9 m (3 ft), under the vehicle wheels where $Z = 0.98$ m (3.2 ft).

The values correspond to the following figures:

- Stresses around the circumference, with LL vehicle located above SS for 0.3 m (1 ft) of cover (Figure C-22);
- Stresses around the circumference, with LL vehicle located above SS for 0.9 m (3 ft) of cover (Figure C-23);
- Stresses around the circumference, with LL vehicle located above SH for 0.3 m (1 ft) of cover (Figure C-24);
- Stresses around the circumference, with LL vehicle located above SH for 0.9 m (3 ft) of cover (Figure C-25);
- Stresses around the circumference, with LL vehicle located above CR for 0.3 m (1 ft) of cover (Figure C-26);
- Stresses around the circumference, with LL vehicle located above CR for 0.9 m (3 ft) of cover (Figure C-27).

Data were recorded at four different circumferential locations: SC, SH, ST, and CR. Consideration of these results

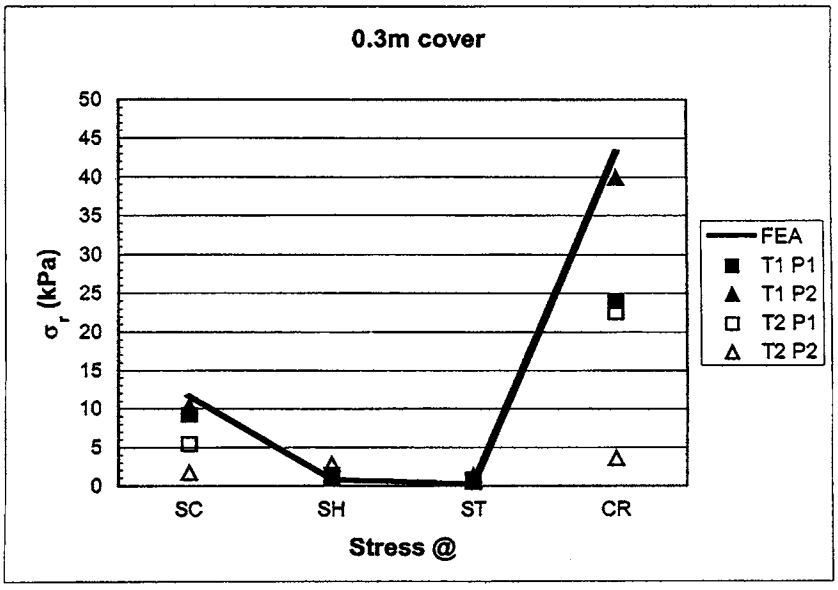

Figure C-22. Radial pressures at z = 0.98 m (3.2 ft): 0.3-m (1-ft) cover, LL above SS.

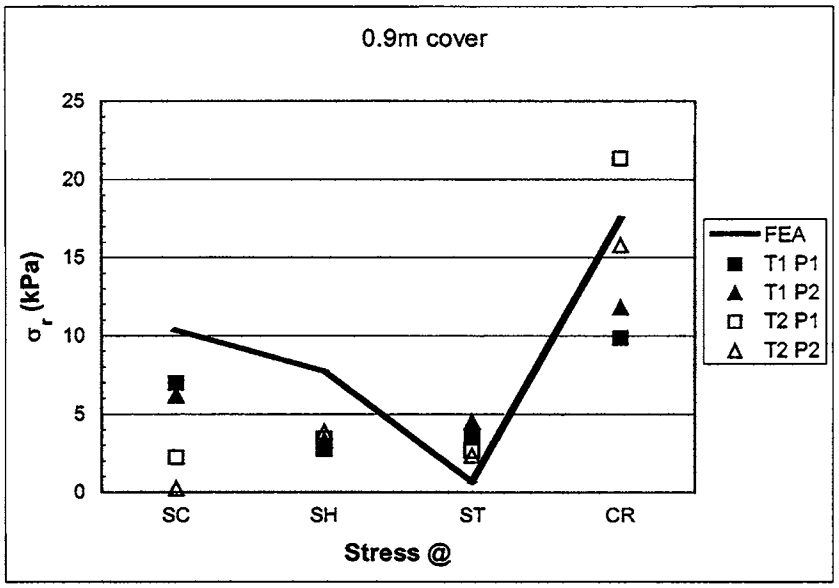

Figure C-23. Radial pressures at z = 0.98 m (3.2 ft): 0.9-m (3-ft) cover, LL above SS.

again indicates that there is generally a reasonable match between finite element calculations and field measurements. With the exception of Figure C-26, where stresses are very small and the stress cells are likely unreliable, the trend of the theoretical and field results is similar, and it appears that reasonable estimates of earth pressures can be expected with the three-dimensional elastic analysis.

CONCRETE CULVERT ANALYSIS: DISCUSSION AND CONCLUSIONS

Based on the preceding results, two-dimensional finite element analysis provides reasonable estimates of soil stresses resulting from earth load. With the exception of discrepancies at the shoulder in the case of culvert in uncompacted backfill, calculations match measurements well. Therefore, the analy-

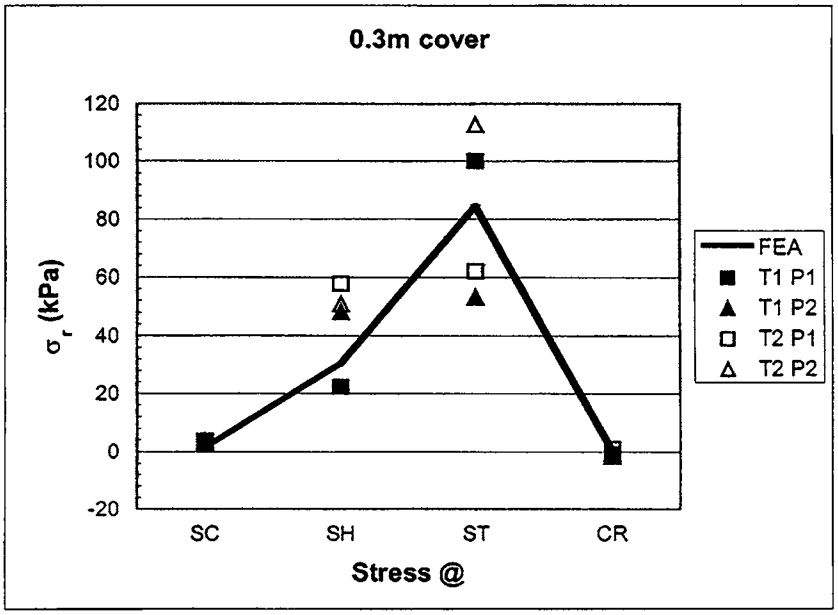

Figure C-24. Radial pressures at z = 0.98 m (3.2 ft): 0.3-m (1-ft) cover, LL above SH.

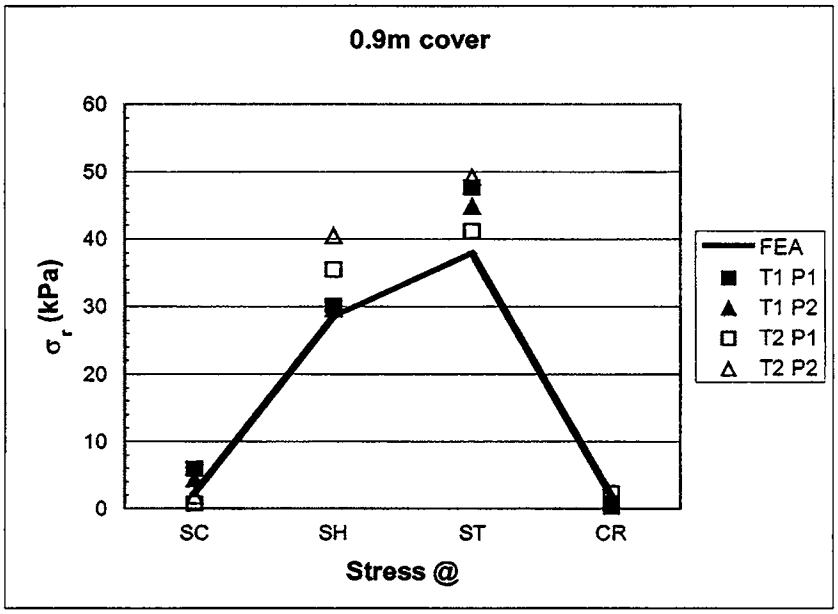

Figure C-25. Radial pressures at z = 0.98 m (3.2 ft): 0.9-m (3-ft) cover, LL above SH.

sis was used without adjustment to evaluate earth pressures for the long-span reinforced concrete culvert structure chosen for the parametric study (Appendix D).

The comprehensive design method features direct evaluation of stress resultant values with the culvert-soil interaction analysis. The few stress resultant values measured in the field were calculated with reasonable success. Changes in the values of thrust with time were observed in the field; these changes are not considered significant to the reinforced concrete design process, because thrust values are small relative to those that influence moment capacity of the reinforced concrete section. Earth-load bending moments were also calculated with reasonable success, so far as field measurements have permitted those values to be assessed. The analysis can therefore be used to undertake a comprehensive design calculation.

The use of elastic solutions to estimate stress distributions as a result of surface loading is a well-accepted, effective technique in the practice of soil mechanics, despite the nonlinear

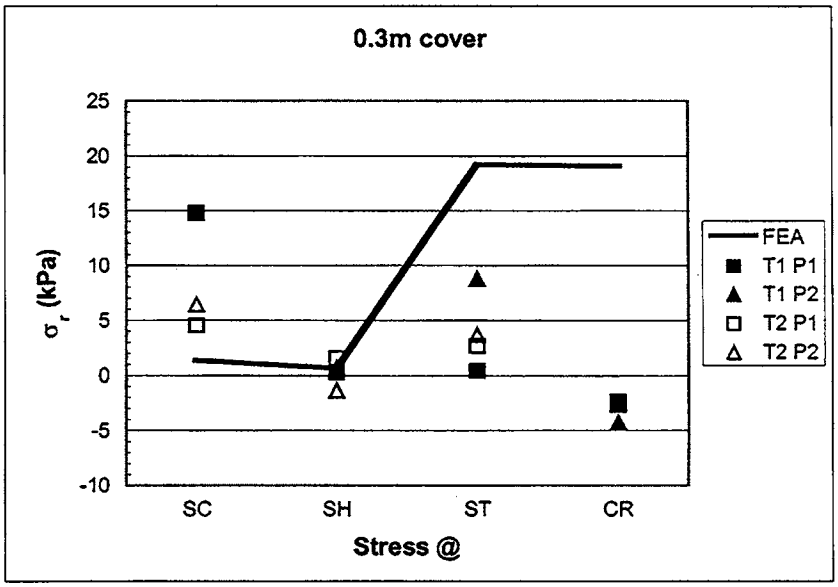

Figure C-26. Radial pressures at z = 0.98 m (3.2 ft): 0.3-m (1-ft) cover, LL above CR.

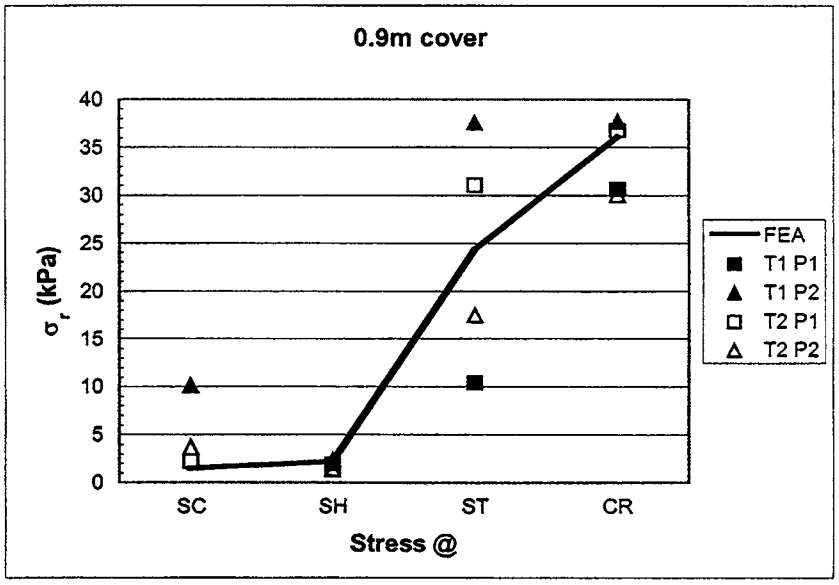

Figure C-27. Radial pressures at z = 0.98 m (3.2 ft): 0.9-m (3-ft) cover, LL above CR.

and nonuniform nature of typical soil deposits. This success of elastic solutions arises from the fact that stress, and therefore stress distributions, are not greatly affected by local variations in soil properties. It appears that earth pressures around the reinforced concrete culvert can be successfully estimated with elastic solutions that account for the impact of soil-culvert interaction but that neglect, for example, the impact of local shear failure as a result of the vehicle load.

The segmented nature of the concrete culvert may have a significant effect on the thrusts and moments that develop within but little impact on the earth pressures that arise in the surrounding soil as a result of live load. The simplified reinforced concrete culvert design method examines earth pressures and then uses these as input in a frame analysis to determine moments, thrusts, and shear forces; it does not use explicit calculations of thrust or moment resulting from dead or live load. The three-dimensional finite element procedure is therefore considered suitable for evaluating earth pressures resulting from live load, despite the fact that it models the structure as continuous (not segmented).